

# ORDER AND SYMMETRY BREAKING IN THE FLUCTUATIONS OF DRIVEN SYSTEMS

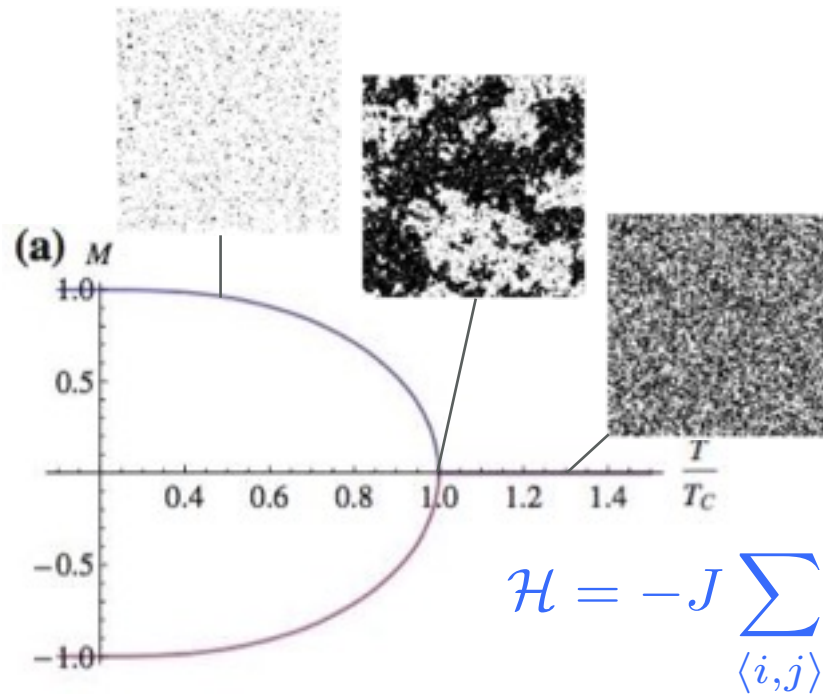
**Pablo I. Hurtado**

Institute Carlos I for Theoretical and Computational Physics  
Departamento de Electromagnetismo y Física de la Materia  
Universidad de Granada (Spain)

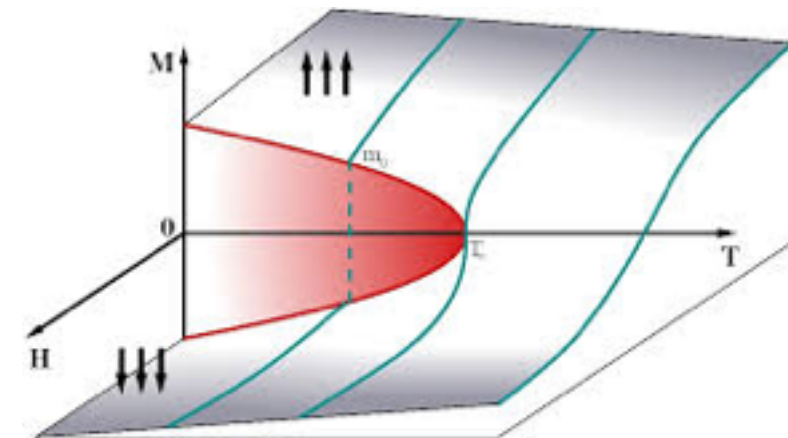
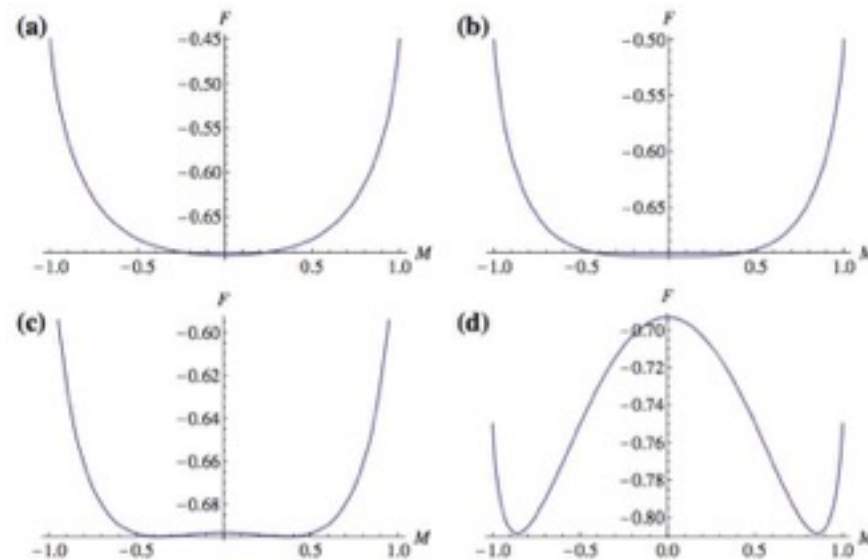
Collaborators  
**N. Tizón**  
**C.P. Espigares**  
**P.L. Garrido**

# DYNAMIC PHASE TRANSITIONS

- Phase transitions are ubiquitous in physics. Typical 2<sup>nd</sup>-order phase transition: **order** + **symmetry-breaking** + **non-analyticity** in thermodynamic potential



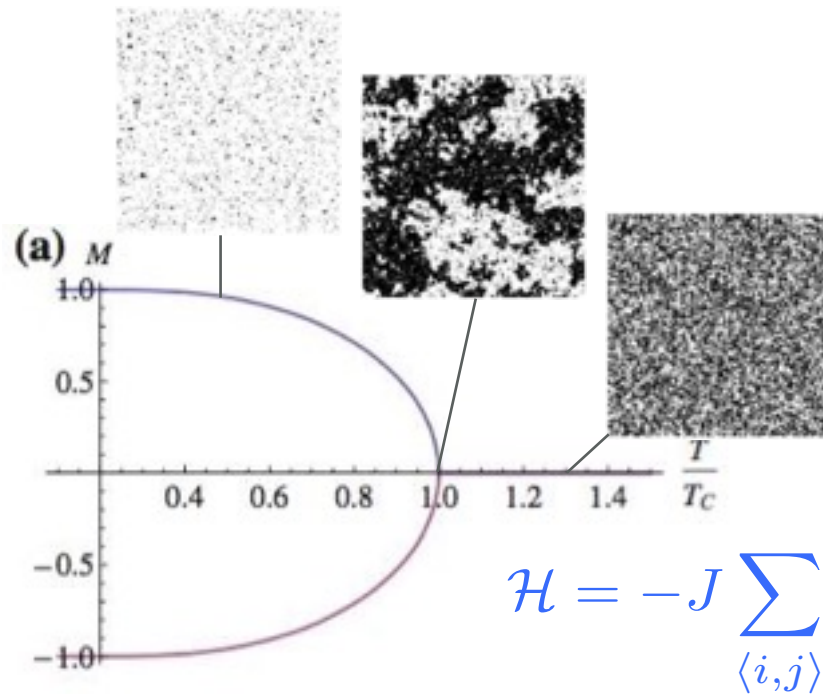
$$\mathcal{H} = -J \sum_{\langle i,j \rangle} s_i s_j$$



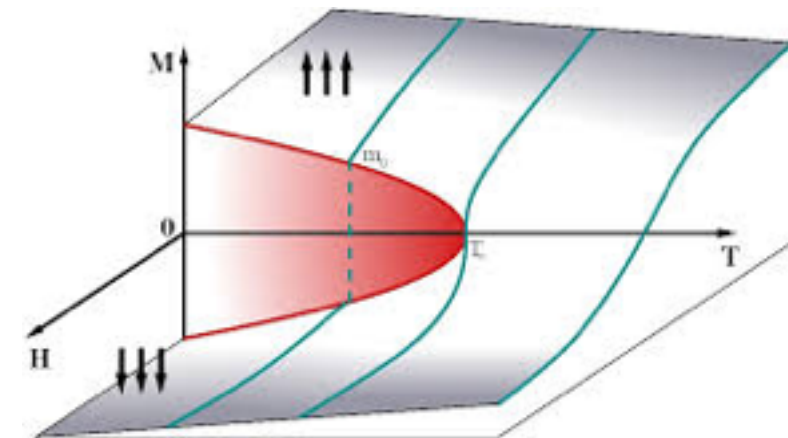
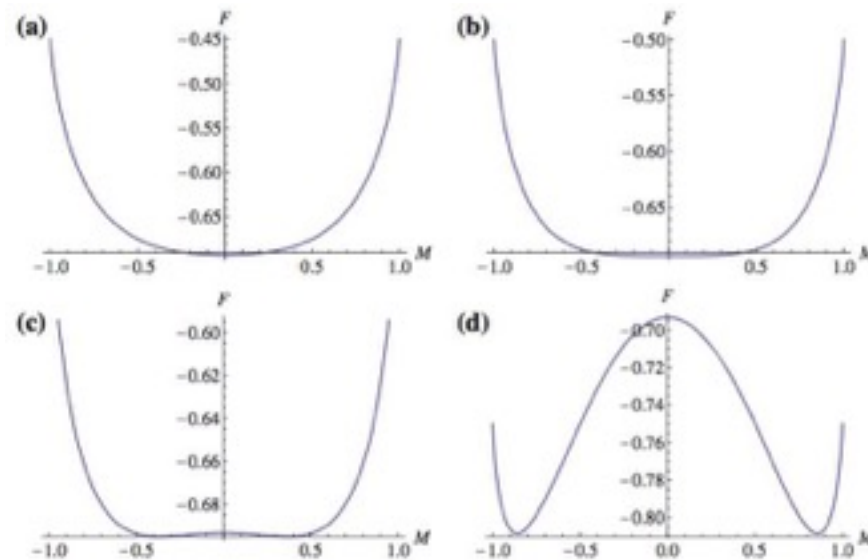
- Typical 1<sup>st</sup>-order phase transition: **abrupt jump** in order parameter + **coexistence** + **metastability**

# DYNAMIC PHASE TRANSITIONS

- Phase transitions are ubiquitous in physics. Typical 2<sup>nd</sup>-order phase transition: **order** + **symmetry-breaking** + **non-analyticity** in thermodynamic potential



$$\mathcal{H} = -J \sum_{\langle i,j \rangle} s_i s_j$$



- Typical 1<sup>st</sup>-order phase transition: **abrupt jump** in order parameter + **coexistence** + **metastability**
- Ideas extended to realm of fluctuations, where **dynamic phase transitions (DPTs)** in the space of trajectories have been identified in **classical and quantum systems**
- **Examples:** glass formers, micromasers, superconducting transistors, etc.  
**Applications:** DPT-based quantum thermal switches

# BUT WHAT ARE DYNAMIC PHASE TRANSITIONS ?

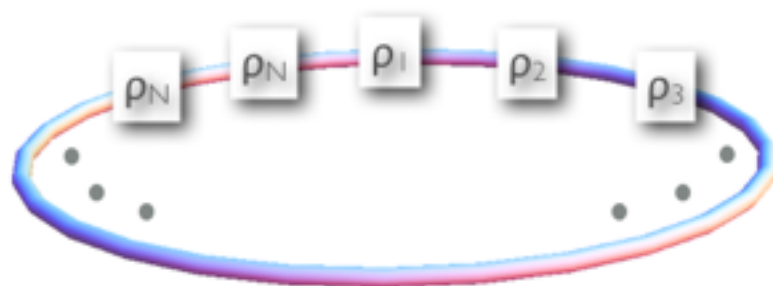
- DPTs appear **when conditioning a system to have a fixed value of some time-integrated observable**, such as, e.g., the **current** or the **activity**
- The **different dynamical phases** correspond to **different types of trajectories** adopted by the system to sustain atypical values of this observable.
- Some dynamical phases may display **emergent order** and **collective rearrangements**, including **symmetry-breaking phenomena**
- The **large deviation functions (LDFs)** controlling the statistics of these fluctuations exhibit **nonanalyticities and Lee-Yang singularities at the DPT** reminiscent of **standard critical behavior**



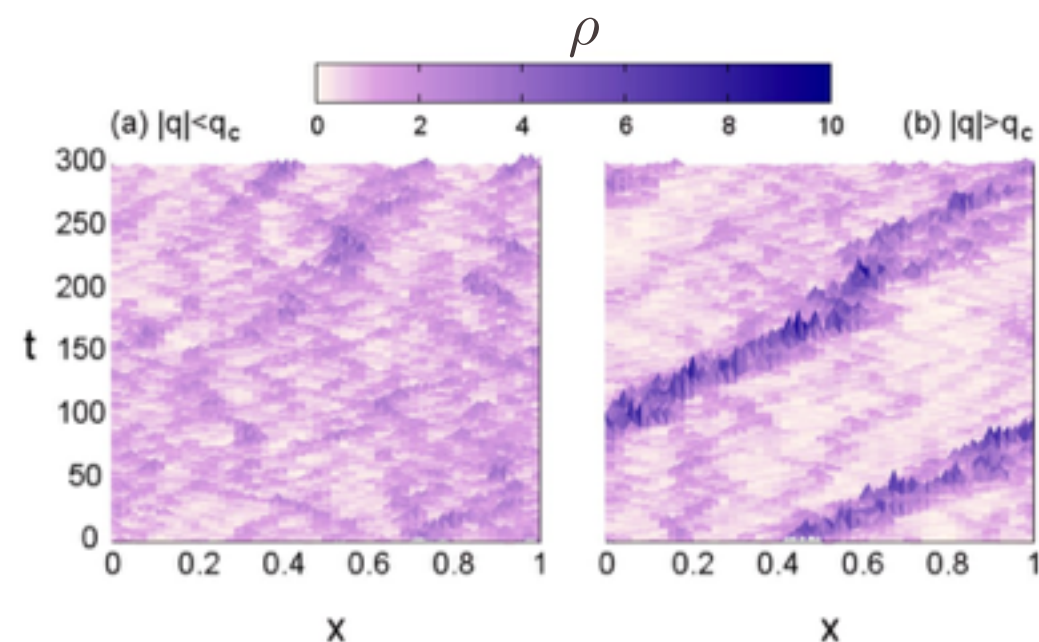
# BUT WHAT ARE DYNAMIC PHASE TRANSITIONS ?

- DPTs appear **when conditioning a system to have a fixed value of some time-integrated observable**, such as, e.g., the **current** or the **activity**
- The **different dynamical phases** correspond to **different types of trajectories** adopted by the system to sustain atypical values of this observable.
- Some dynamical phases may display **emergent order** and **collective rearrangements**, including **symmetry-breaking phenomena**
- The **large deviation functions (LDFs)** controlling the statistics of these fluctuations exhibit **nonanalyticities and Lee-Yang singularities at the DPT** reminiscent of **standard critical behavior**

Kipnis-Marchioro-Presutti (KMP) model

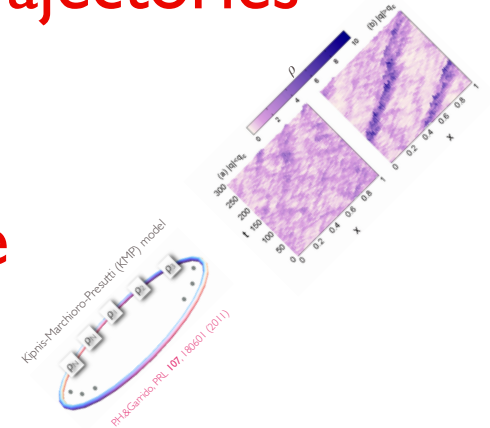


P.H.&Garrido, PRL **107**, 180601 (2011)



# BUT WHAT ARE DYNAMIC PHASE TRANSITIONS ?

- DPTs appear **when conditioning a system to have a fixed value of some time-integrated observable**, such as, e.g., the **current** or the **activity**
- The **different dynamical phases** correspond to **different types of trajectories** adopted by the system to sustain atypical values of this observable.
- Some dynamical phases may display **emergent order** and **collective rearrangements**, including **symmetry-breaking phenomena**
- The **large deviation functions (LDFs)** controlling the statistics of these fluctuations exhibit **nonanalyticities and Lee-Yang singularities at the DPT** reminiscent of **standard critical behavior**
- **Important out of equilibrium**: LDFs play a role akin to thermodynamic potentials for nonequilibrium systems
- **Rare events far more probable than anticipated** due to self-organized structures
- **Control-theory (or active) interpretation of fluctuations** allows to see **DPTs as singular changes in optimal control field** (experimentally observable)



# DYNAMIC PHASE TRANSITIONS IN $d > 1$

- However, discovery and study of DPTs **restricted** to **toy 1d transport models** or **fluctuations of scalar observables in  $d > 1$**

Pérez-Espigares et al, PRE **87**, 032115 (2013); Vaikuntanathan et al PRE **89**, 062108 (2014); Jack et al PRL **114**, 060601 (2015); Shpielberg et al, PRL **116**, 240603 (2016); Zarfaty et al J. Stat. Mech. (2016) P033304; Baek et al, PRL **118**, 030604 (2017); Karevski et al, PRL **118**, 030601 (2017); Garrahan et al, PRL **104**, 160601 (2010); Lesanovsky et al, PRL **110**, 150401 (2013).

Garrahan et al, PRL **98**, 195702 (2007); Garrahan et al J. Phys. A **42**, 075007 (2009); Hedges et al, Science **323**, 1309 (2009); Chandler et al, Annu. Rev. Phys. Chem. **61**, 191 (2010); Pitard et al, EPL **96**, 56002 (2011); Speck et al, PRL **109**, 195703 (2012); Pinchaipat et al, PRL **119**, 028004 (2017).

- **Challenge**: bridge the gap to **fluctuations of fully vectorial observables in  $d > 1$**  and how they are affected by the **(possible) system anisotropy**

# DYNAMIC PHASE TRANSITIONS IN $d > 1$

- However, discovery and study of DPTs **restricted** to **toy 1d transport models** or **fluctuations of scalar observables in  $d > 1$**

Pérez-Espigares et al, PRE **87**, 032115 (2013); Vaikuntanathan et al PRE **89**, 062108 (2014); Jack et al PRL **114**, 060601 (2015); Shpielberg et al, PRL **116**, 240603 (2016); Zarfaty et al J. Stat. Mech. (2016) P033304; Baek et al, PRL **118**, 030604 (2017); Karevski et al, PRL **118**, 030601 (2017); Garrahan et al, PRL **104**, 160601 (2010); Lesanovsky et al, PRL **110**, 150401 (2013).

Garrahan et al, PRL **98**, 195702 (2007); Garrahan et al J. Phys. A **42**, 075007 (2009); Hedges et al, Science **323**, 1309 (2009); Chandler et al, Annu. Rev. Phys. Chem. **61**, 191 (2010); Pitard et al, EPL **96**, 56002 (2011); Speck et al, PRL **109**, 195703 (2012); Pinchaipat et al, PRL **119**, 028004 (2017).

- **Challenge**: bridge the gap to **fluctuations of fully vectorial observables in  $d > 1$**  and how they are affected by the **(possible) system anisotropy**
- **Current statistics**: main objective of nonequilibrium statistical physics.  
Fundamental observable: **current LDF**
- **Aim**: DPTs in the vectorial current statistics of  $d > 1$  driven diffusive systems

# DYNAMIC PHASE TRANSITIONS IN $d > 1$

- However, discovery and study of DPTs **restricted** to **toy 1d transport models** or **fluctuations of scalar observables in  $d > 1$**

Pérez-Espigares et al, PRE **87**, 032115 (2013); Vaikuntanathan et al PRE **89**, 062108 (2014); Jack et al PRL **114**, 060601 (2015); Shpielberg et al, PRL **116**, 240603 (2016); Zarfaty et al J. Stat. Mech. (2016) P033304; Baek et al, PRL **118**, 030604 (2017); Karevski et al, PRL **118**, 030601 (2017); Garrahan et al, PRL **104**, 160601 (2010); Lesanovsky et al, PRL **110**, 150401 (2013).

Garrahan et al, PRL **98**, 195702 (2007); Garrahan et al J. Phys. A **42**, 075007 (2009); Hedges et al, Science **323**, 1309 (2009); Chandler et al, Annu. Rev. Phys. Chem. **61**, 191 (2010); Pitard et al, EPL **96**, 56002 (2011); Speck et al, PRL **109**, 195703 (2012); Pinchaipat et al, PRL **119**, 028004 (2017).

- **Challenge**: bridge the gap to **fluctuations of fully vectorial observables in  $d > 1$**  and how they are affected by the **(possible) system anisotropy**
- **Current statistics**: main objective of nonequilibrium statistical physics.  
Fundamental observable: **current LDF**
- **Aim**: DPTs in the vectorial current statistics of  $d > 1$  driven diffusive systems
- **Tools**: Macroscopic Fluctuation Theory (**MFT**) and advanced **simulations of rare events**
- **Ideal lab**: stochastic lattice gases



# MODEL: 2D WEAKLY ASYMMETRIC SIMPLE EXCLUSION PROCESS

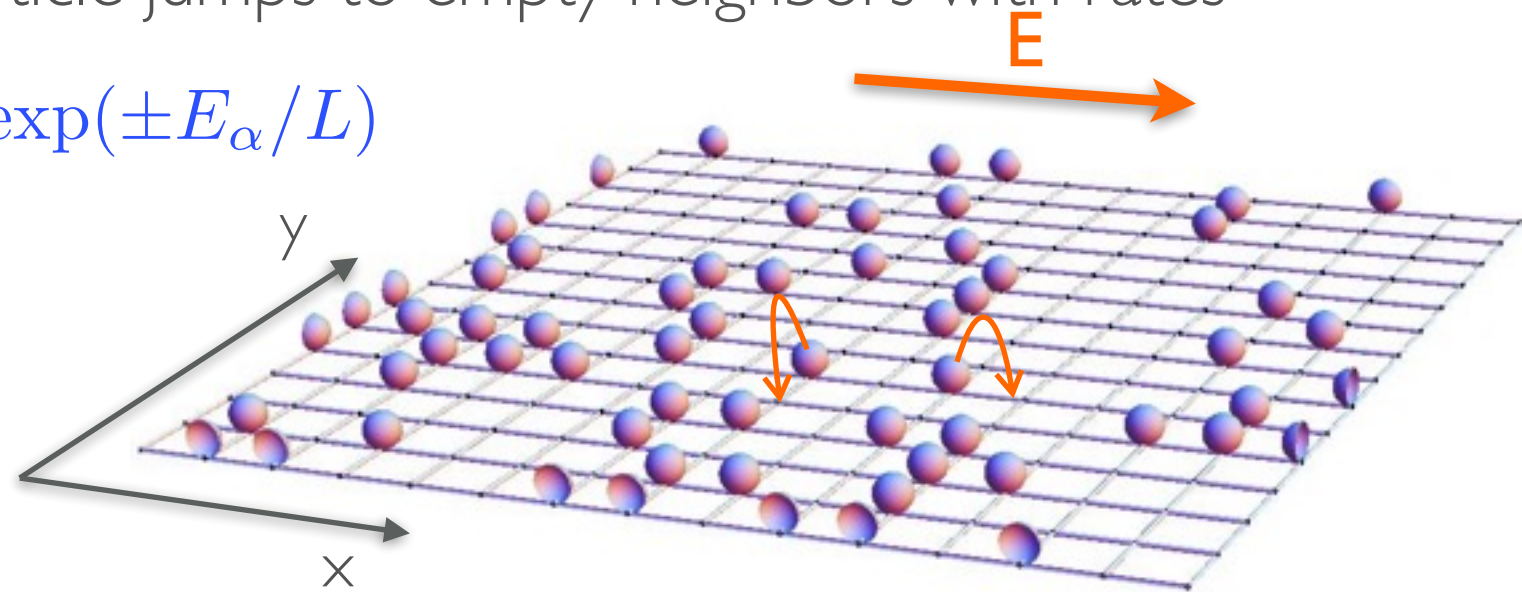
- **WASEP** in 2d: Diffusive particle transport under external field
- Occupation numbers  $n_i = 0, 1$  + particle jumps to empty neighbors with rates

$$r_{\pm}^{(\alpha)} \equiv \frac{1}{2} \exp(\pm E_{\alpha}/L)$$

- Periodic boundary conditions

$$\mathbf{n} \equiv \{n_{ij} = 0, 1; i, j \in [1, L]\}$$

$$N = L^2 \quad M = \sum_{i,j=1}^L n_{ij} \quad \rho_0 = \frac{M}{N}$$



# MODEL: 2D WEAKLY ASYMMETRIC SIMPLE EXCLUSION PROCESS

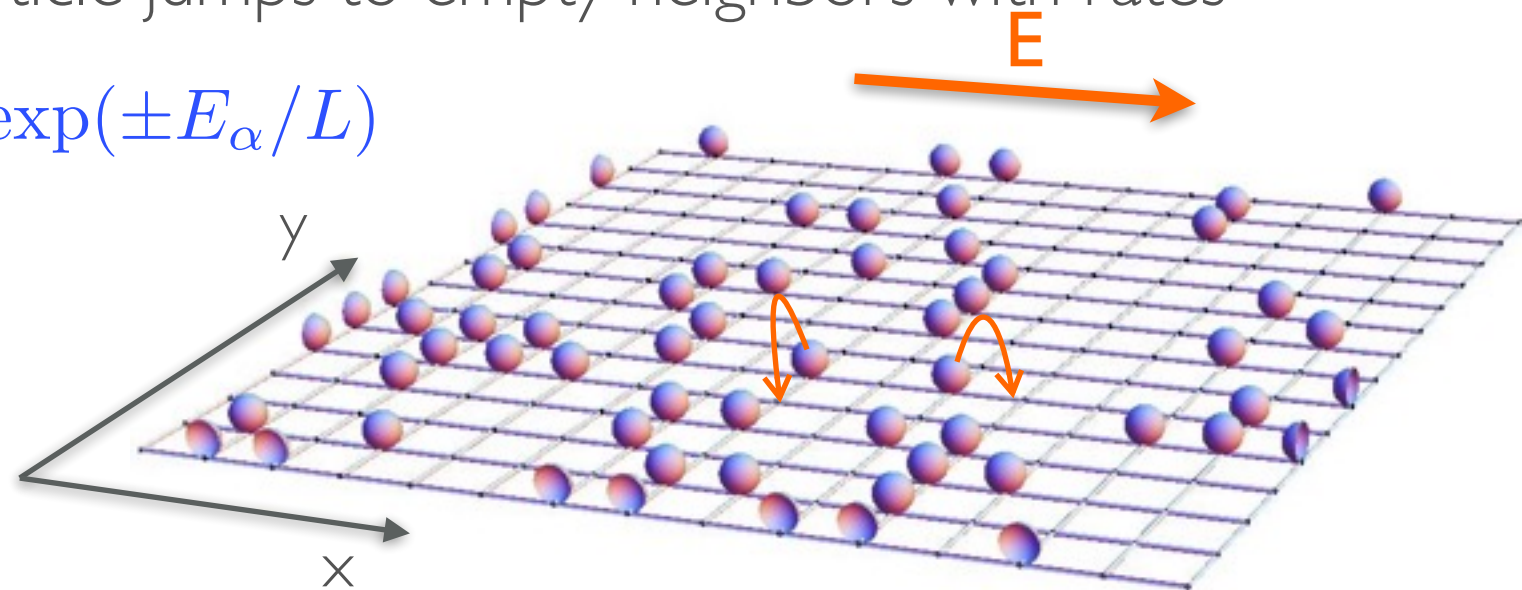
- **WASEP** in 2d: **Diffusive** particle transport under external field
- Occupation numbers  $n_i=0,1$  + particle jumps to empty neighbors with rates

$$r_{\pm}^{(\alpha)} \equiv \frac{1}{2} \exp(\pm E_{\alpha}/L)$$

- **Periodic boundary conditions**

$$\mathbf{n} \equiv \{n_{ij} = 0, 1; i, j \in [1, L]\}$$

$$N = L^2 \quad M = \sum_{i,j=1}^L n_{ij} \quad \rho_0 = \frac{M}{N}$$



- For large E and moderate L, **the field per unit length E/L is strong**  $\Rightarrow$  **effective anisotropy  $\epsilon$** , enhancing diffusivity and mobility along E.

- **Macroscopic transport coefficients:**

$$\hat{D}(\rho) = D(\rho)\hat{A}$$

$$\hat{\sigma}(\rho) = \sigma(\rho)\hat{A}$$

$$D(\rho) = 1/2$$

$$\sigma(\rho) = \rho(1 - \rho)$$

$$\hat{A} = \begin{pmatrix} 1 + \epsilon & 0 \\ 0 & 1 - \epsilon \end{pmatrix}$$

- **Simulations:** Cloning Monte Carlo method for rare events. **Extraordinary number of clones, up to  $N_c=5.12 \times 10^5$  !!**

# MACROSCOPIC FLUCTUATION THEORY (MFT)

Bertini, Gabrielli, De Sole, Jona-Lasinio & Landim, 2001-2016

Rev. Mod. Phys. **87**, 593 (2015)

- Evolution equation for **broad family of systems**:

$$\partial_t \rho(\mathbf{r}, t) + \nabla \cdot \left( -\hat{D}(\rho) \cdot \nabla \rho(\mathbf{r}, t) + \hat{\sigma}(\rho) \cdot \mathbf{E} + \boldsymbol{\xi}(\mathbf{r}, t) \right) = 0 \quad \mathbf{r} \in \Lambda \equiv [0, 1]^d$$

# MACROSCOPIC FLUCTUATION THEORY (MFT)

Bertini, Gabrielli, De Sole, Jona-Lasinio & Landim, 2001-2016  
Rev. Mod. Phys. **87**, 593 (2015)

- Evolution equation for **broad family of systems**:  $\mathbf{j}(\mathbf{r}, t)$  fluctuating current

$$\partial_t \rho(\mathbf{r}, t) + \nabla \cdot \left( -\hat{D}(\rho) \cdot \nabla \rho(\mathbf{r}, t) + \hat{\sigma}(\rho) \cdot \mathbf{E} + \boldsymbol{\xi}(\mathbf{r}, t) \right) = 0 \quad \mathbf{r} \in \Lambda \equiv [0, 1]^d$$

# MACROSCOPIC FLUCTUATION THEORY (MFT)

Bertini, Gabrielli, De Sole, Jona-Lasinio & Landim, 2001-2016  
Rev. Mod. Phys. **87**, 593 (2015)

- Evolution equation for **broad family of systems**:  $\mathbf{j}(\mathbf{r}, t)$  fluctuating current

$$\partial_t \rho(\mathbf{r}, t) + \nabla \cdot \left( -\hat{D}(\rho) \cdot \nabla \rho(\mathbf{r}, t) + \hat{\sigma}(\rho) \cdot \mathbf{E} + \boldsymbol{\xi}(\mathbf{r}, t) \right) = 0 \quad \mathbf{r} \in \Lambda \equiv [0, 1]^d$$

- **Gaussian white noise**: Accounts for microscopic fluctuations at the macroscale

$$\langle \boldsymbol{\xi}(\mathbf{r}, t) \rangle = 0 \quad \langle \xi_\alpha(\mathbf{r}, t) \xi_\beta(\mathbf{r}', t') \rangle = L^{-d} \sigma_\alpha(\rho) \delta_{\alpha\beta} \delta(\mathbf{r} - \mathbf{r}') \delta(t - t') \quad \alpha, \beta \in [1, d]$$



# MACROSCOPIC FLUCTUATION THEORY (MFT)

Bertini, Gabrielli, De Sole, Jona-Lasinio & Landim, 2001-2016  
Rev. Mod. Phys. **87**, 593 (2015)

- Evolution equation for **broad family of systems**:  $\mathbf{j}(\mathbf{r}, t)$  fluctuating current

$$\partial_t \rho(\mathbf{r}, t) + \nabla \cdot \left( -\hat{D}(\rho) \cdot \nabla \rho(\mathbf{r}, t) + \hat{\sigma}(\rho) \cdot \mathbf{E} + \boldsymbol{\xi}(\mathbf{r}, t) \right) = 0 \quad \mathbf{r} \in \Lambda \equiv [0, 1]^d$$

- **Gaussian white noise**: Accounts for microscopic fluctuations at the macroscale

$$\langle \boldsymbol{\xi}(\mathbf{r}, t) \rangle = 0 \quad \langle \xi_\alpha(\mathbf{r}, t) \xi_\beta(\mathbf{r}', t') \rangle = L^{-d} \sigma_\alpha(\rho) \delta_{\alpha\beta} \delta(\mathbf{r} - \mathbf{r}') \delta(t - t') \quad \alpha, \beta \in [1, d]$$

- **Anisotropy** in diffusivity and mobility matrices and **local Einstein relation**:

$$\begin{aligned} \hat{D}(\rho) &= D(\rho) \hat{A} & \hat{A}_{\alpha\beta} &= a_\alpha \delta_{\alpha\beta} = (1 \pm \epsilon) \delta_{\alpha\beta} & \hat{D}(\rho) &= f_0''(\rho) \hat{\sigma}(\rho) \\ \hat{\sigma}(\rho) &= \sigma(\rho) \hat{A} \end{aligned}$$

# MACROSCOPIC FLUCTUATION THEORY (MFT)

Bertini, Gabrielli, De Sole, Jona-Lasinio & Landim, 2001-2016  
 Rev. Mod. Phys. **87**, 593 (2015)

- Evolution equation for **broad family of systems**:  $\mathbf{j}(\mathbf{r}, t)$  fluctuating current

$$\partial_t \rho(\mathbf{r}, t) + \nabla \cdot \left( -\hat{D}(\rho) \cdot \nabla \rho(\mathbf{r}, t) + \hat{\sigma}(\rho) \cdot \mathbf{E} + \boldsymbol{\xi}(\mathbf{r}, t) \right) = 0 \quad \mathbf{r} \in \Lambda \equiv [0, 1]^d$$

- **Gaussian white noise**: Accounts for microscopic fluctuations at the macroscale

$$\langle \boldsymbol{\xi}(\mathbf{r}, t) \rangle = 0 \quad \langle \xi_\alpha(\mathbf{r}, t) \xi_\beta(\mathbf{r}', t') \rangle = L^{-d} \sigma_\alpha(\rho) \delta_{\alpha\beta} \delta(\mathbf{r} - \mathbf{r}') \delta(t - t') \quad \alpha, \beta \in [1, d]$$

- **Anisotropy** in diffusivity and mobility matrices and **local Einstein relation**:

$$\begin{aligned} \hat{D}(\rho) &= D(\rho) \hat{A} & \hat{A}_{\alpha\beta} &= a_\alpha \delta_{\alpha\beta} = (1 \pm \epsilon) \delta_{\alpha\beta} & \hat{D}(\rho) &= f_0''(\rho) \hat{\sigma}(\rho) \\ \hat{\sigma}(\rho) &= \sigma(\rho) \hat{A} \end{aligned}$$

- Probability of a **trajectory**  $\{\rho(\mathbf{r}, t), \mathbf{j}(\mathbf{r}, t)\}_0^\tau \longrightarrow P(\{\rho, \mathbf{j}\}_0^\tau) \sim e^{+L^d I_\tau[\rho, \mathbf{j}]}$

$$I_\tau[\rho, \mathbf{j}] = -\frac{1}{2} \int_0^\tau dt \int_\Lambda d\mathbf{r} [\mathbf{j} - \mathbf{Q}_E(\rho)]^T \cdot \hat{\Sigma}(\rho) \cdot [\mathbf{j} - \mathbf{Q}_E(\rho)] \quad \left| \begin{array}{l} \mathbf{Q}_E(\rho) \equiv -\hat{D}(\rho) \cdot \nabla \rho + \hat{\sigma}(\rho) \cdot \mathbf{E} \\ \Sigma_\alpha(\rho) \equiv \sigma_\alpha^{-1}(\rho) \end{array} \right.$$

- Density and current fields coupled via **continuity equation**:  $\partial_t \rho(\mathbf{r}, t) + \nabla \cdot \mathbf{j}(\mathbf{r}, t) = 0$

- Periodic boundaries  $\Rightarrow$  **conserved mass**:  $\rho_0 = \int_\Lambda d\mathbf{r} \rho(\mathbf{r}, t)$

# CURRENT STATISTICS IN MFT

- Space- and time-averaged **empirical current  $\mathbf{J}$  and current LDF  $G(\mathbf{J})$**

$$\mathbf{J} = \frac{1}{\tau} \int_0^\tau dt \int_\Lambda d\mathbf{r} \mathbf{j}(\mathbf{r}, t) \longrightarrow P_\tau(\mathbf{J}) \sim e^{+\tau L^d G(\mathbf{J})} \longrightarrow G(\mathbf{J}) = \lim_{\tau \rightarrow \infty} \frac{1}{\tau} \max_{\{\rho, \mathbf{j}\}_0^\tau} I_\tau[\rho, \mathbf{j}]$$

- Also interesting: **scaled cumulant generating function (SCGF)**

$$\mu(\boldsymbol{\lambda}) \equiv \lim_{t \rightarrow \infty} t^{-1} \ln \langle e^{t\boldsymbol{\lambda} \cdot \mathbf{J}} \rangle = \max_{\mathbf{J}} [G(\mathbf{J}) + \boldsymbol{\lambda} \cdot \mathbf{J}]$$

# CURRENT STATISTICS IN MFT

- Space- and time-averaged **empirical current  $\mathbf{J}$  and current LDF  $G(\mathbf{J})$**

$$\mathbf{J} = \frac{1}{\tau} \int_0^\tau dt \int_\Lambda d\mathbf{r} \mathbf{j}(\mathbf{r}, t) \longrightarrow P_\tau(\mathbf{J}) \sim e^{+\tau L^d G(\mathbf{J})} \longrightarrow G(\mathbf{J}) = \lim_{\tau \rightarrow \infty} \frac{1}{\tau} \max_{\{\rho, \mathbf{j}\}_0^\tau} I_\tau[\rho, \mathbf{j}]$$

- Also interesting: **scaled cumulant generating function (SCGF)**

$$\mu(\boldsymbol{\lambda}) \equiv \lim_{t \rightarrow \infty} t^{-1} \ln \langle e^{t \boldsymbol{\lambda} \cdot \mathbf{J}} \rangle = \max_{\mathbf{J}} [G(\mathbf{J}) + \boldsymbol{\lambda} \cdot \mathbf{J}]$$

- Optimal trajectory  $\neq$  steady profile:  $\rho_{\mathbf{J}}(\mathbf{r}, t)$   $\mathbf{j}_{\mathbf{J}}(\mathbf{r}, t)$

- **Homogeneous steady state:**  $\rho_{\text{st}}(\mathbf{r}) = \rho_0$   $\mathbf{j}_{\text{st}}(\mathbf{r}) = \langle \mathbf{J} \rangle = \sigma_0 \hat{A} \mathbf{E}$

$$D_0 \equiv D(\rho_0)$$
$$\sigma_0 \equiv \sigma(\rho_0)$$

# CURRENT STATISTICS IN MFT

- Space- and time-averaged **empirical current  $\mathbf{J}$  and current LDF  $G(\mathbf{J})$**

$$\mathbf{J} = \frac{1}{\tau} \int_0^\tau dt \int_\Lambda d\mathbf{r} \mathbf{j}(\mathbf{r}, t) \longrightarrow P_\tau(\mathbf{J}) \sim e^{+\tau L^d G(\mathbf{J})} \longrightarrow G(\mathbf{J}) = \lim_{\tau \rightarrow \infty} \frac{1}{\tau} \max_{\{\rho, \mathbf{j}\}_0^\tau} I_\tau[\rho, \mathbf{j}]$$

- Also interesting: **scaled cumulant generating function (SCGF)**

$$\mu(\boldsymbol{\lambda}) \equiv \lim_{t \rightarrow \infty} t^{-1} \ln \langle e^{t \boldsymbol{\lambda} \cdot \mathbf{J}} \rangle = \max_{\mathbf{J}} [G(\mathbf{J}) + \boldsymbol{\lambda} \cdot \mathbf{J}]$$

- Optimal trajectory  $\neq$  steady profile:  $\rho_{\mathbf{J}}(\mathbf{r}, t)$   $\mathbf{j}_{\mathbf{J}}(\mathbf{r}, t)$

- Homogeneous steady state:**  $\rho_{\text{st}}(\mathbf{r}) = \rho_0$   $\mathbf{j}_{\text{st}}(\mathbf{r}) = \langle \mathbf{J} \rangle = \sigma_0 \hat{A} \mathbf{E}$   $D_0 \equiv D(\rho_0)$   
 $\sigma_0 \equiv \sigma(\rho_0)$

- Small current fluctuations** result from weakly-correlated local events which sum incoherently  $\Rightarrow$  **homogeneous optimal fields**

$$|\mathbf{J} - \langle \mathbf{J} \rangle| \ll 1 \Rightarrow \begin{cases} \rho_{\mathbf{J}}(\mathbf{r}, t) = \rho_0 \\ \mathbf{j}_{\mathbf{J}}(\mathbf{r}, t) = \langle \mathbf{J} \rangle \end{cases}$$

- Leads to quadratic current LDF and **Gaussian current statistics**

$$G_G(\mathbf{J}) = -(\mathbf{J} - \hat{\sigma}_0 \mathbf{E}) \cdot \hat{\sigma}_0^{-1} (\mathbf{J} - \hat{\sigma}_0 \mathbf{E}) / 2 \quad \Rightarrow \quad \mu_G(\mathbf{z}) = (\mathbf{z} \cdot \hat{\sigma}_0 \mathbf{z} - \mathbf{E} \cdot \hat{\sigma}_0 \mathbf{E}) / 2$$

$$\mathbf{z} \equiv \boldsymbol{\lambda} + \mathbf{E}$$

- Stability of this homogeneous solution?



# DPT FOR STRONG CURRENT FLUCTUATIONS

- **Local stability analysis:** the **Gaussian regime eventually becomes unstable** against small but otherwise arbitrary spatiotemporal perturbations. **Critical line** ( $\sigma''(\rho) < 0$ )

$$\mathbf{J} \cdot \hat{A}^{-1} \mathbf{J} \leq \sigma_0^2 \Xi_c \quad \Leftrightarrow \quad \mathbf{z} \cdot \hat{A} \mathbf{z} \leq \Xi_c \quad \Xi_c \equiv \Sigma_c + \mathbf{E} \cdot \hat{A} \mathbf{E}$$

- This DPT appears for **strong fields**,  $\mathbf{E} \cdot \hat{A} \mathbf{E} \geq |\Sigma_c|$

$$\Sigma_c \equiv 8\pi^2 D_0^2 \frac{a_{\min}}{\sigma_0 \sigma_0''}$$

$$a_{\min} = \min(a_x, a_y)$$

# DPT FOR STRONG CURRENT FLUCTUATIONS

- **Local stability analysis:** the **Gaussian regime eventually becomes unstable** against small but otherwise arbitrary spatiotemporal perturbations. **Critical line** ( $\sigma''(\rho) < 0$ )

$$\mathbf{J} \cdot \hat{A}^{-1} \mathbf{J} \leq \sigma_0^2 \Xi_c \quad \Leftrightarrow \quad \mathbf{z} \cdot \hat{A} \mathbf{z} \leq \Xi_c \quad \Xi_c \equiv \Sigma_c + \mathbf{E} \cdot \hat{A} \mathbf{E}$$

- This DPT appears for **strong fields**,  $\mathbf{E} \cdot \hat{A} \mathbf{E} \geq |\Sigma_c|$

$$\Sigma_c \equiv 8\pi^2 D_0^2 \frac{a_{\min}}{\sigma_0 \sigma_0''}$$

$$a_{\min} = \min(a_x, a_y)$$

- **Dominant perturbation** beyond instability: **Id density traveling wave**

$$\rho_{\mathbf{J}}(\mathbf{r}, t) = \omega_{\mathbf{J}}(x_{\parallel} - vt)$$

- This solution **breaks the system spatiotemporal translation symmetry** by localizing particles in a **jammed region** to facilitate a low-current fluctuation
- **Different Id density waves dominate different subcritical current regimes**, depending on the anisotropy parameter  $\epsilon$

# DPT FOR STRONG CURRENT FLUCTUATIONS

- Local stability analysis: the **Gaussian regime eventually becomes unstable** against small but otherwise arbitrary spatiotemporal perturbations. **Critical line** ( $\sigma''(\rho) < 0$ )

$$\mathbf{J} \cdot \hat{A}^{-1} \mathbf{J} \leq \sigma_0^2 \Xi_c \Leftrightarrow \mathbf{z} \cdot \hat{A} \mathbf{z} \leq \Xi_c \quad \Xi_c \equiv \Sigma_c + \mathbf{E} \cdot \hat{A} \mathbf{E}$$

- This DPT appears for **strong fields**,  $\mathbf{E} \cdot \hat{A} \mathbf{E} \geq |\Sigma_c|$

$$\Sigma_c \equiv 8\pi^2 D_0^2 \frac{a_{\min}}{\sigma_0 \sigma_0''}$$

$$a_{\min} = \min(a_x, a_y)$$

- Dominant perturbation** beyond instability: **Id density traveling wave**

$$\rho_{\mathbf{J}}(\mathbf{r}, t) = \omega_{\mathbf{J}}(x_{\parallel} - vt)$$

- This solution **breaks the system spatiotemporal translation symmetry** by localizing particles in a **jammed region** to facilitate a low-current fluctuation

- Different Id density waves dominate different subcritical current regimes**, depending on the anisotropy parameter  $\epsilon$

- This enriching degeneracy stems from a **structured divergence-free vector field coupled to the current**

$$\mathbf{j}_{\mathbf{J}}(\mathbf{r}, t) = \mathbf{J} - \mathbf{v} [\rho_0 - \omega_{\mathbf{J}}(\mathbf{r} - \mathbf{v}t)] + \phi_{\mathbf{J}}(\mathbf{r} - \mathbf{v}t)$$

$$\int_{\Lambda} \phi_{\mathbf{J}}(\mathbf{r}) d\mathbf{r} = 0$$

$$\nabla \cdot \phi_{\mathbf{J}}(\mathbf{r}) = 0$$

Pérez-Espigares, Garrido, PH, PRE **93**, 040103(R) (2016)

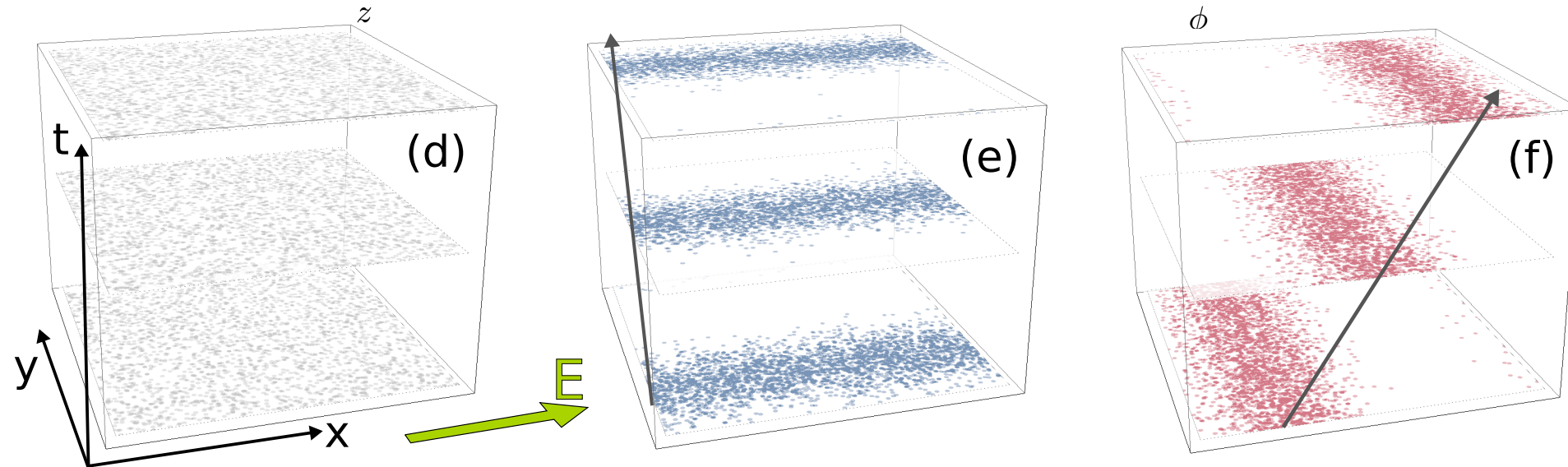
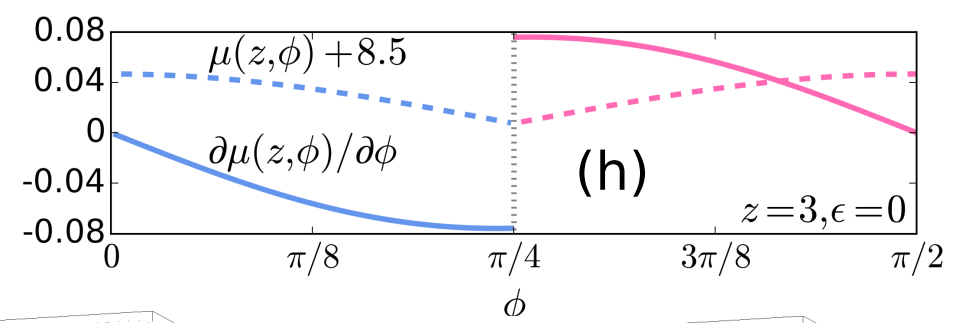
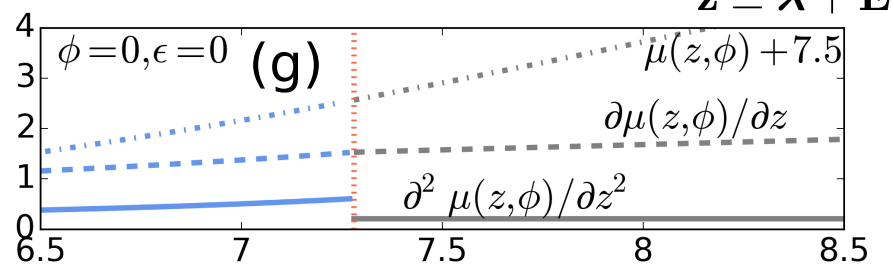
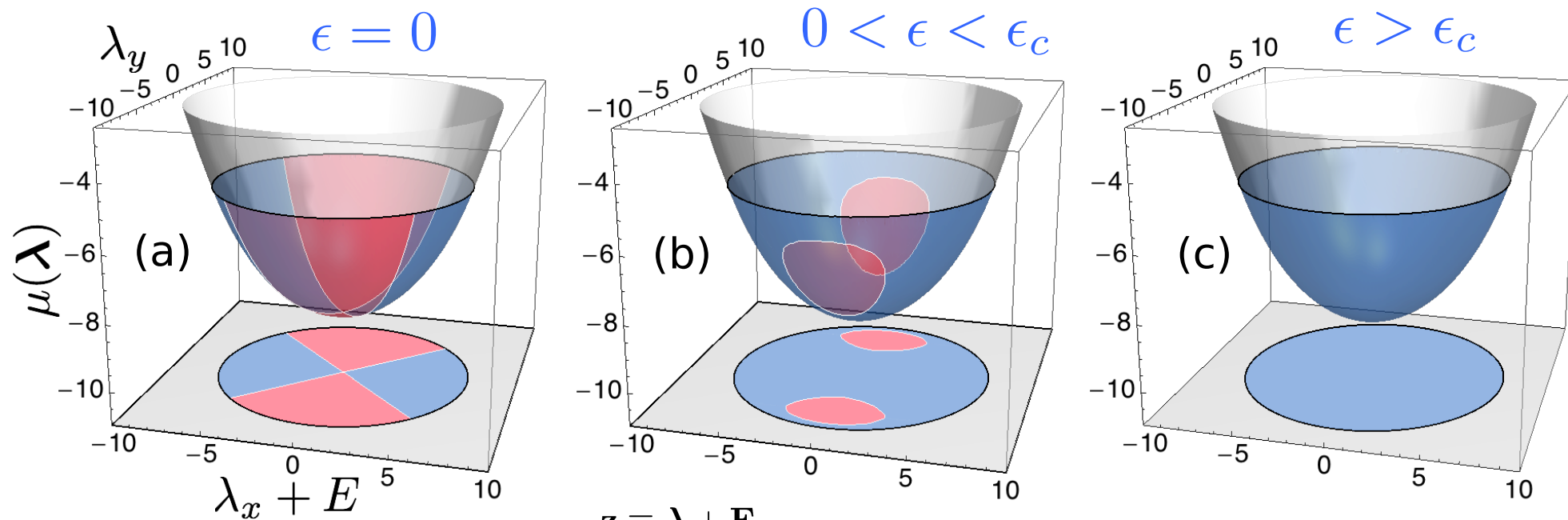
Villavicencio, Harris, PRE **93**, 032134 (2016)

Tizón, PH, Garrido, PRE **95**, 032119 (2017)

# A RICH PHASE DIAGRAM (2D WASEP)

$$\mathbf{J} \cdot \hat{\mathbf{A}}^{-1} \mathbf{J} \leq \sigma_0^2 \Xi_c$$

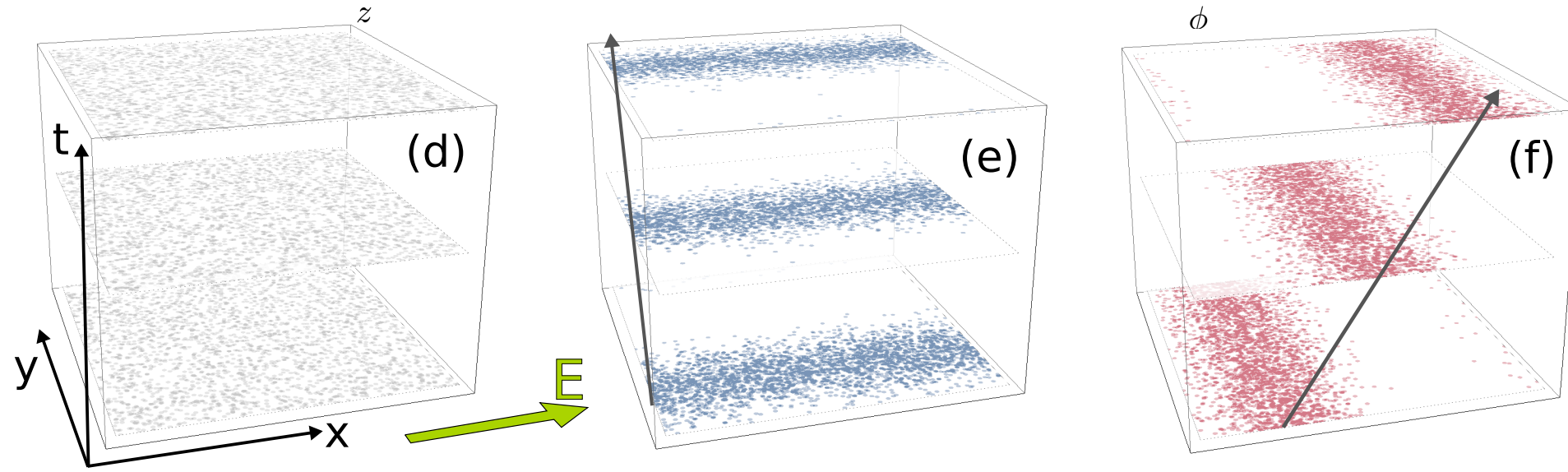
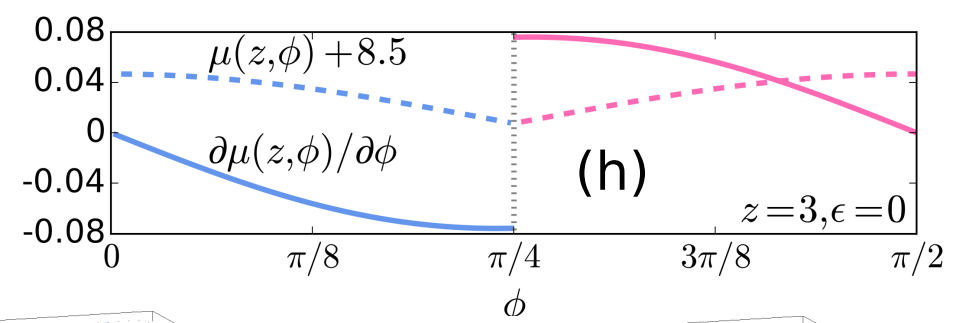
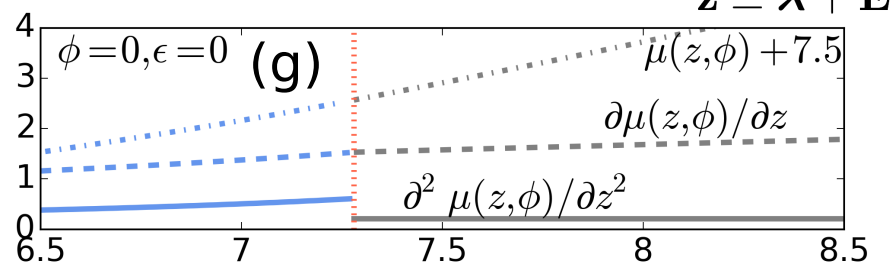
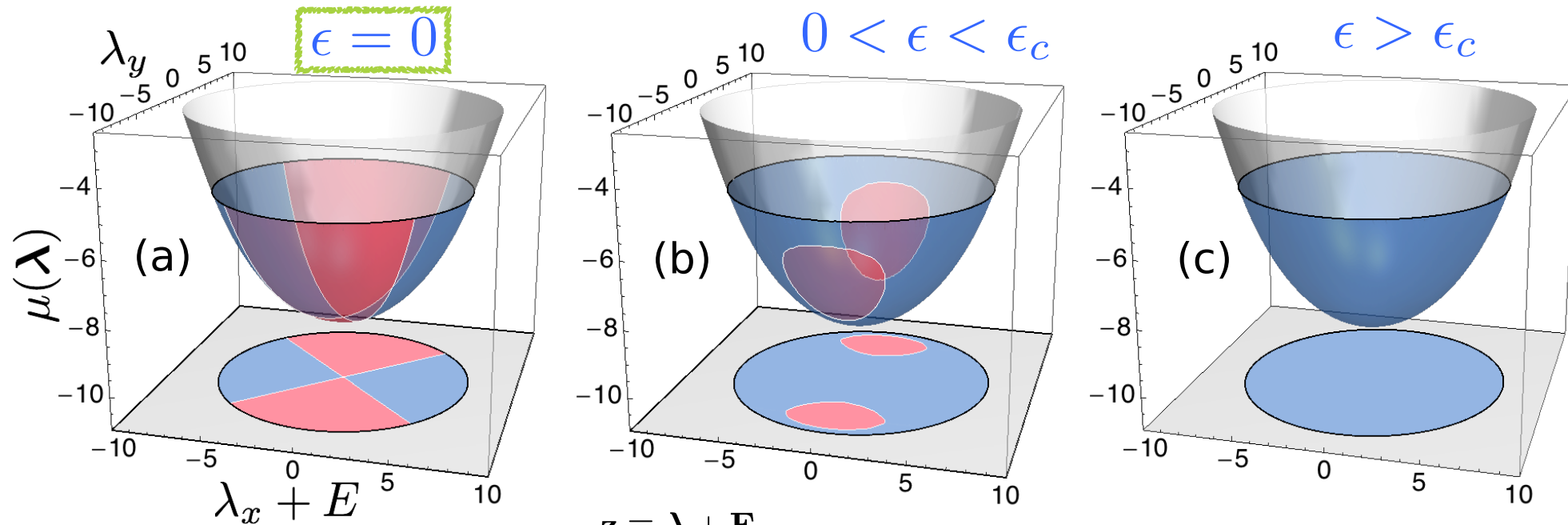
$$\hat{\mathbf{A}} = \begin{pmatrix} 1 + \epsilon & 0 \\ 0 & 1 - \epsilon \end{pmatrix}$$



# A RICH PHASE DIAGRAM (2D WASEP)

$$\mathbf{J} \cdot \hat{\mathbf{A}}^{-1} \mathbf{J} \leq \sigma_0^2 \Xi_c$$

$$\hat{\mathbf{A}} = \begin{pmatrix} 1 + \epsilon & 0 \\ 0 & 1 - \epsilon \end{pmatrix}$$



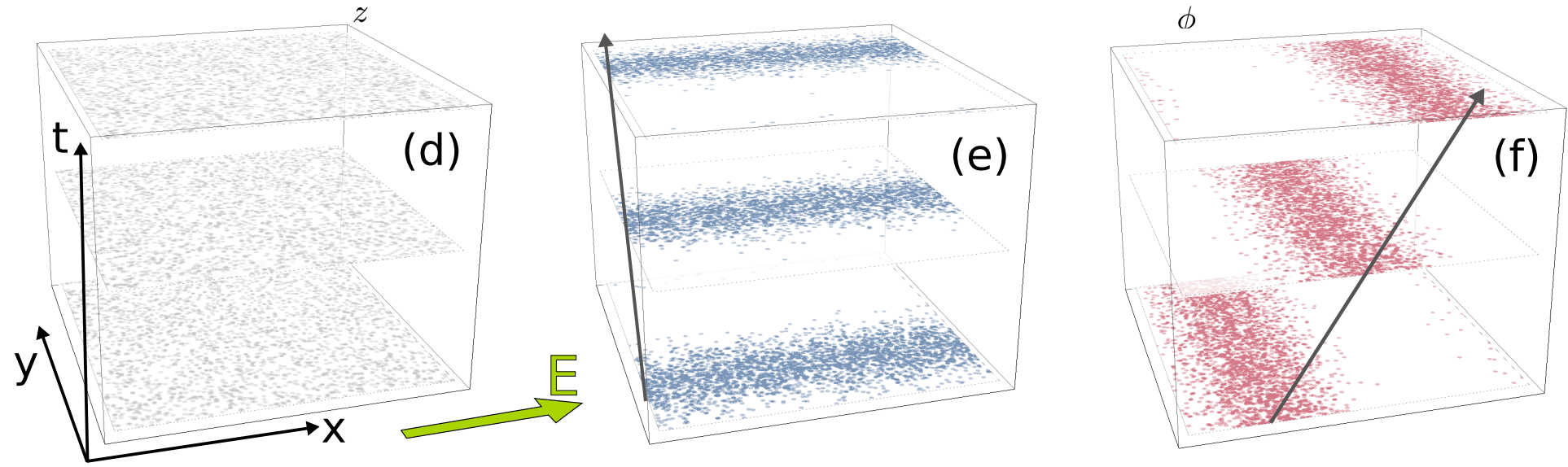
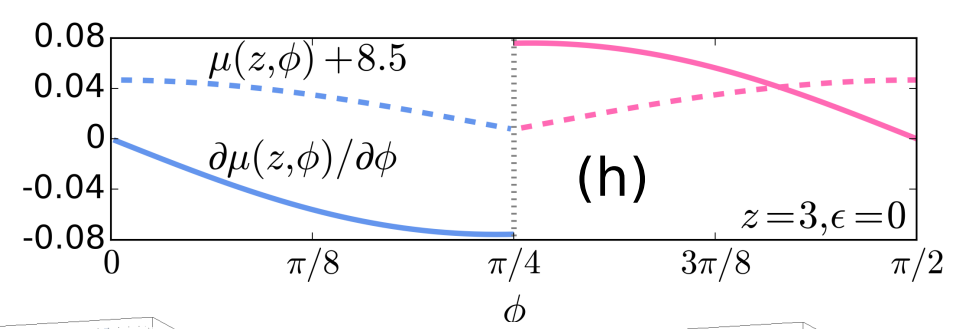
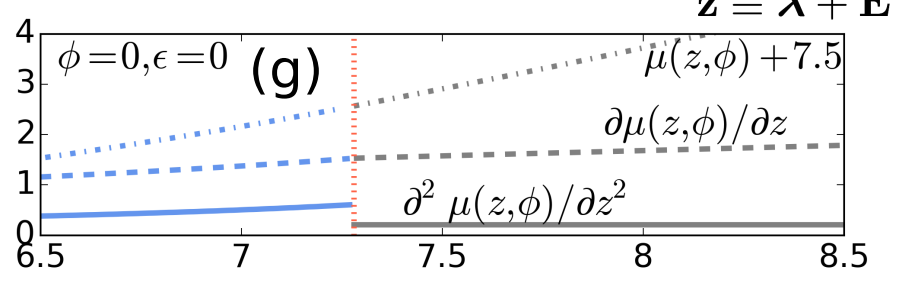
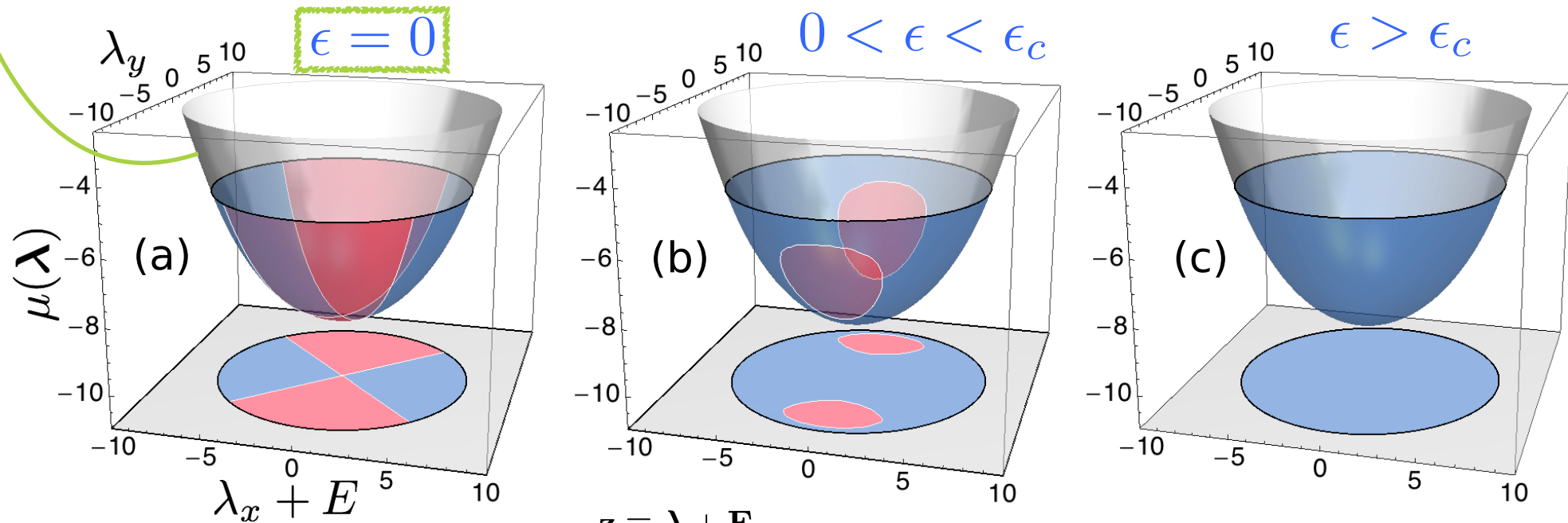


# A RICH PHASE DIAGRAM (2D WASEP)

$$\mathbf{J} \cdot \hat{\mathbf{A}}^{-1} \mathbf{J} \leq \sigma_0^2 \Xi_c$$

$$\hat{\mathbf{A}} = \begin{pmatrix} 1 + \epsilon & 0 \\ 0 & 1 - \epsilon \end{pmatrix}$$

Gaussian current statistics  $\mu_G(\boldsymbol{\lambda})$

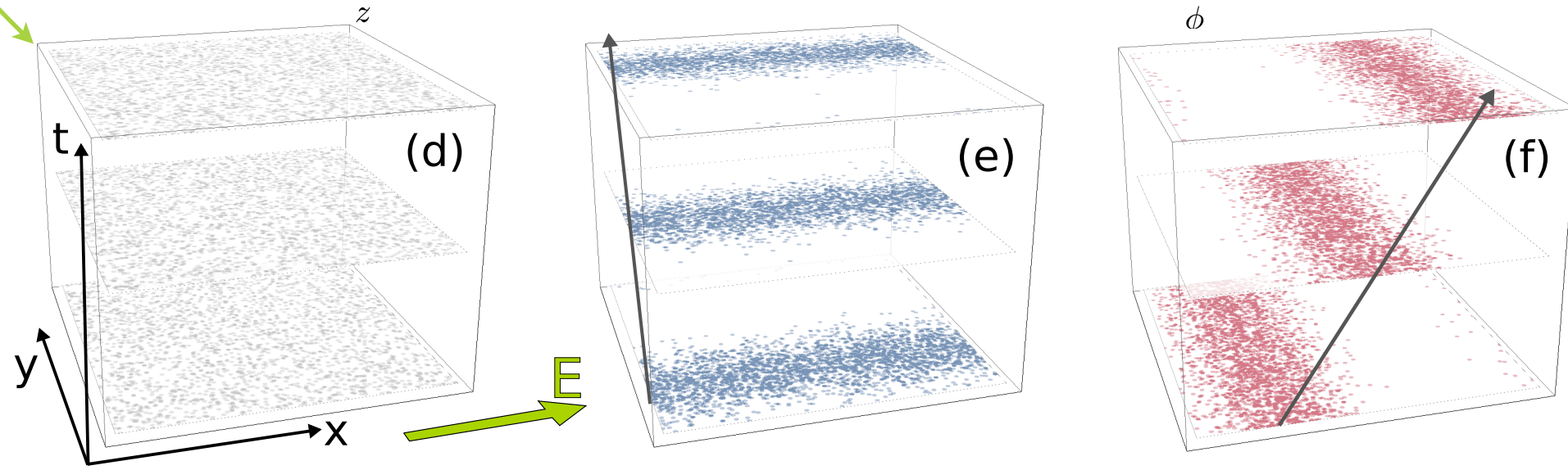
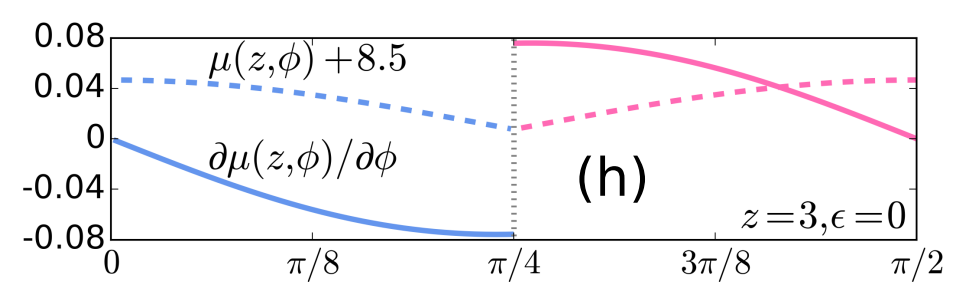
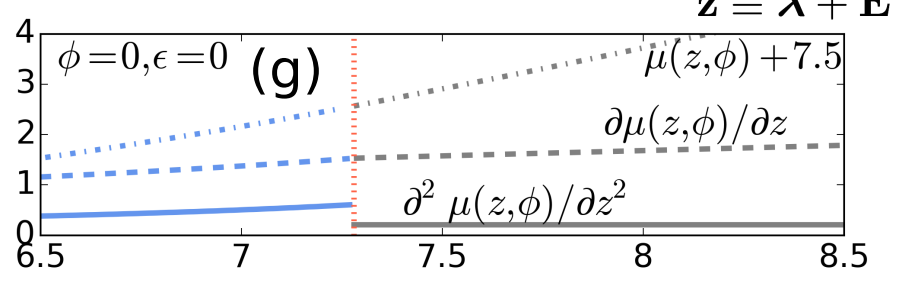
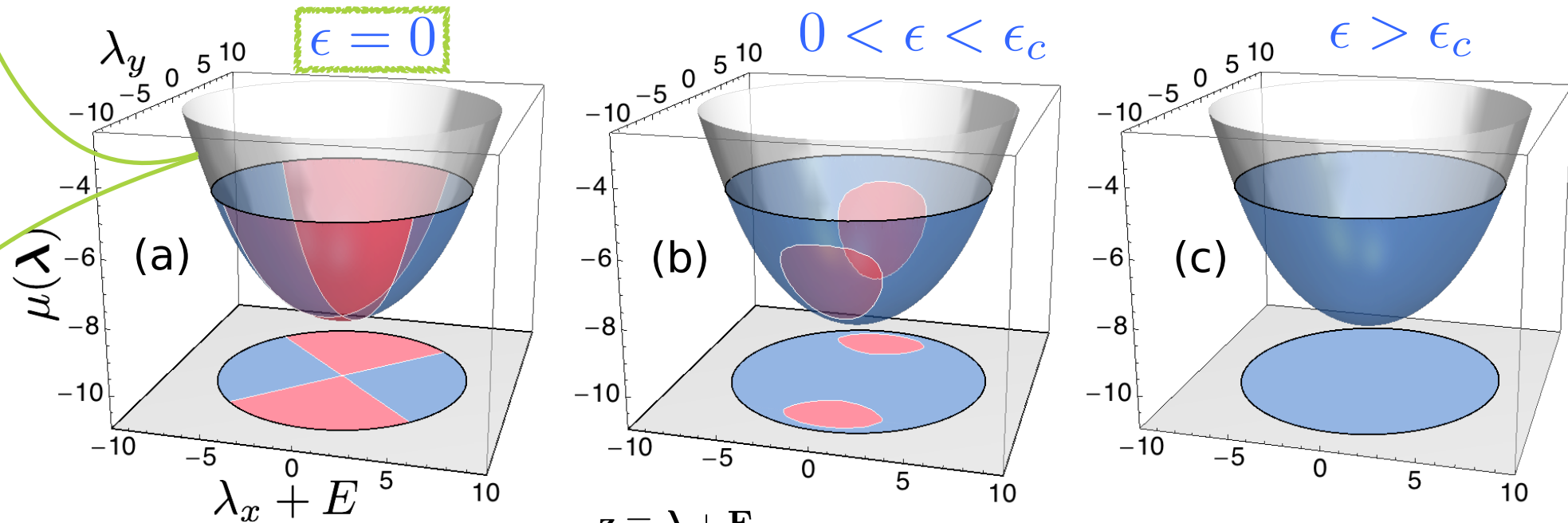


# A RICH PHASE DIAGRAM (2D WASEP)

$$\mathbf{J} \cdot \hat{\mathbf{A}}^{-1} \mathbf{J} \leq \sigma_0^2 \Xi_c$$

$$\hat{\mathbf{A}} = \begin{pmatrix} 1 + \epsilon & 0 \\ 0 & 1 - \epsilon \end{pmatrix}$$

Gaussian current statistics  $\mu_G(\boldsymbol{\lambda})$



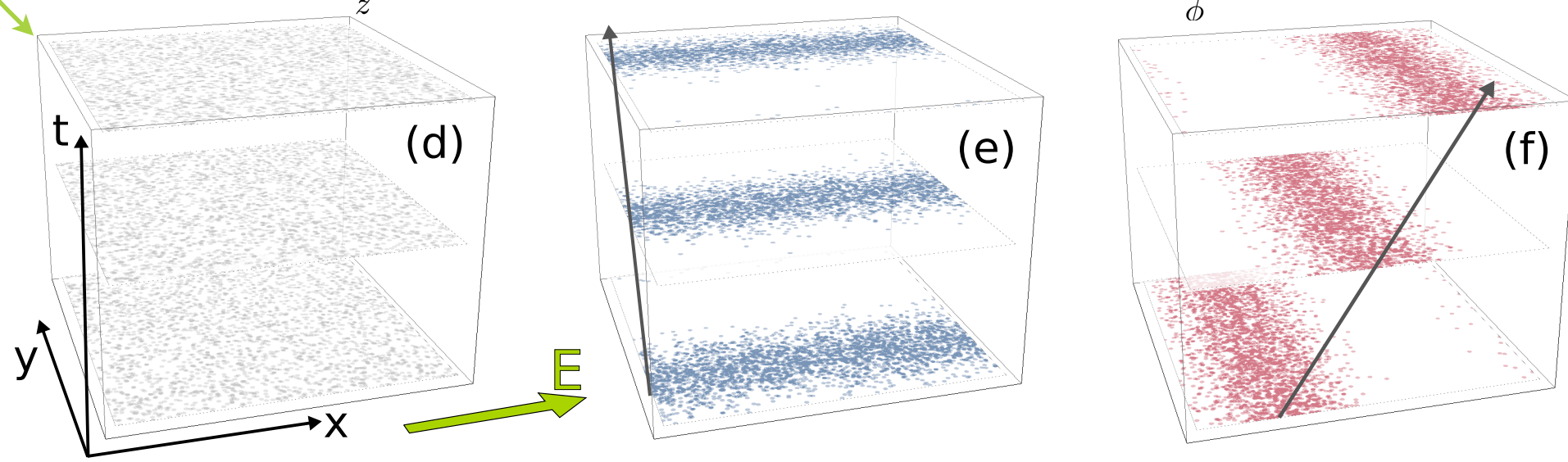
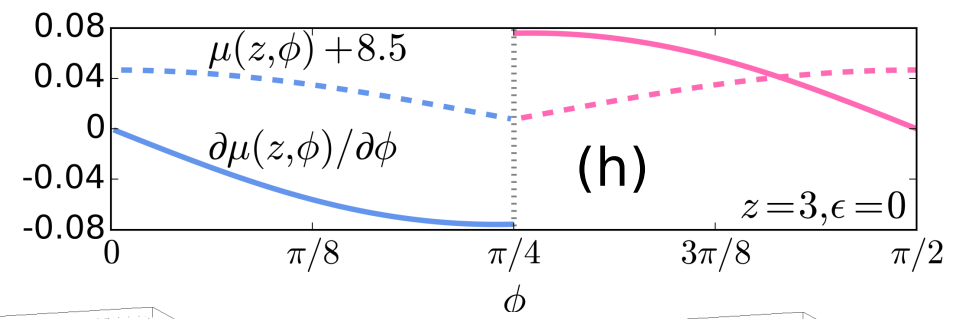
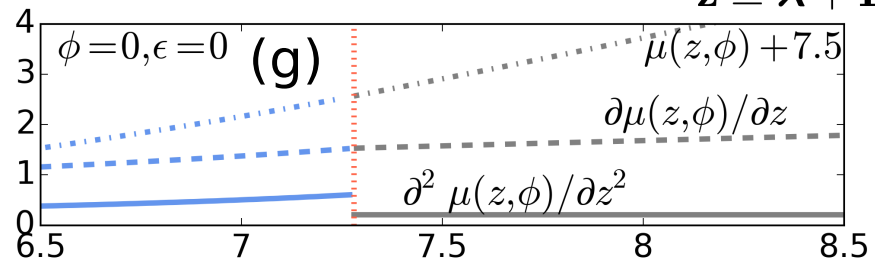
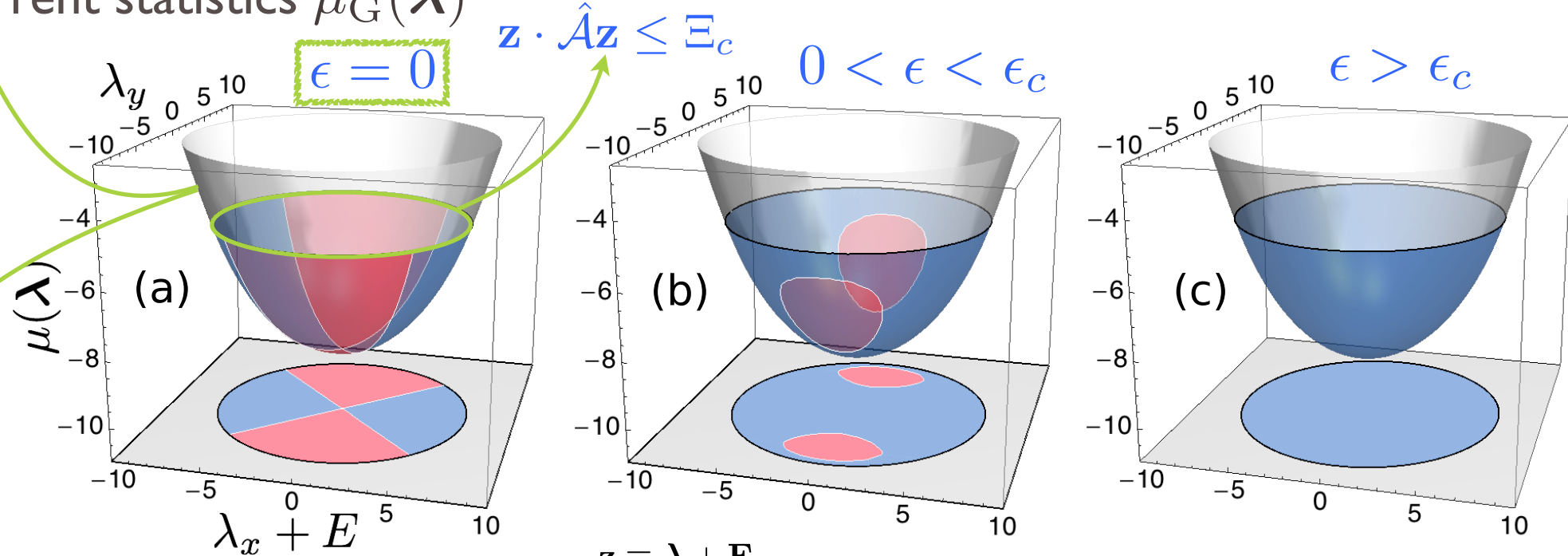
Homogeneous, structureless typical trajectories

# A RICH PHASE DIAGRAM (2D WASEP)

$$\mathbf{J} \cdot \hat{\mathbf{A}}^{-1} \mathbf{J} \leq \sigma_0^2 \Xi_c$$

$$\hat{\mathbf{A}} = \begin{pmatrix} 1 + \epsilon & 0 \\ 0 & 1 - \epsilon \end{pmatrix}$$

Gaussian current statistics  $\mu_G(\boldsymbol{\lambda})$



Homogeneous, structureless typical trajectories

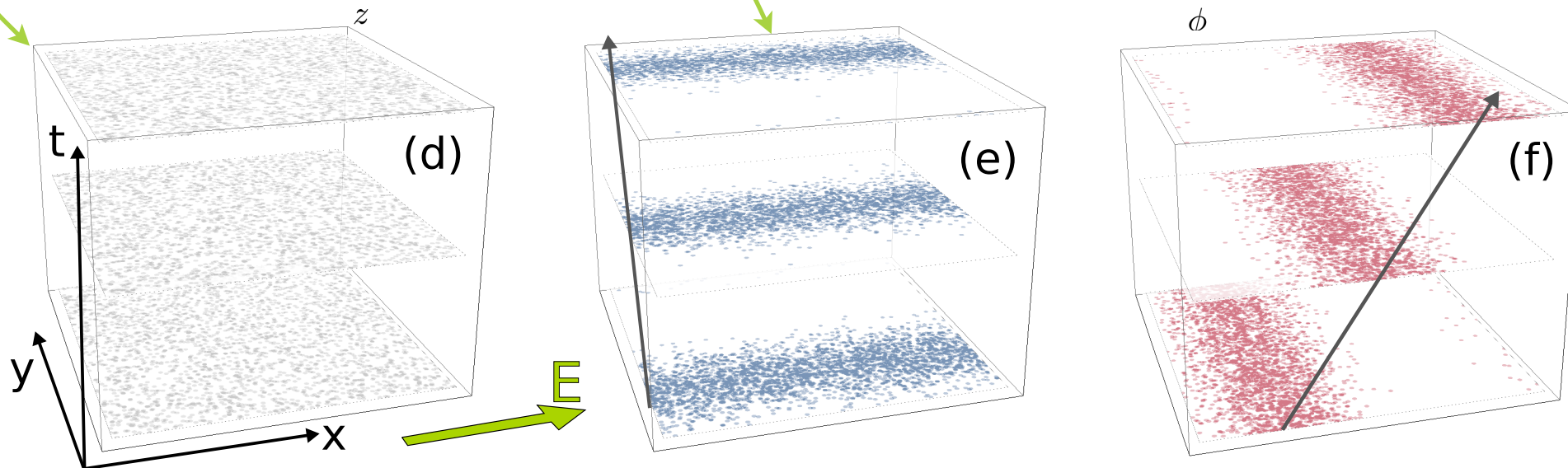
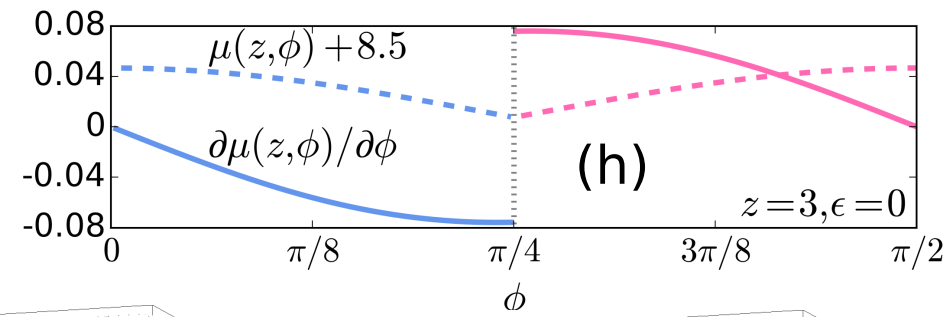
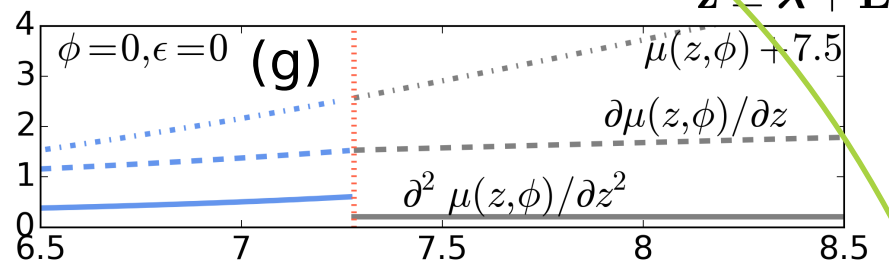
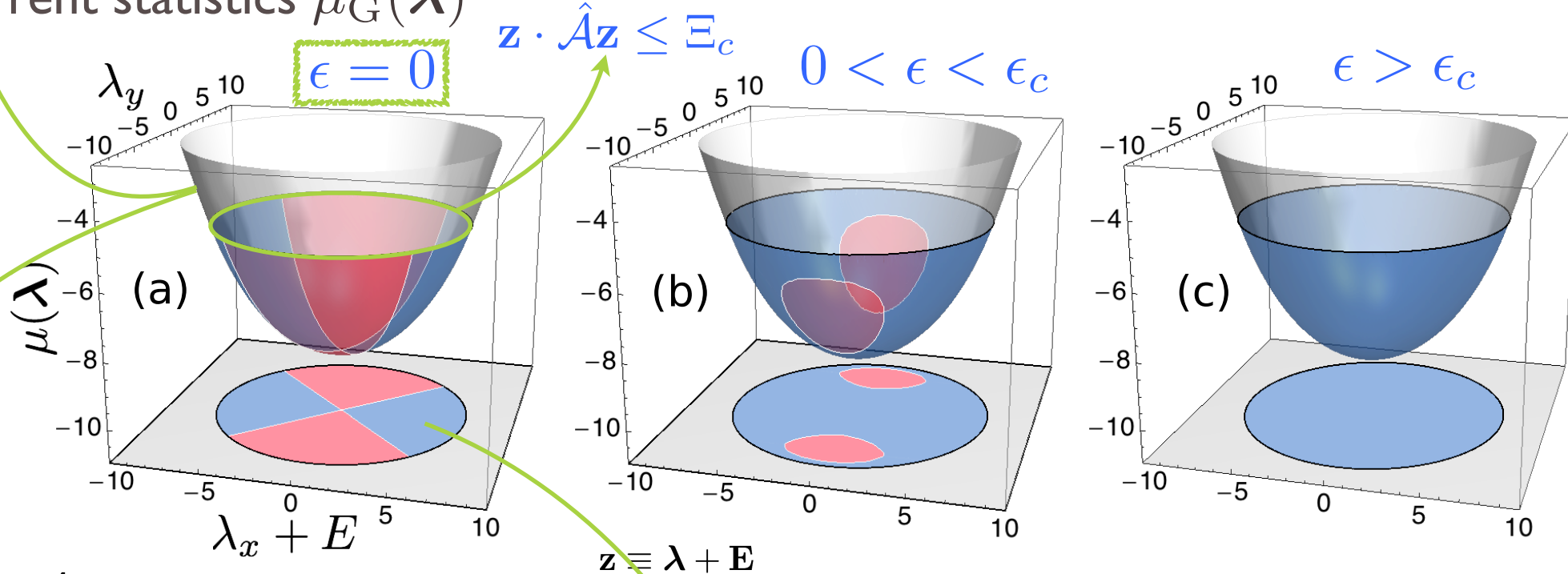


# A RICH PHASE DIAGRAM (2D WASEP)

$$\mathbf{J} \cdot \hat{\mathbf{A}}^{-1} \mathbf{J} \leq \sigma_0^2 \Xi_c$$

$$\hat{\mathbf{A}} = \begin{pmatrix} 1 + \epsilon & 0 \\ 0 & 1 - \epsilon \end{pmatrix}$$

Gaussian current statistics  $\mu_G(\boldsymbol{\lambda})$



Homogeneous, structureless typical trajectories

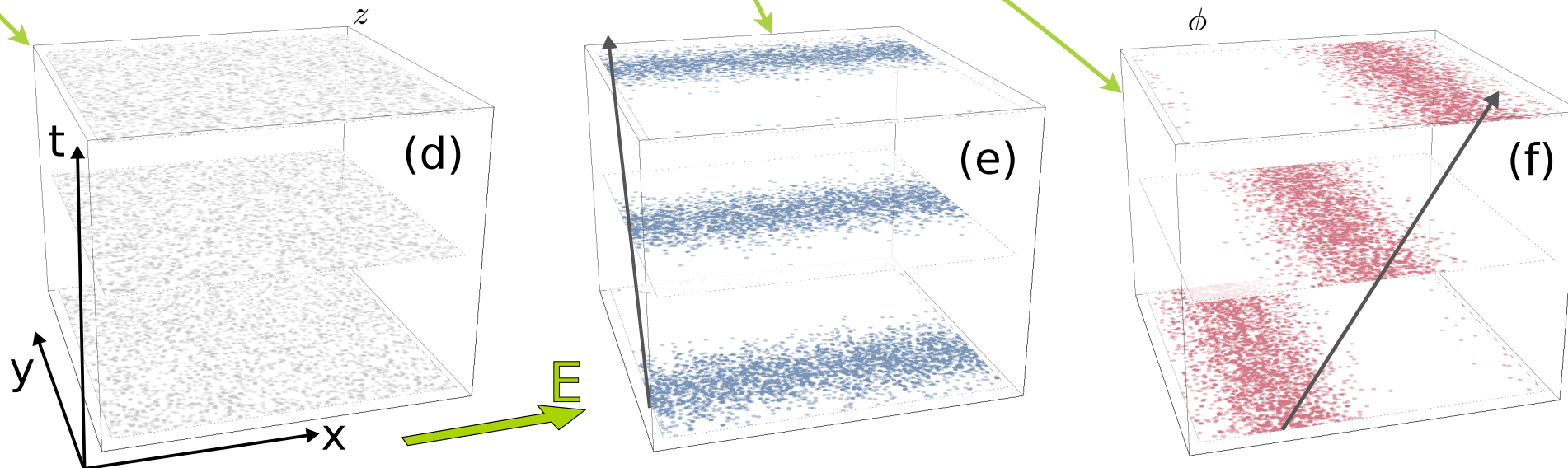
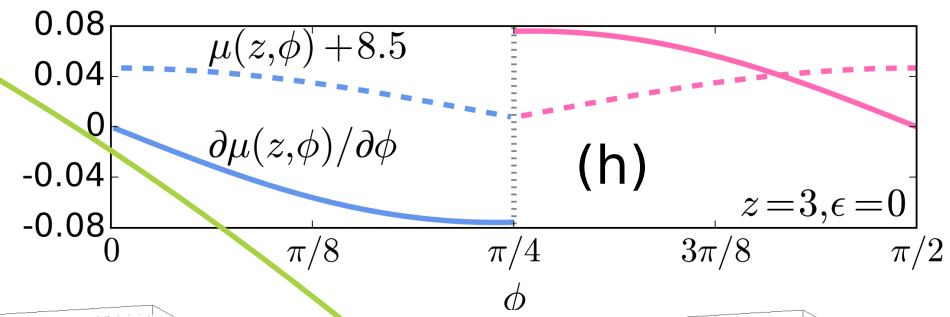
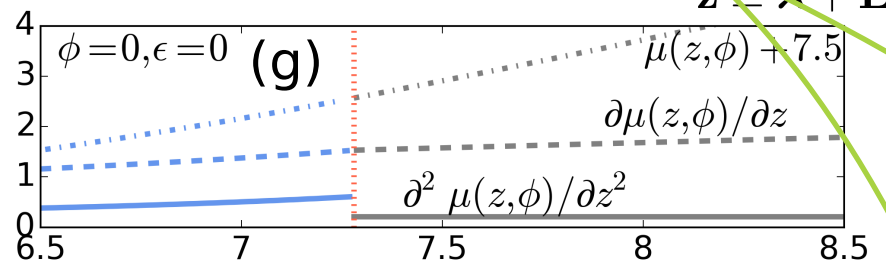
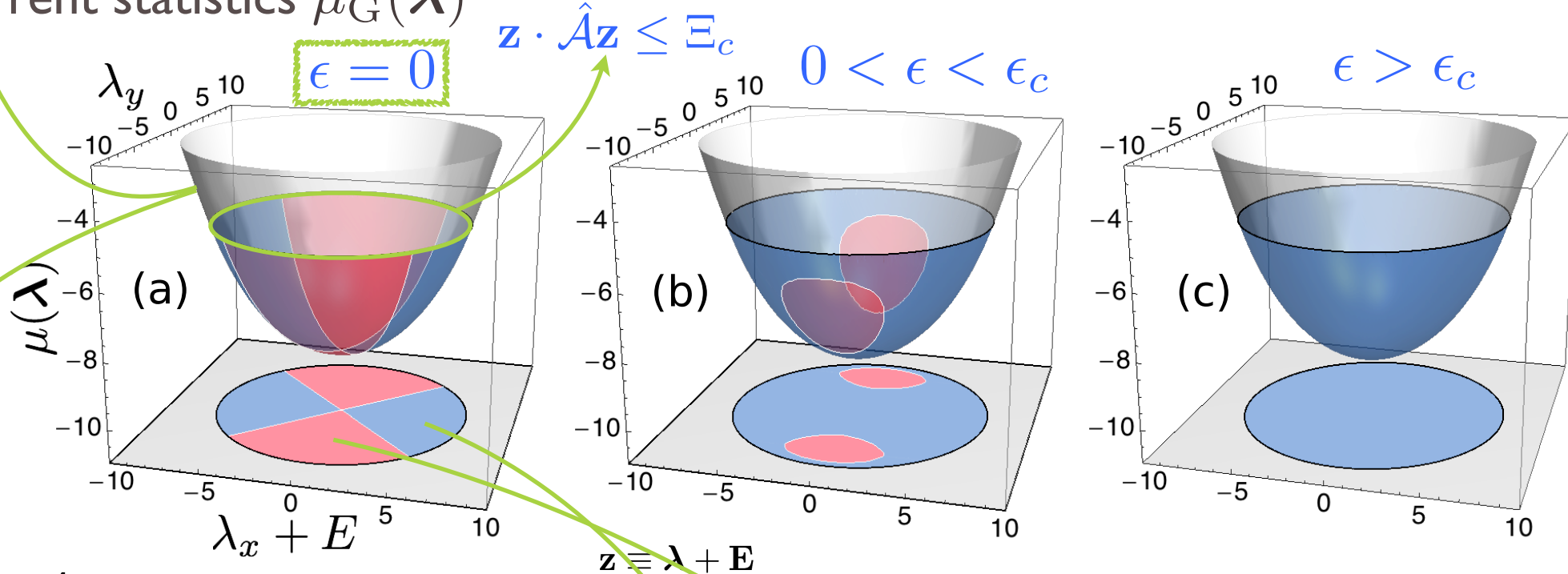
$\omega_{\mathbf{J}}(y - vt)$   
Traveling wave in  $y$ , jam in  $x$   
Broken spacetime symmetry

# A RICH PHASE DIAGRAM (2D WASEP)

$$\mathbf{J} \cdot \hat{\mathbf{A}}^{-1} \mathbf{J} \leq \sigma_0^2 \Xi_c$$

$$\hat{\mathbf{A}} = \begin{pmatrix} 1 + \epsilon & 0 \\ 0 & 1 - \epsilon \end{pmatrix}$$

Gaussian current statistics  $\mu_G(\boldsymbol{\lambda})$



Homogeneous, structureless typical trajectories

$\omega_J(y - vt)$   
Traveling wave in  $y$ , jam in  $x$   
Broken spacetime symmetry

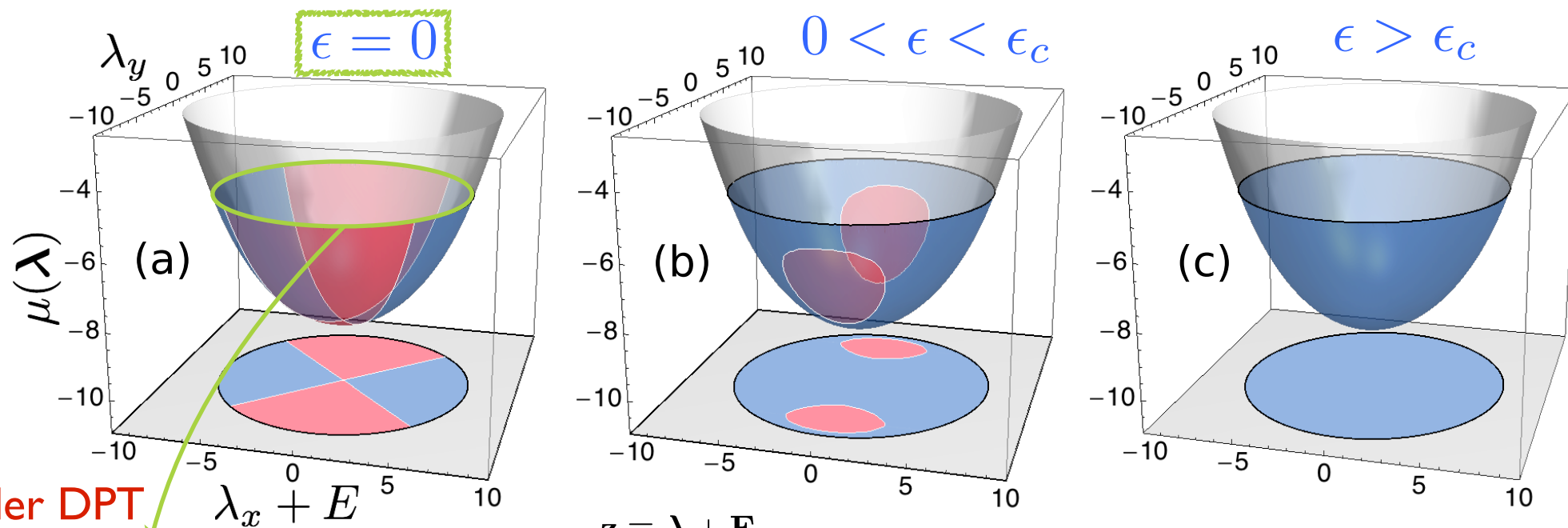
$\omega_J(x - vt)$   
Traveling wave in  $x$ , jam in  $y$   
Broken spacetime symmetry



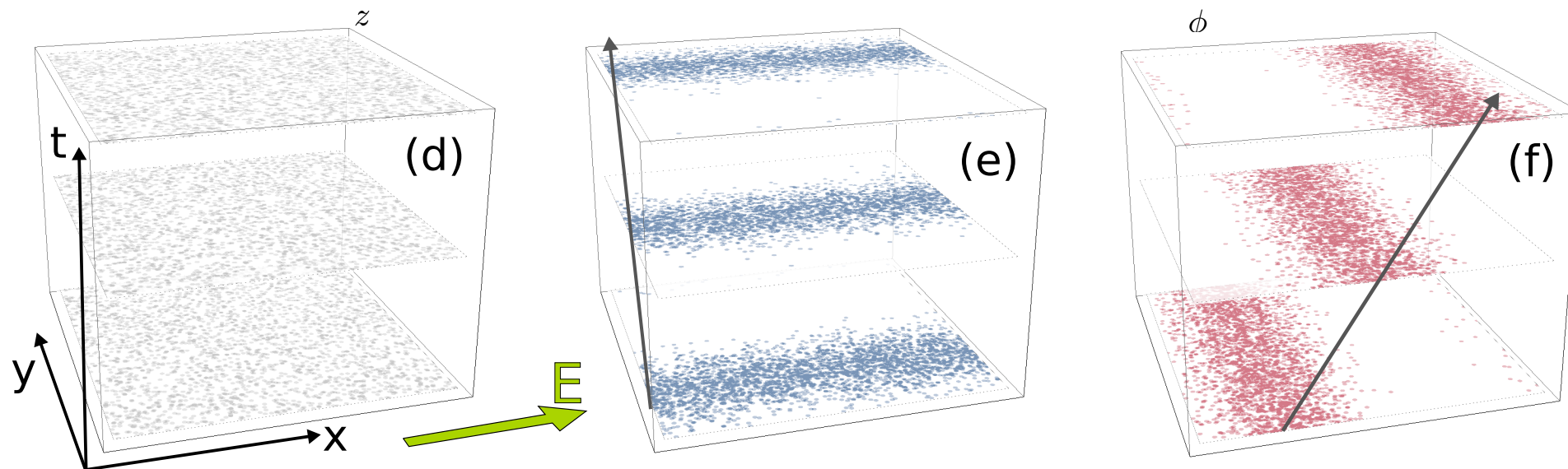
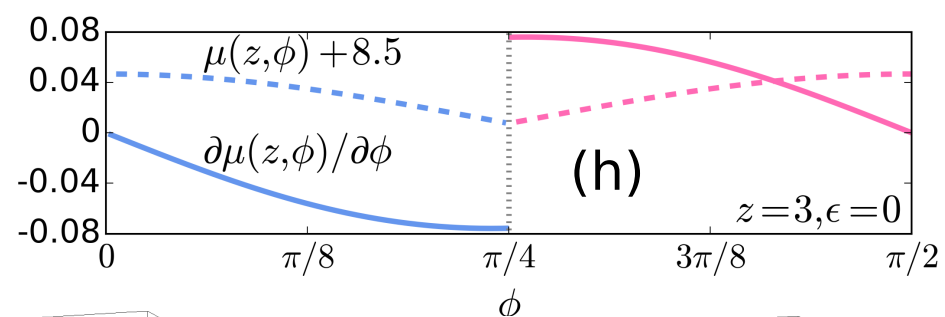
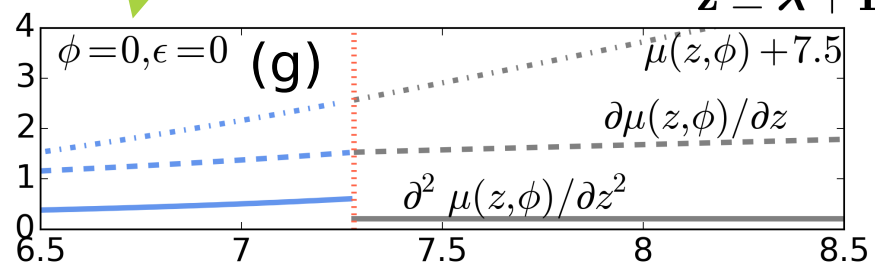
# A RICH PHASE DIAGRAM (2D WASEP)

$$\mathbf{J} \cdot \hat{\mathbf{A}}^{-1} \mathbf{J} \leq \sigma_0^2 \Xi_c$$

$$\hat{\mathbf{A}} = \begin{pmatrix} 1 + \epsilon & 0 \\ 0 & 1 - \epsilon \end{pmatrix}$$



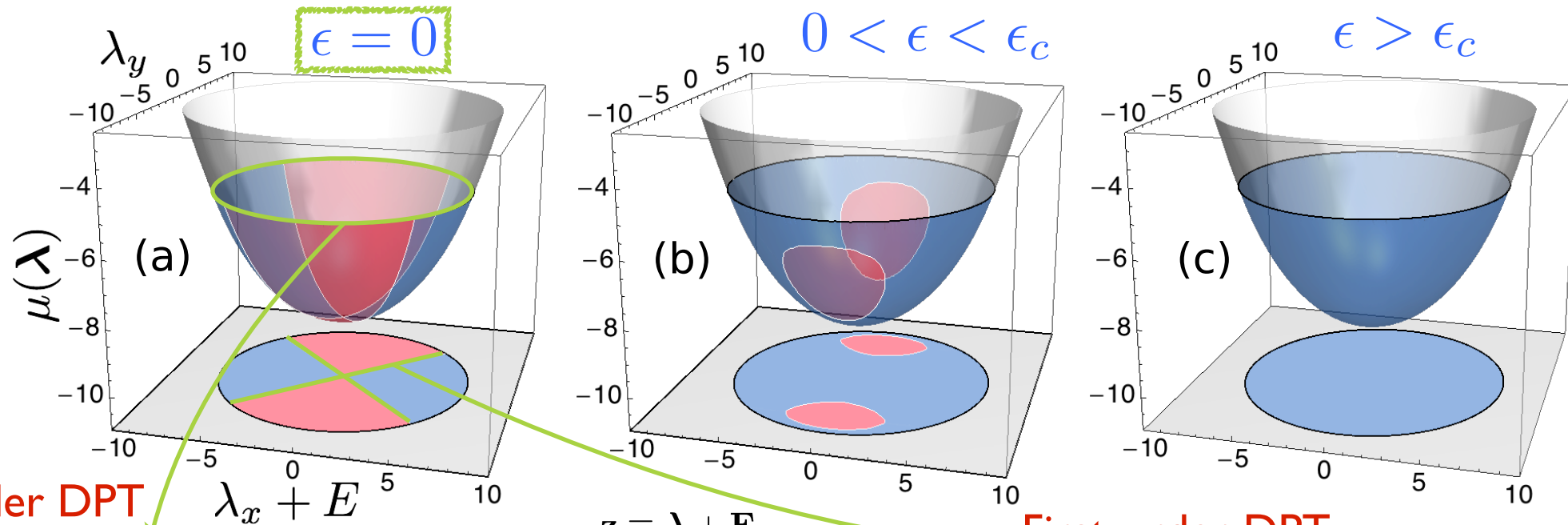
Second-order DPT



# A RICH PHASE DIAGRAM (2D WASEP)

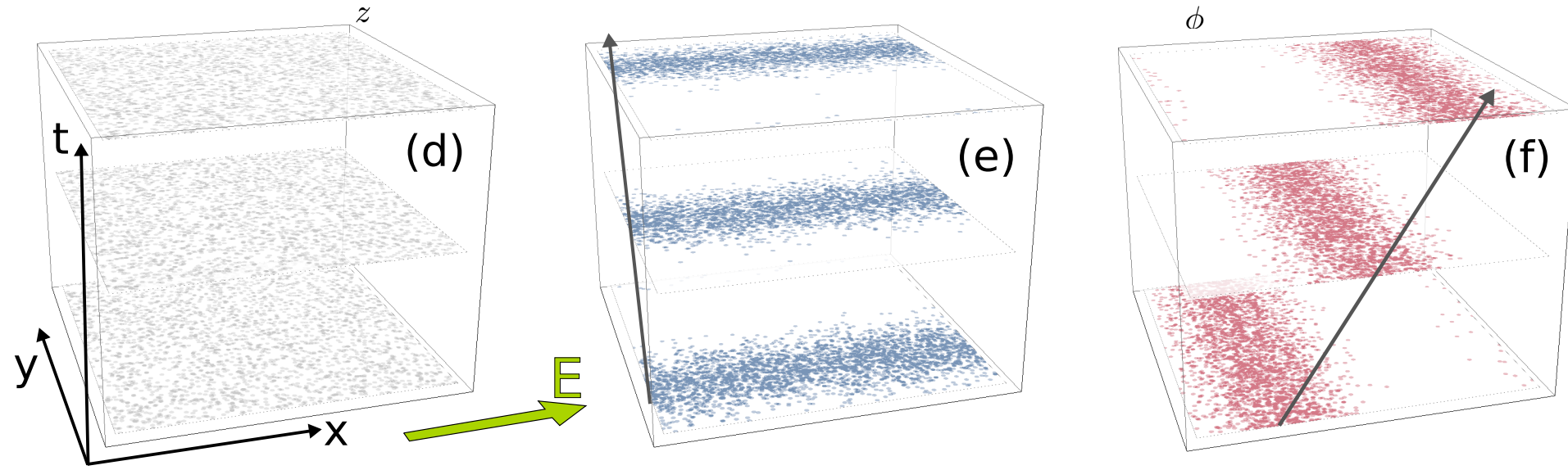
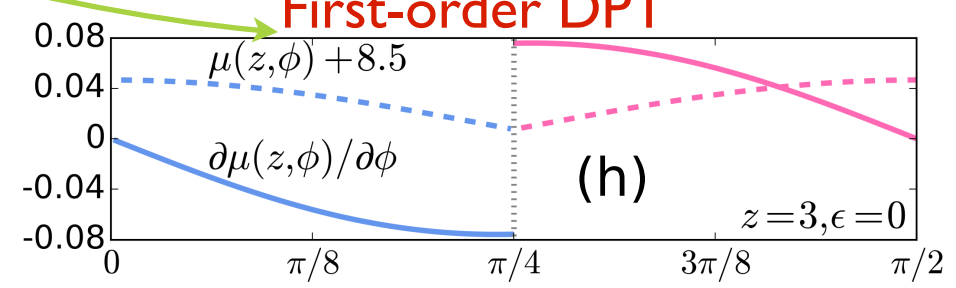
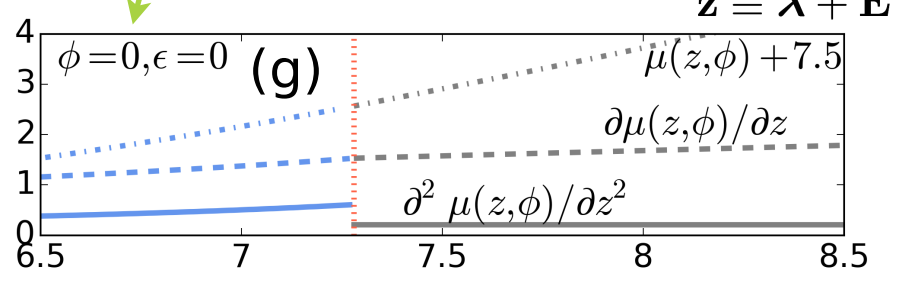
$$\mathbf{J} \cdot \hat{\mathbf{A}}^{-1} \mathbf{J} \leq \sigma_0^2 \Xi_c$$

$$\hat{\mathbf{A}} = \begin{pmatrix} 1 + \epsilon & 0 \\ 0 & 1 - \epsilon \end{pmatrix}$$



Second-order DPT

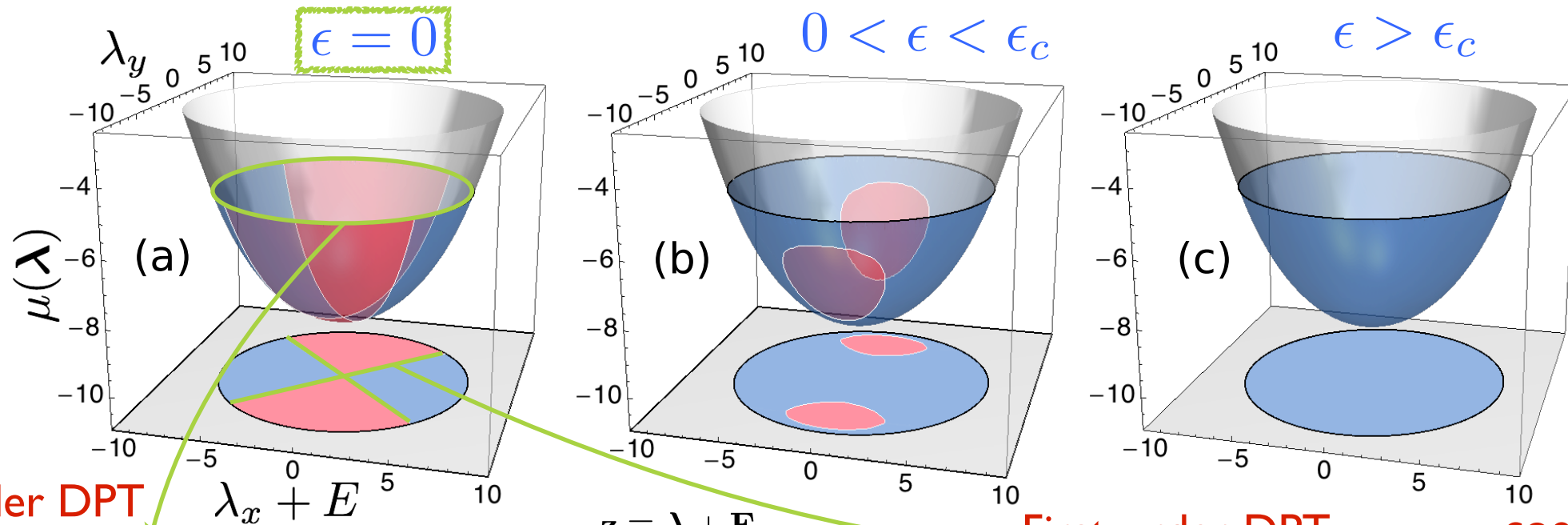
First-order DPT



# A RICH PHASE DIAGRAM (2D WASEP)

$$\mathbf{J} \cdot \hat{\mathbf{A}}^{-1} \mathbf{J} \leq \sigma_0^2 \Xi_c$$

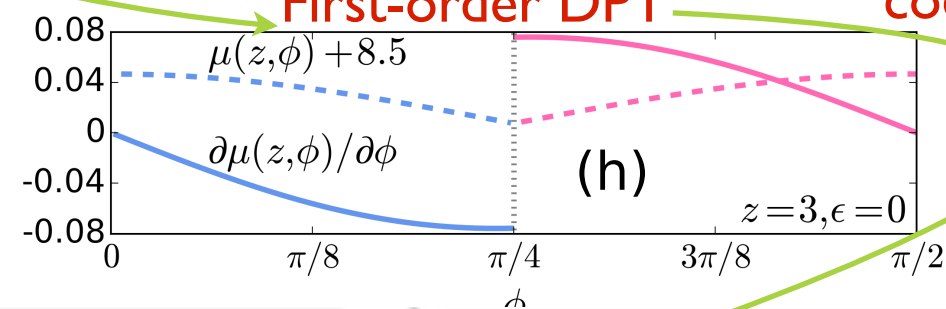
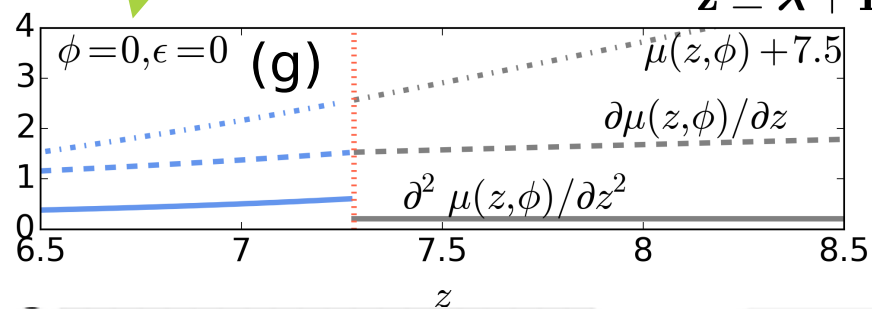
$$\hat{\mathbf{A}} = \begin{pmatrix} 1+\epsilon & 0 \\ 0 & 1-\epsilon \end{pmatrix}$$



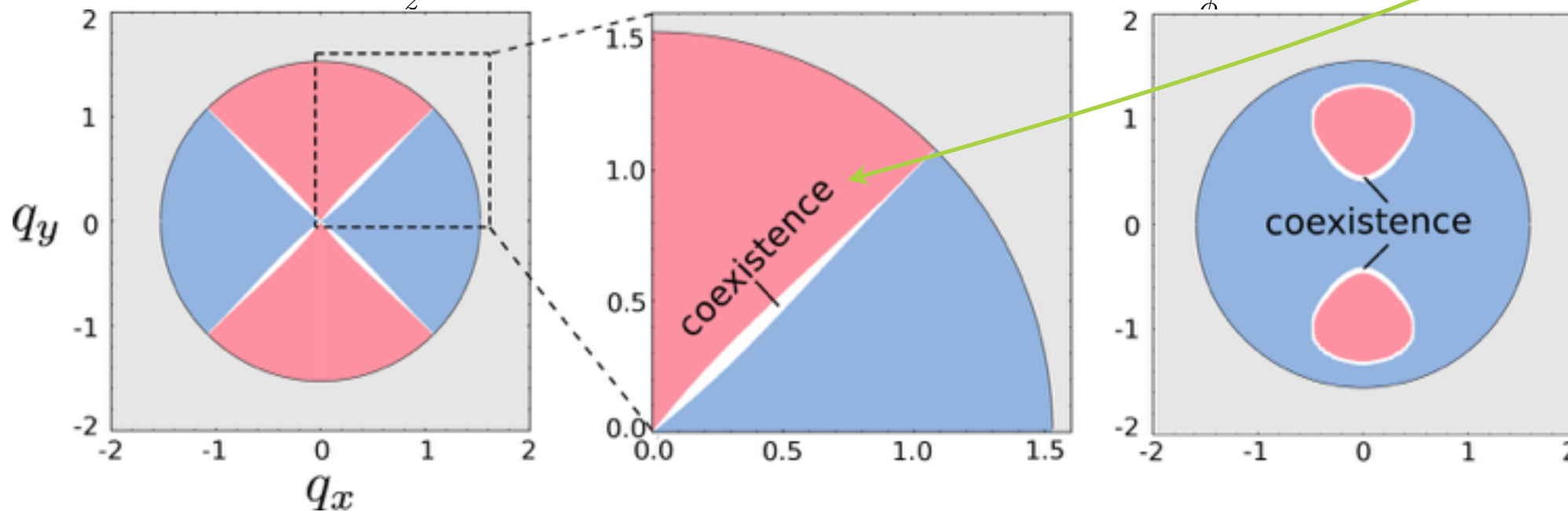
Second-order DPT

First-order DPT

Shows up as coexistence region in q-space



$$\mathbf{q}_\lambda = \nabla \mu(\lambda)$$



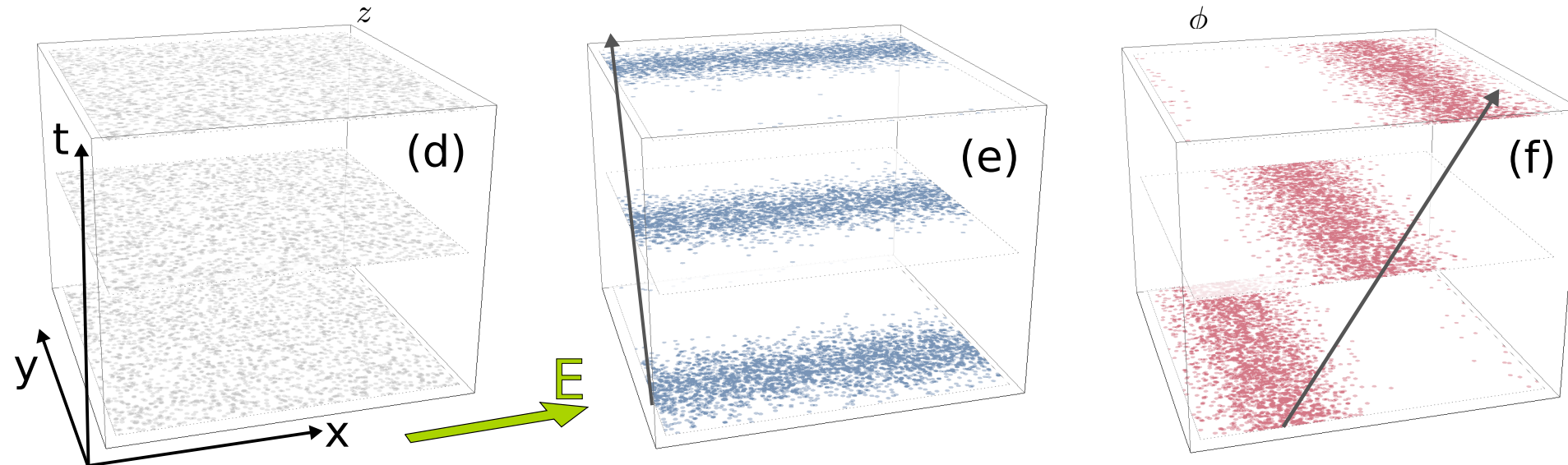
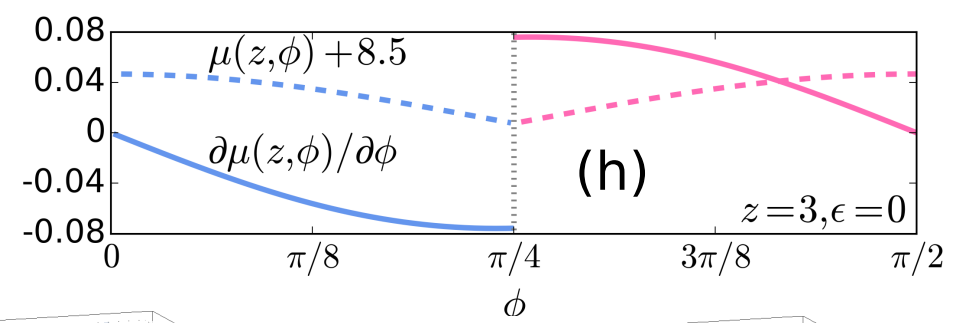
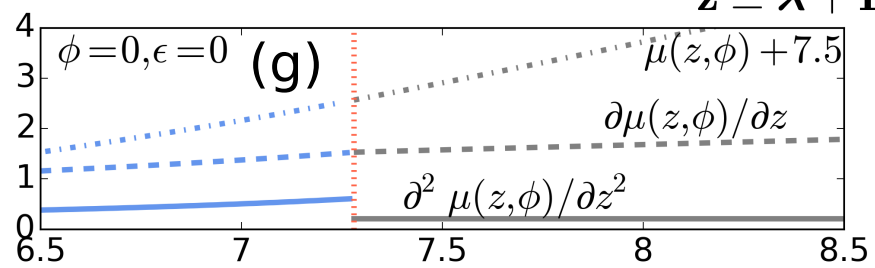
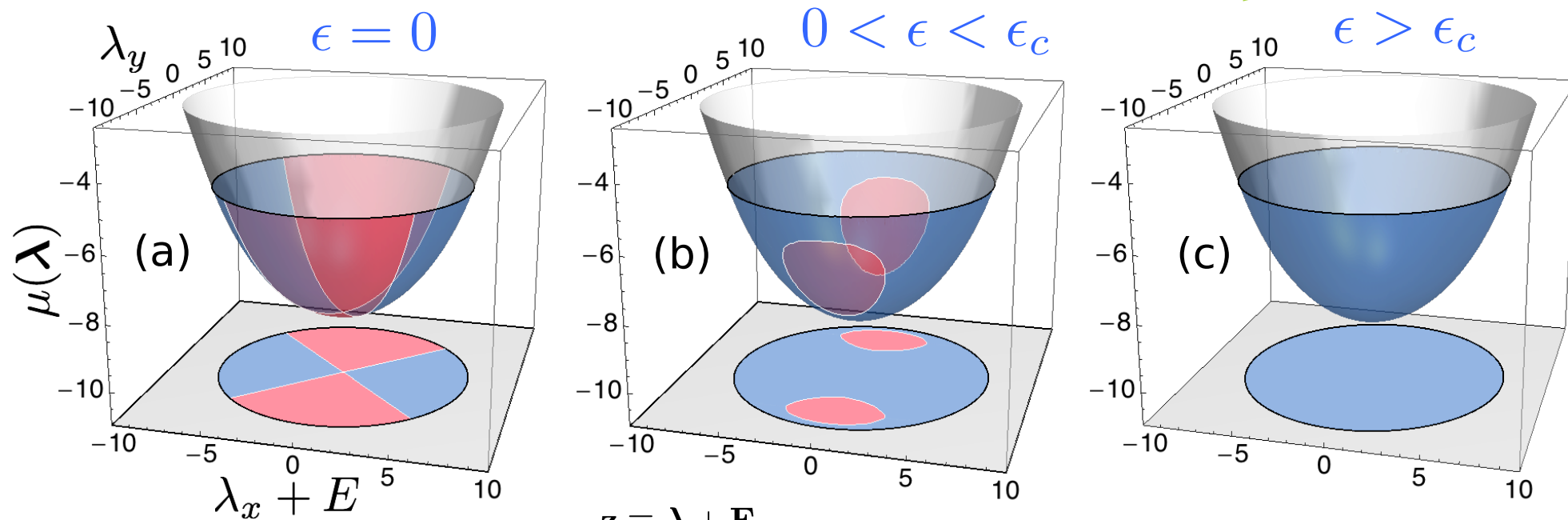


# A RICH PHASE DIAGRAM (2D WASEP)

$$\mathbf{J} \cdot \hat{\mathbf{A}}^{-1} \mathbf{J} \leq \sigma_0^2 \Xi_c$$

$$\hat{\mathbf{A}} = \begin{pmatrix} 1 + \epsilon & 0 \\ 0 & 1 - \epsilon \end{pmatrix}$$

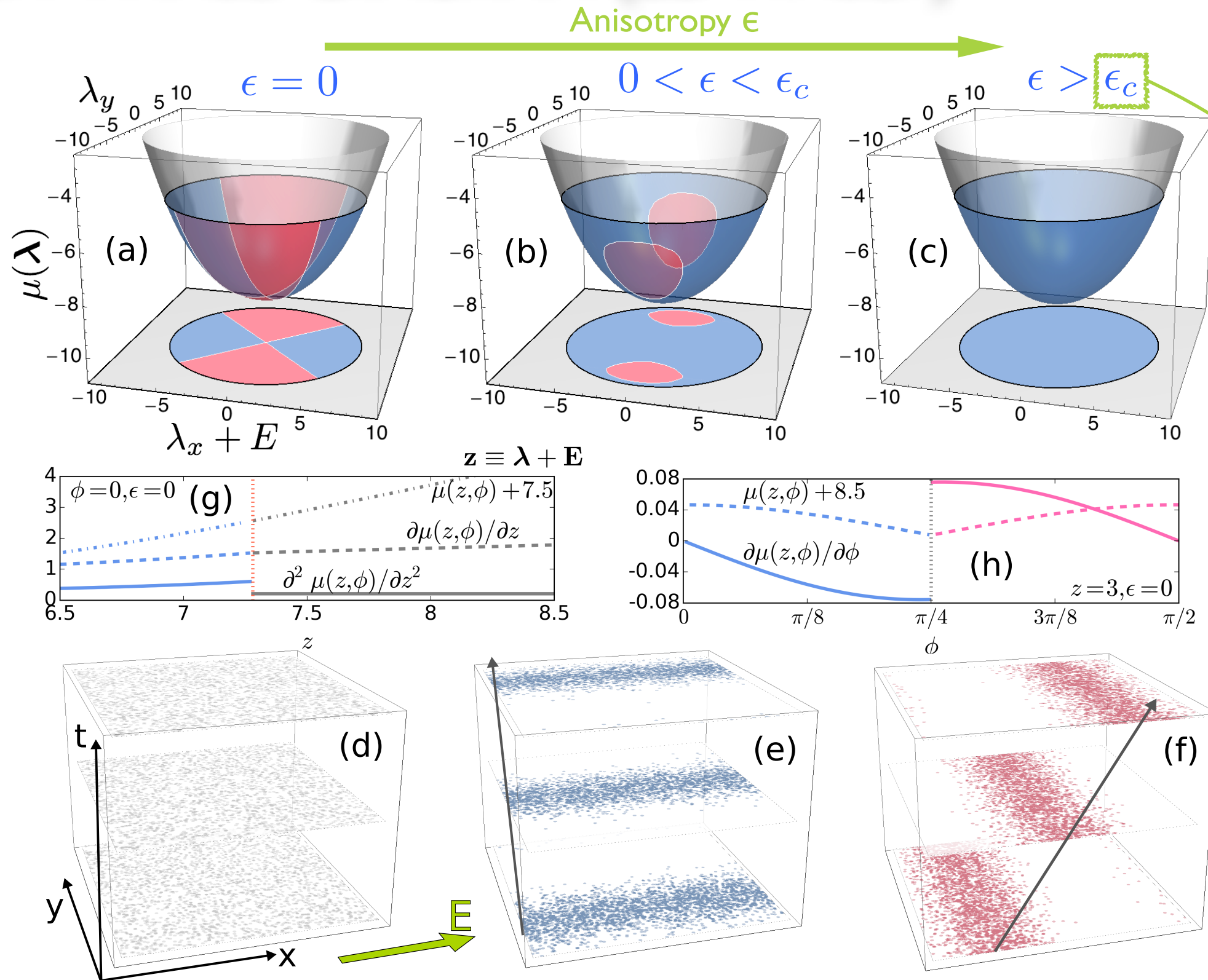
Anisotropy  $\epsilon$



# A RICH PHASE DIAGRAM (2D WASEP)

$$\mathbf{J} \cdot \hat{\mathbf{A}}^{-1} \mathbf{J} \leq \sigma_0^2 \Xi_c$$

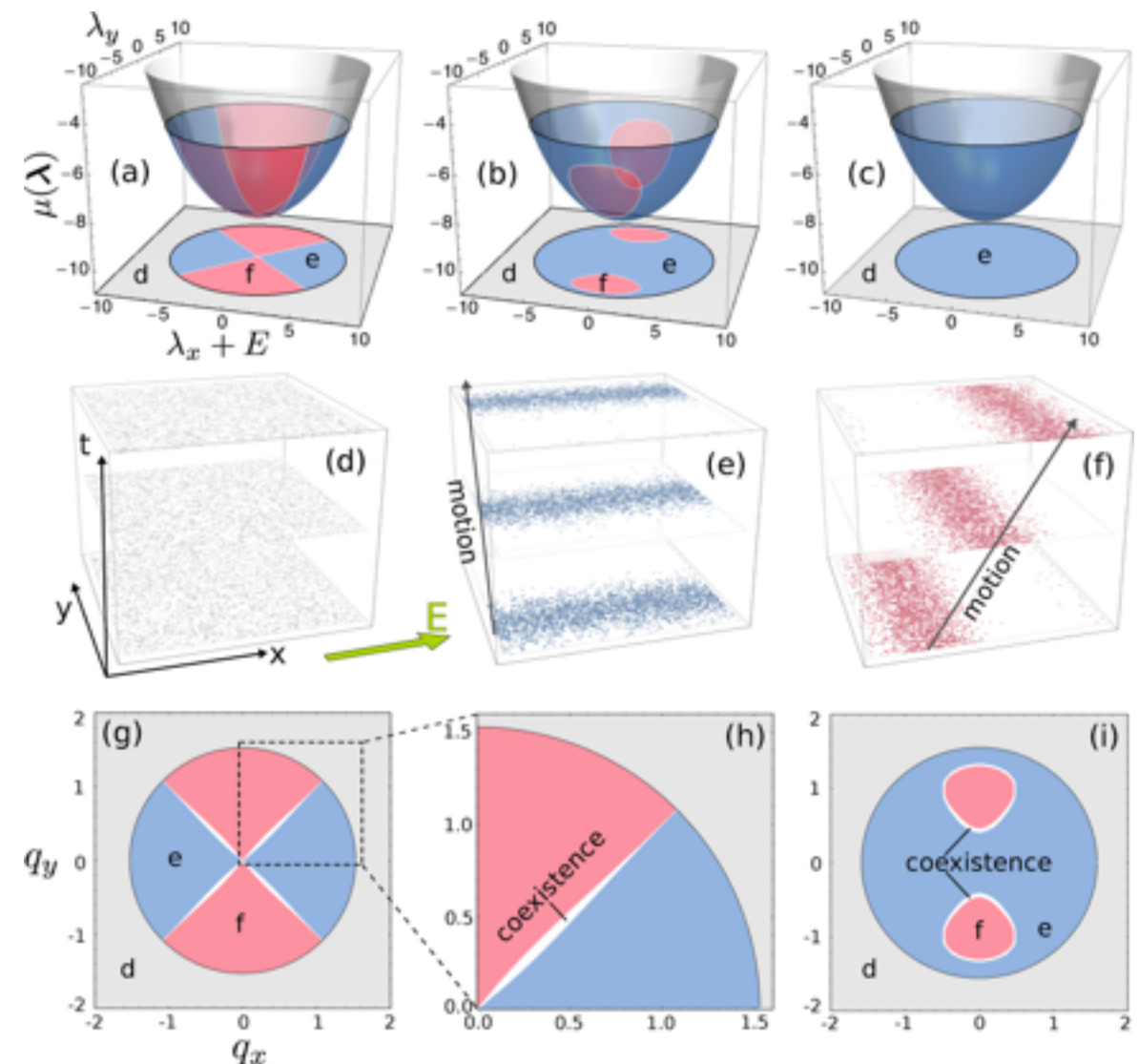
$$\hat{\mathbf{A}} = \begin{pmatrix} 1+\epsilon & 0 \\ 0 & 1-\epsilon \end{pmatrix}$$



There exists a critical anisotropy  $\epsilon_c \approx 0.035$  beyond which only one symmetry-broken phase appears

# KEY INGREDIENTS BEHIND NEW PHYSICS ?

- What are the **key ingredients** responsible of the new physics observed?
- First, by considering **vectorial currents**, it becomes apparent that **current rotations can trigger first-order transitions** between different dynamical phases.
- This is certainly **not present in simpler 1d models and cannot show up when studying fluctuations of scalar observables in  $d > 1$**



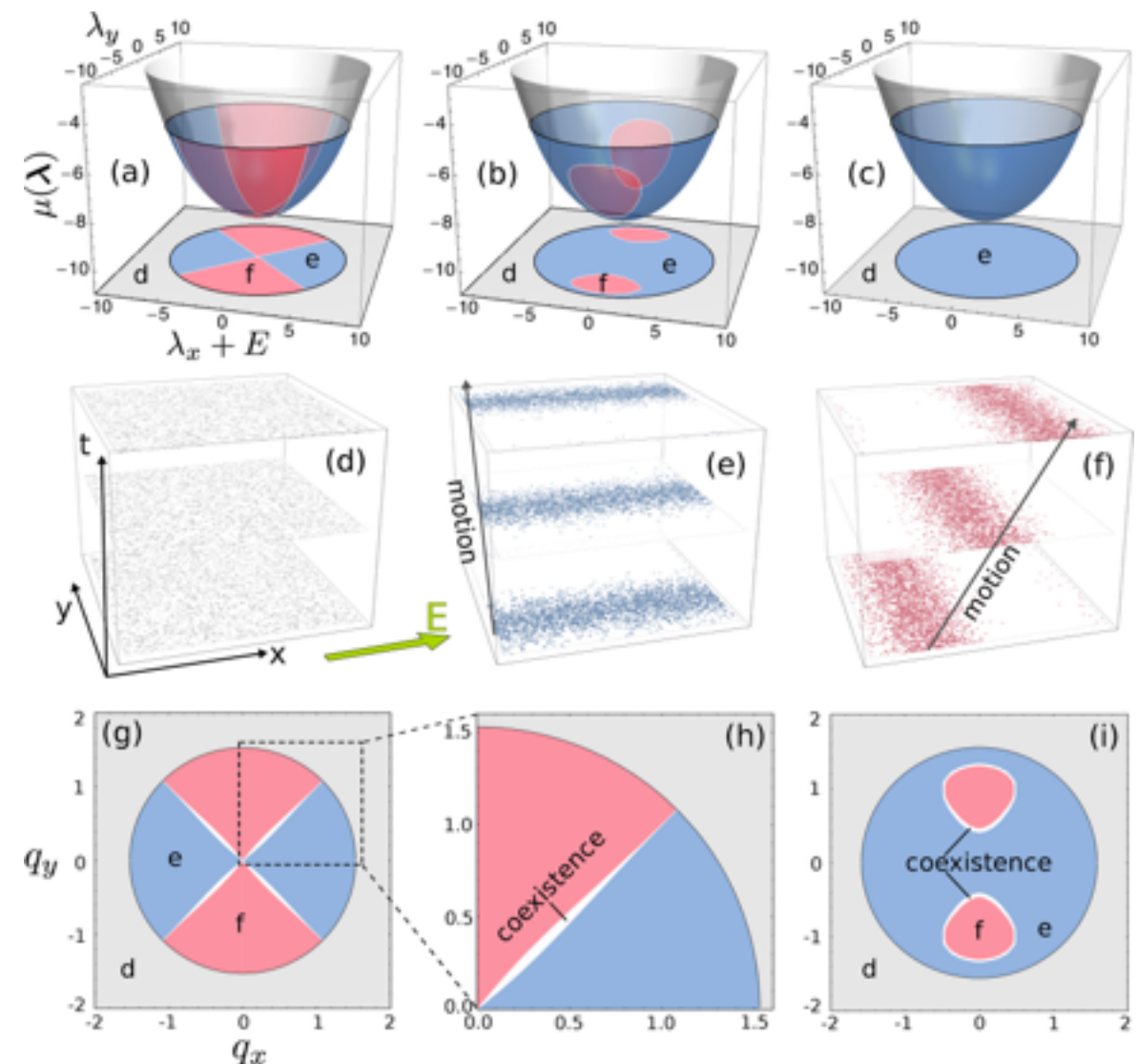


# KEY INGREDIENTS BEHIND NEW PHYSICS ?

- What are the **key ingredients** responsible of the new physics observed?
- First, by considering **vectorial currents**, it becomes apparent that **current rotations can trigger first-order transitions** between different dynamical phases.
- This is certainly **not present in simpler 1d models and cannot show up when studying fluctuations of scalar observables in  $d > 1$**

- Second, by including **anisotropy** it becomes clear its **strong effect on the relative shape and position of the different jammed phases**

- In this way, it is the **interplay between vectorial currents and anisotropy in  $d > 1$**  that gives rise to the rich and complex dynamical phase diagram here described.



# CURRENT STATISTICS FOR 2D WASEP

- Parameters:

$$\rho_0 = 0.3$$

$$N \leq 144$$

$$\mathbf{E} = (10, 0)$$

$$\Downarrow$$
$$\mathbf{E} \cdot \hat{\mathcal{A}}\mathbf{E} \geq |\Sigma_c|$$

# CURRENT STATISTICS FOR 2D WASEP

$$\mathbf{z} \equiv \lambda + \mathbf{E}$$

$$z = |\mathbf{z}|$$

$$\phi = \tan^{-1}(z_y/z_x)$$

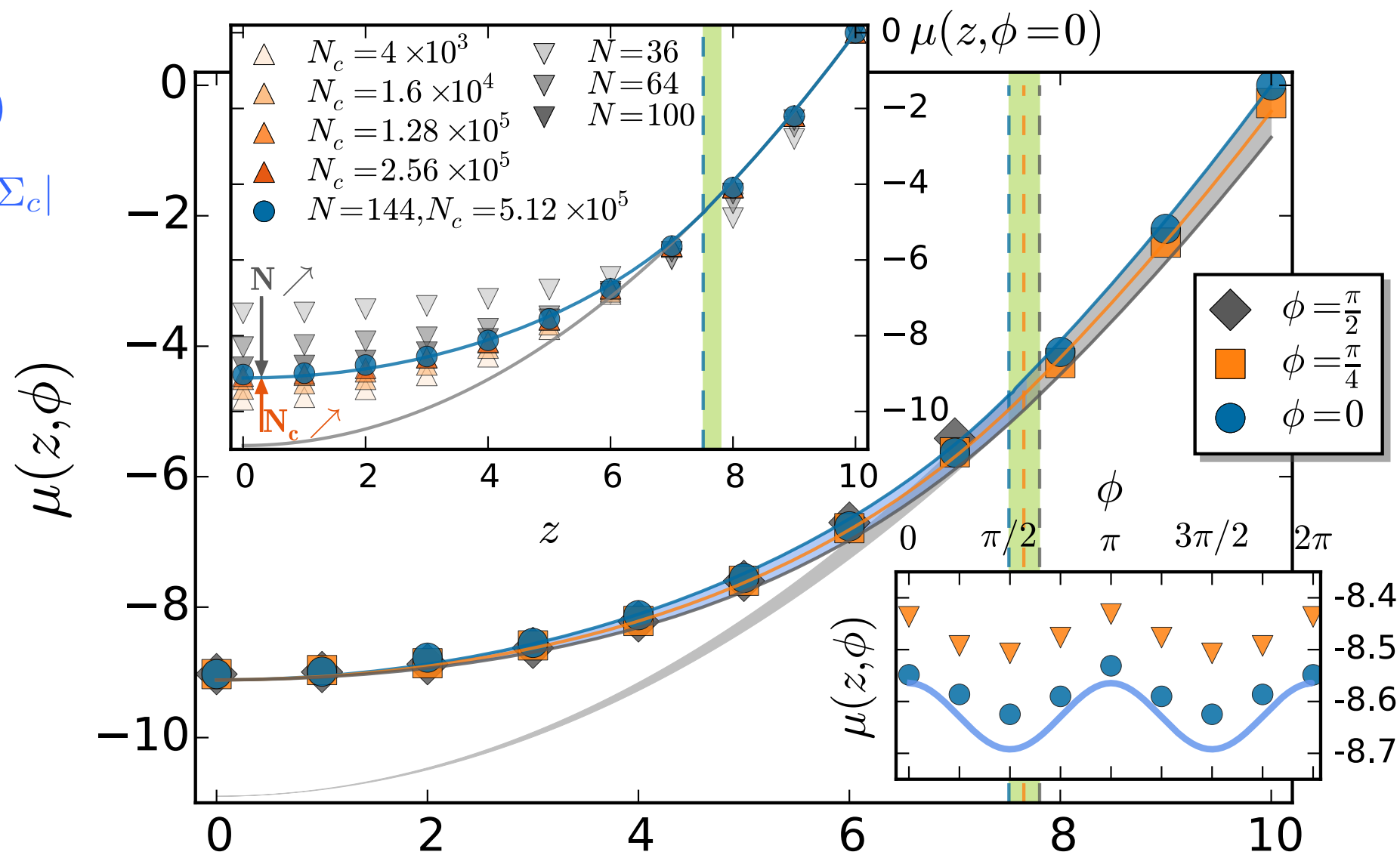
● Parameters:

$$\rho_0 = 0.3$$

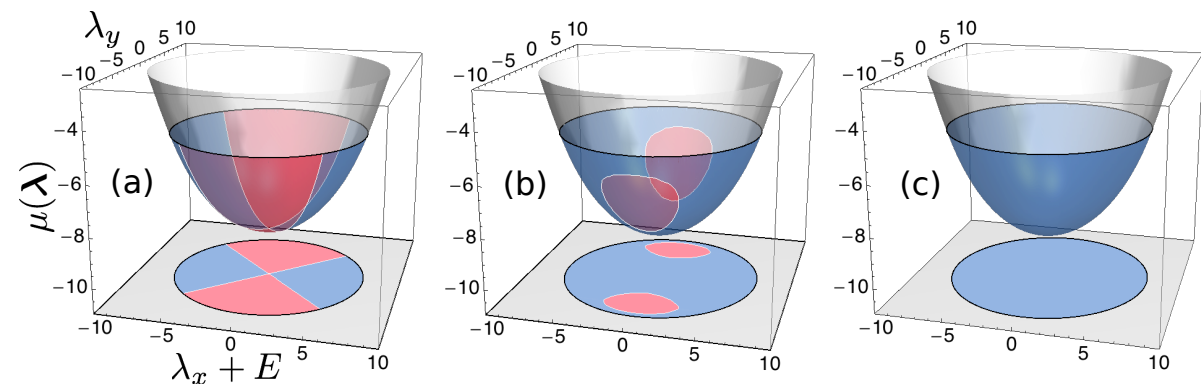
$$N \leq 144$$

$$\mathbf{E} = (10, 0)$$

$$\mathbf{E} \cdot \hat{\mathbf{A}}\mathbf{E} \geq |\Sigma_c|$$



$z$



# CURRENT STATISTICS FOR 2D WASEP

$$\mathbf{z} \equiv \lambda + \mathbf{E}$$

$$z = |\mathbf{z}|$$

$$\phi = \tan^{-1}(z_y/z_x)$$

Parameters:

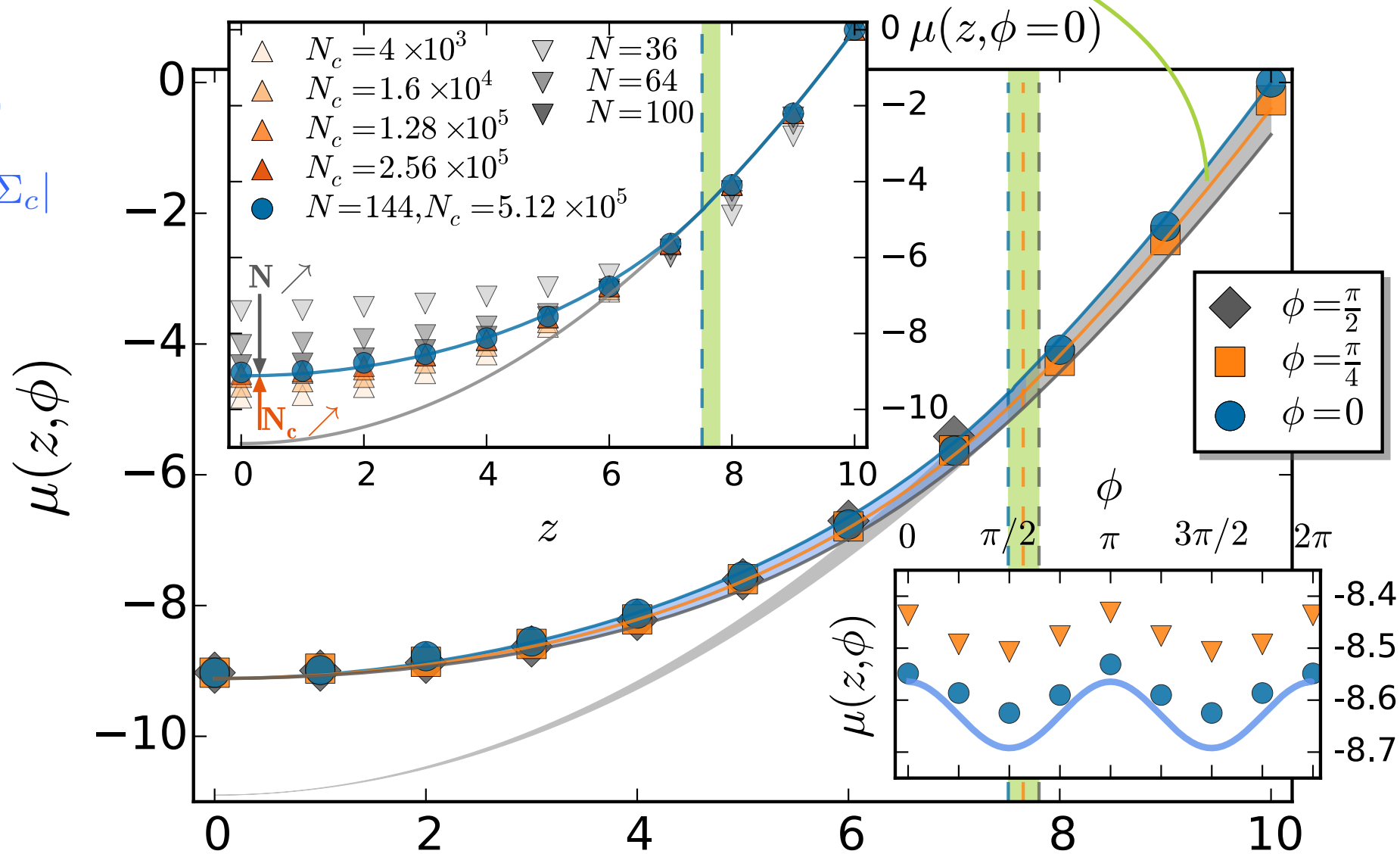
$$\rho_0 = 0.3$$

$$N \leq 144$$

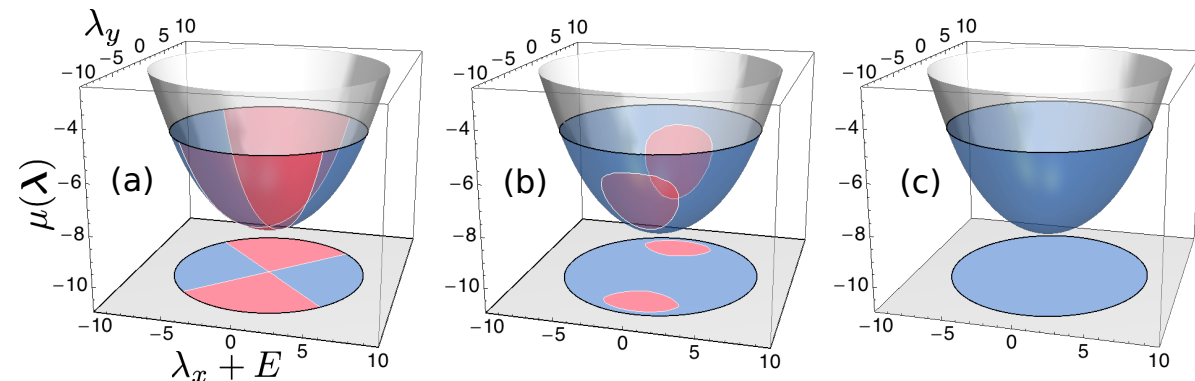
$$\mathbf{E} = (10, 0)$$

$$\mathbf{E} \cdot \hat{\mathbf{A}}\mathbf{E} \geq |\Sigma_c|$$

**Gaussian current statistics**  $\mu_G(\lambda)$   
for mild current fluctuations



$z$



# CURRENT STATISTICS FOR 2D WASEP

$$\mathbf{z} \equiv \boldsymbol{\lambda} + \mathbf{E}$$

$$z = |\mathbf{z}|$$

$$\phi = \tan^{-1}(z_y/z_x)$$

Parameters:

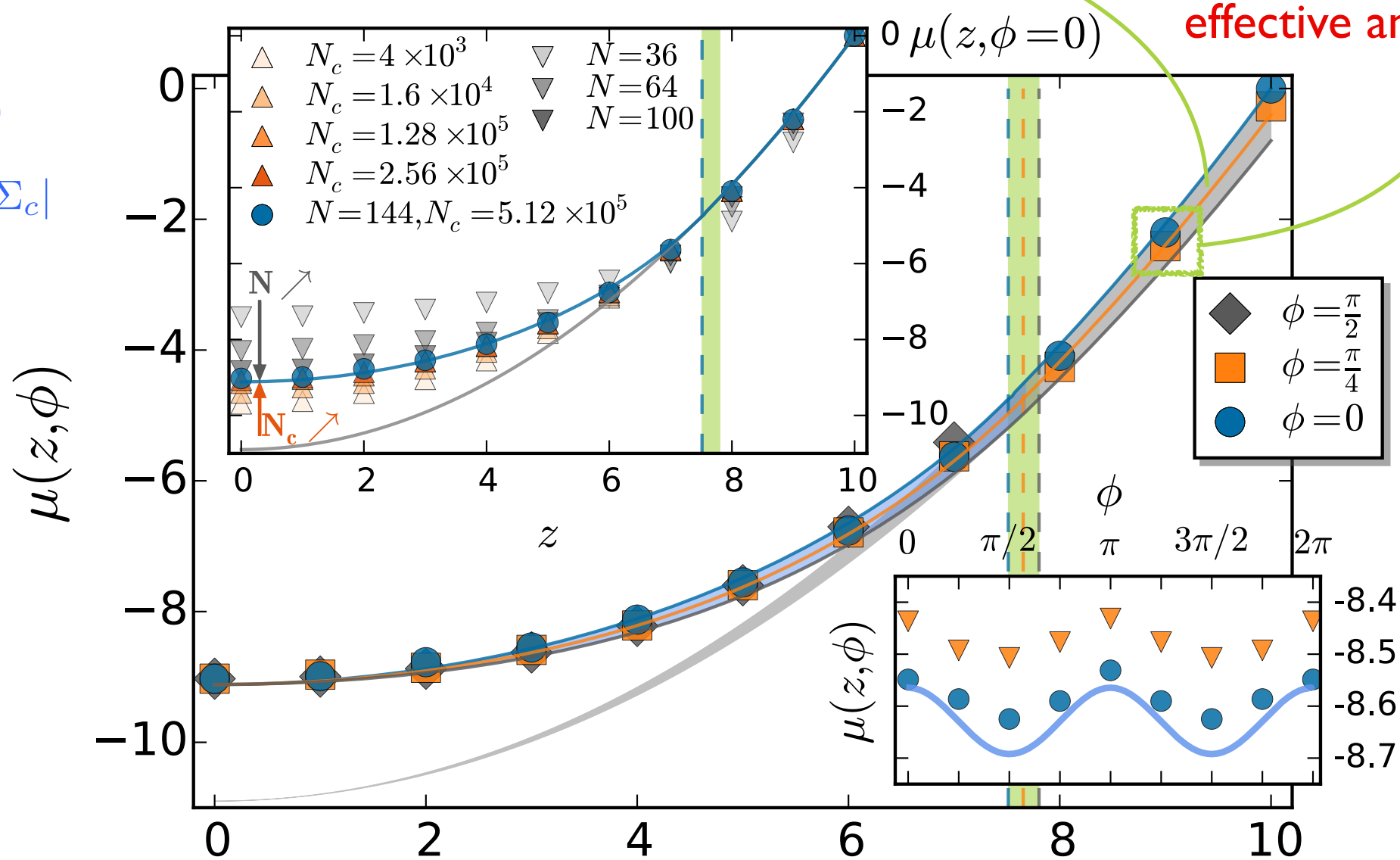
$$\rho_0 = 0.3$$

$$N \leq 144$$

$$\mathbf{E} = (10, 0)$$

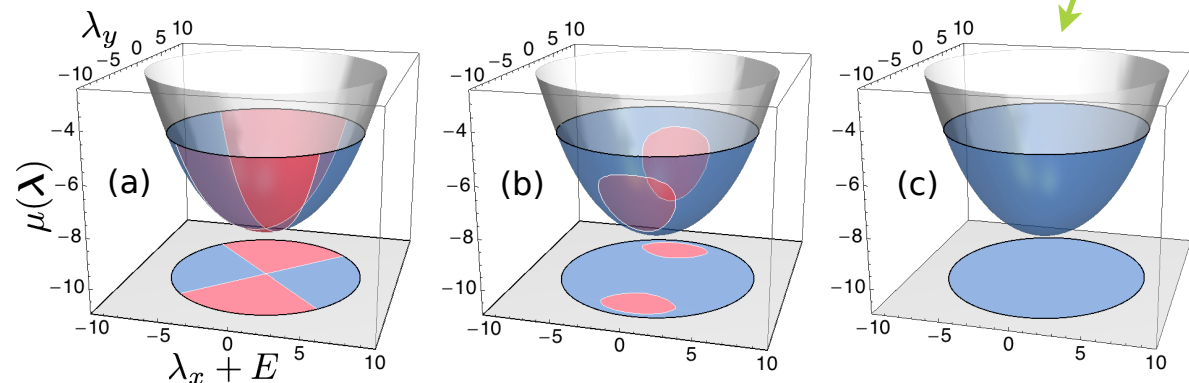
$$\mathbf{E} \cdot \hat{\mathbf{A}}\mathbf{E} \geq |\Sigma_c|$$

**Gaussian current statistics**  $\mu_G(\boldsymbol{\lambda})$   
for mild current fluctuations



$\phi$ -dependence of  $\mu(\mathbf{z}) \Rightarrow$   
**effective anisotropy  $\epsilon > \epsilon_c$**

$z$



# CURRENT STATISTICS FOR 2D WASEP

$$\mathbf{z} \equiv \boldsymbol{\lambda} + \mathbf{E}$$

$$z = |\mathbf{z}|$$

$$\phi = \tan^{-1}(z_y/z_x)$$

Parameters:

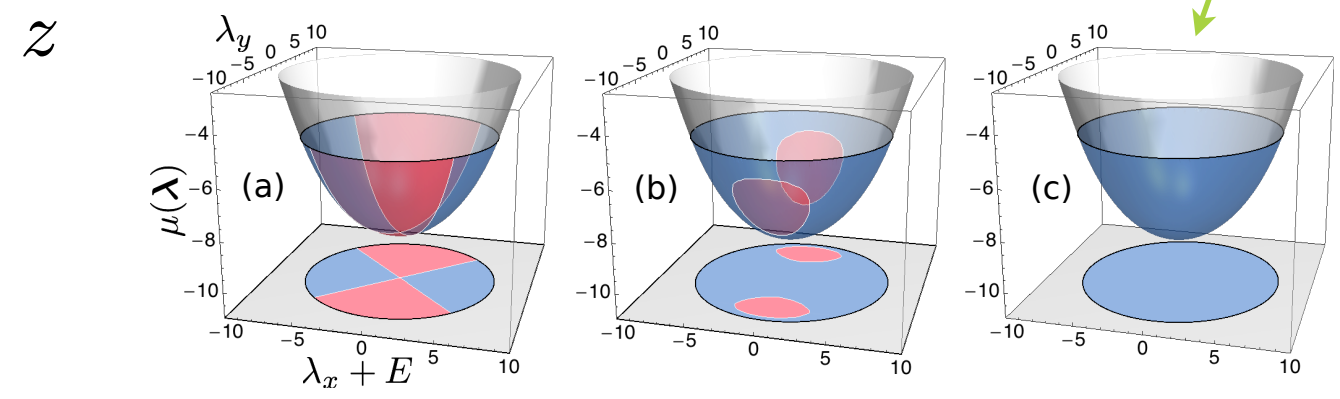
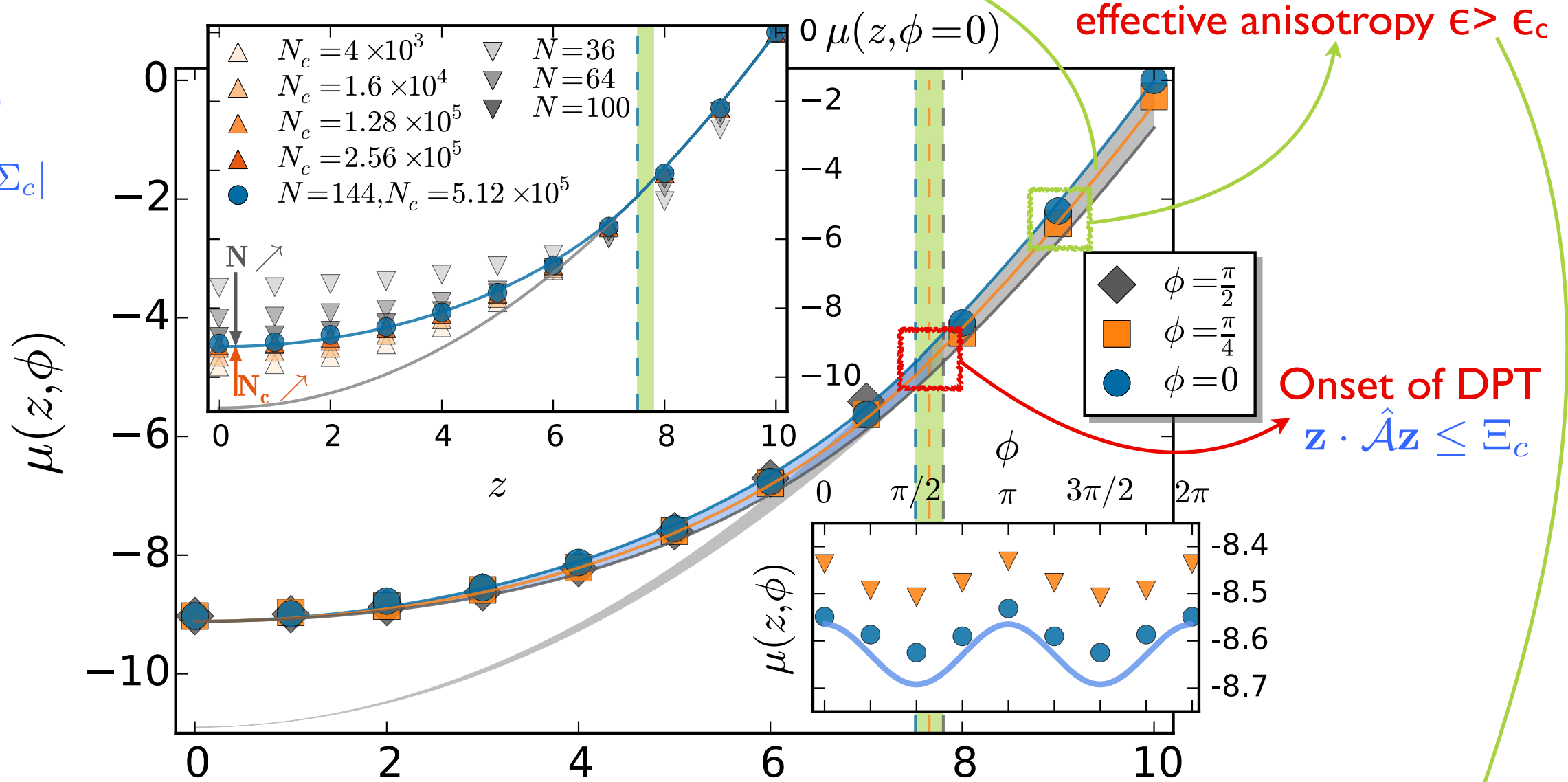
$$\rho_0 = 0.3$$

$$N \leq 144$$

$$\mathbf{E} = (10, 0)$$

$$\mathbf{E} \cdot \hat{\mathbf{A}}\mathbf{E} \geq |\Sigma_c|$$

Gaussian current statistics  $\mu_G(\boldsymbol{\lambda})$   
for mild current fluctuations





# CURRENT STATISTICS FOR 2D WASEP

$$\mathbf{z} \equiv \boldsymbol{\lambda} + \mathbf{E}$$

$$z = |\mathbf{z}|$$

$$\phi = \tan^{-1}(z_y/z_x)$$

Parameters:

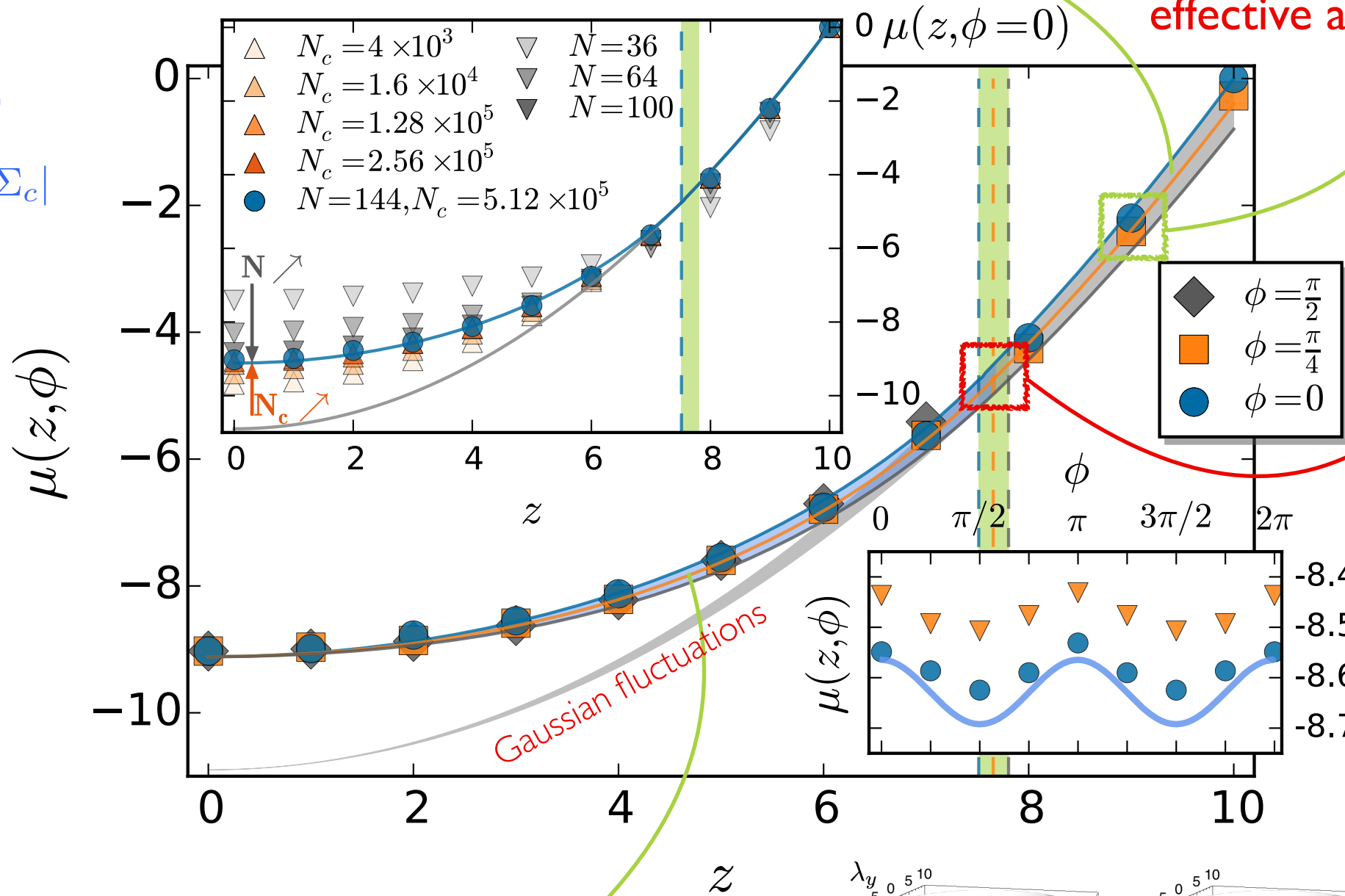
$$\rho_0 = 0.3$$

$$N \leq 144$$

$$\mathbf{E} = (10, 0)$$

$$\mathbf{E} \cdot \hat{\mathbf{A}}\mathbf{E} \geq |\Sigma_c|$$

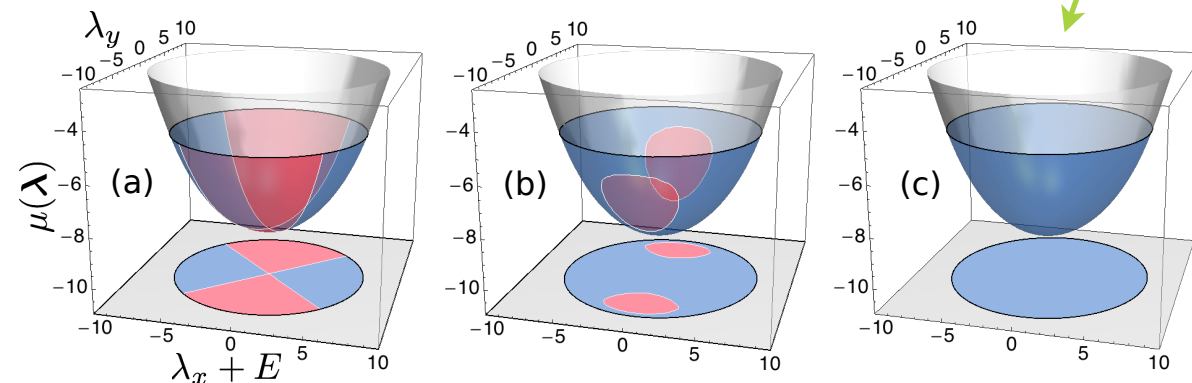
**Gaussian current statistics**  $\mu_G(\boldsymbol{\lambda})$   
for mild current fluctuations



$\phi$ -dependence of  $\mu(\mathbf{z}) \Rightarrow$   
**effective anisotropy**  $\epsilon > \epsilon_c$

**Onset of DPT**  
 $\mathbf{z} \cdot \hat{\mathbf{A}}\mathbf{z} \leq \Xi_c$

**Non-Gaussian current fluctuations**



# CURRENT STATISTICS FOR 2D WASEP

$$\mathbf{z} \equiv \lambda + \mathbf{E}$$

$$z = |\mathbf{z}|$$

$$\phi = \tan^{-1}(z_y/z_x)$$

Parameters:

$$\rho_0 = 0.3$$

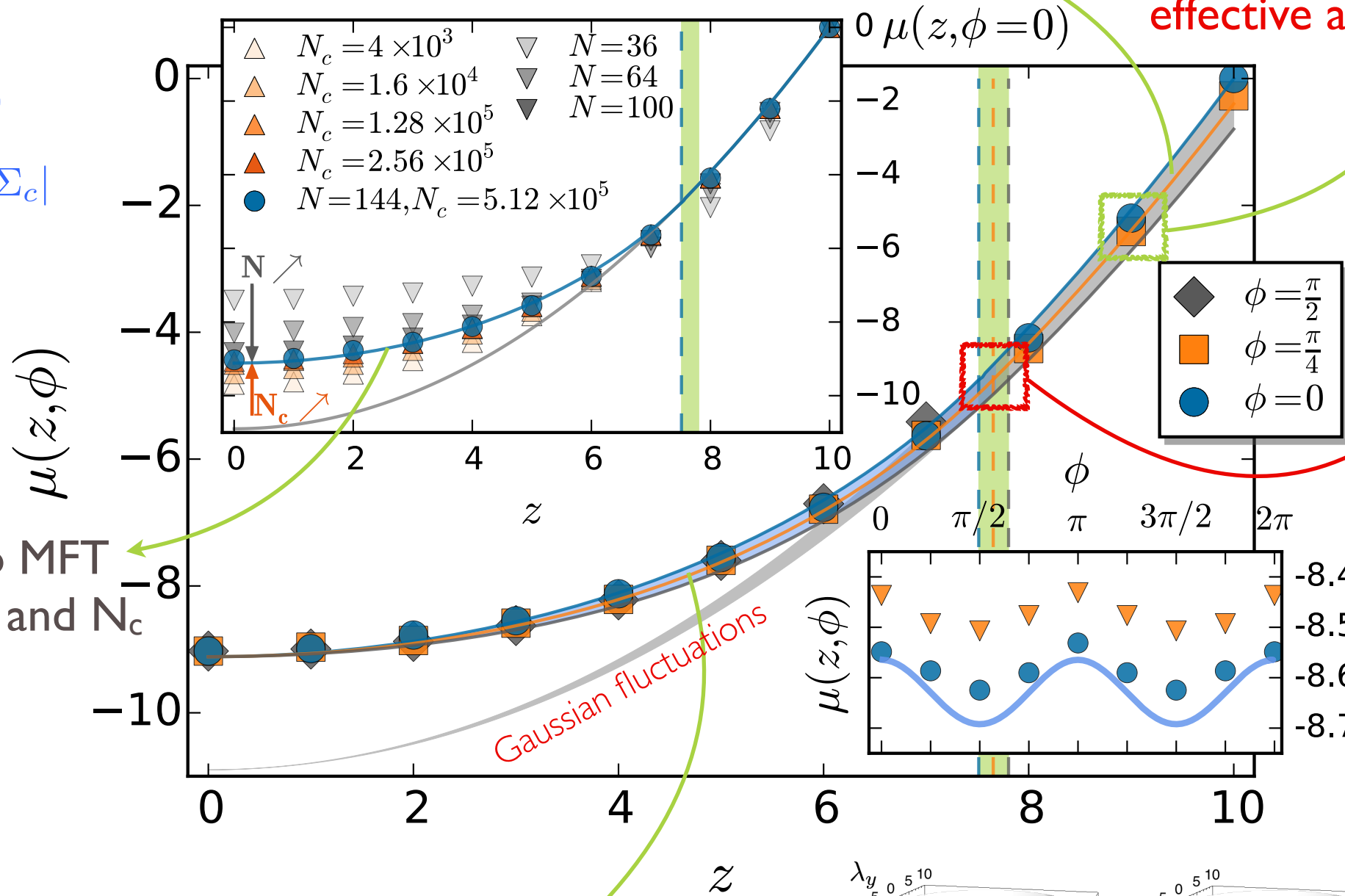
$$N \leq 144$$

$$\mathbf{E} = (10, 0)$$

$$\mathbf{E} \cdot \hat{\mathbf{A}}\mathbf{E} \geq |\Sigma_c|$$

Gaussian current statistics  $\mu_G(\lambda)$   
for mild current fluctuations

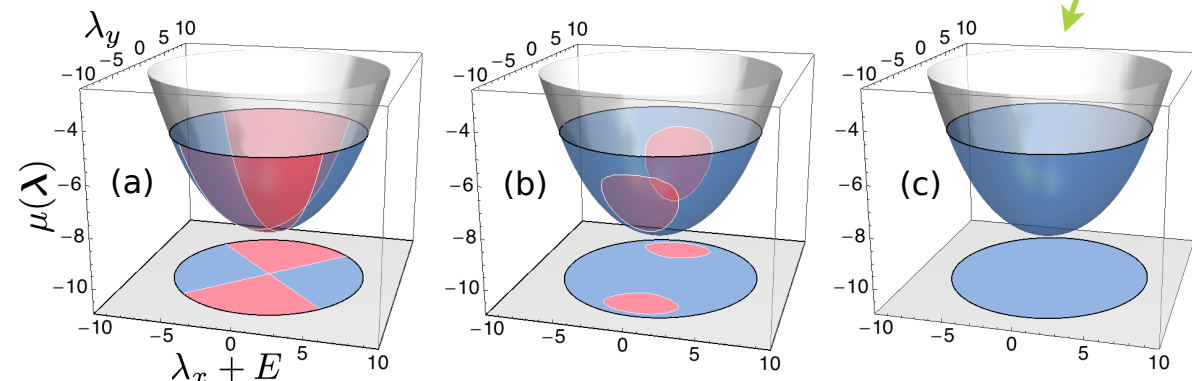
$\phi$ -dependence of  $\mu(\mathbf{z}) \Rightarrow$   
effective anisotropy  $\epsilon > \epsilon_c$



Onset of DPT  
 $\mathbf{z} \cdot \hat{\mathbf{A}}\mathbf{z} \leq \Xi_c$

Convergence to MFT prediction as  $N$  and  $N_c$  increase

Non-Gaussian current fluctuations



# CURRENT STATISTICS FOR 2D WASEP

$$\mathbf{z} \equiv \boldsymbol{\lambda} + \mathbf{E}$$

$$z = |\mathbf{z}|$$

$$\phi = \tan^{-1}(z_y/z_x)$$

Parameters:

$$\rho_0 = 0.3$$

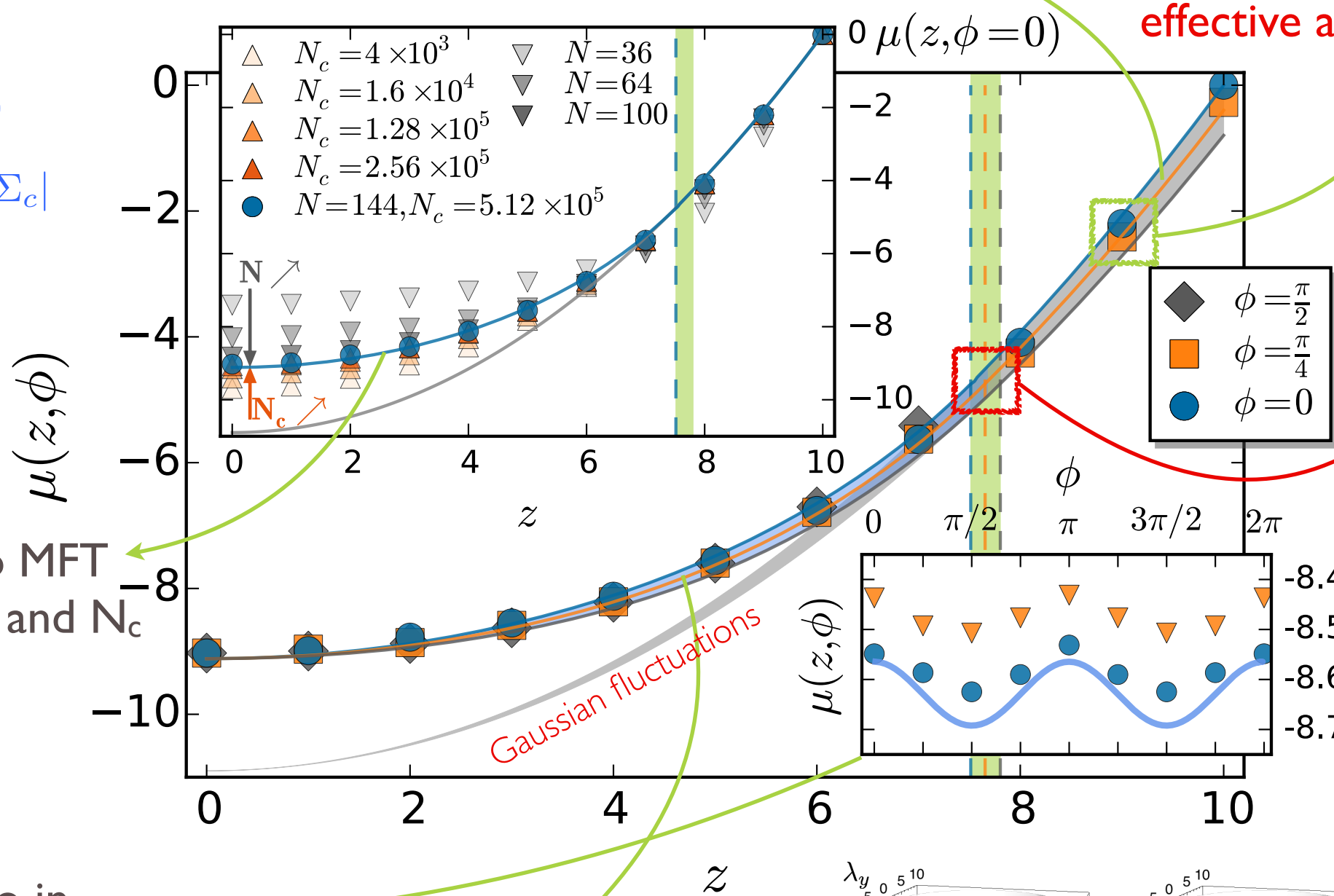
$$N \leq 144$$

$$\mathbf{E} = (10, 0)$$

$$\mathbf{E} \cdot \hat{\mathbf{A}}\mathbf{E} \geq |\Sigma_c|$$

**Gaussian current statistics**  $\mu_G(\boldsymbol{\lambda})$   
for mild current fluctuations

$\phi$ -dependence of  $\mu(\mathbf{z}) \Rightarrow$   
**effective anisotropy**  $\epsilon > \epsilon_c$

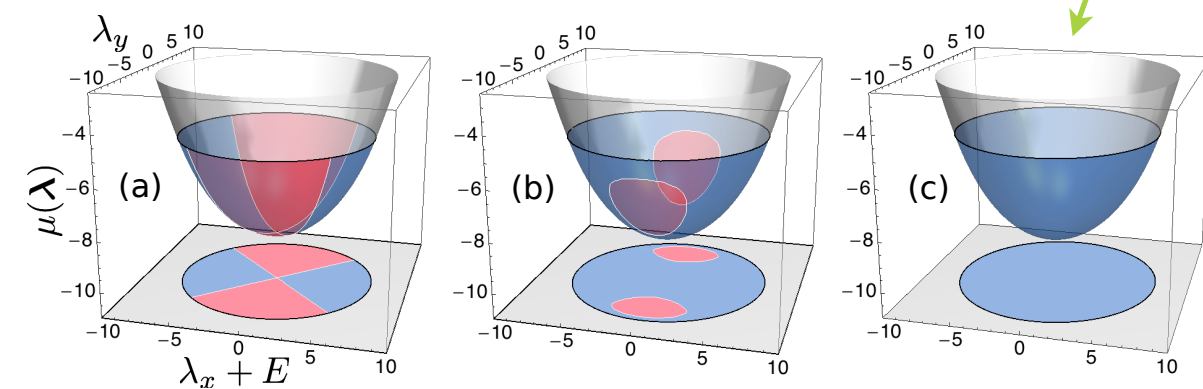


**Onset of DPT**  
 $\mathbf{z} \cdot \hat{\mathbf{A}}\mathbf{z} \leq \Xi_c$

**Convergence to MFT**  
prediction as  $N$  and  $N_c$   
increase

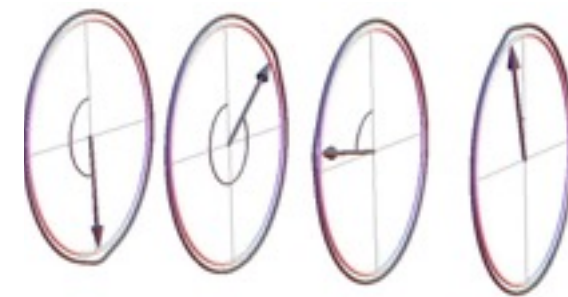
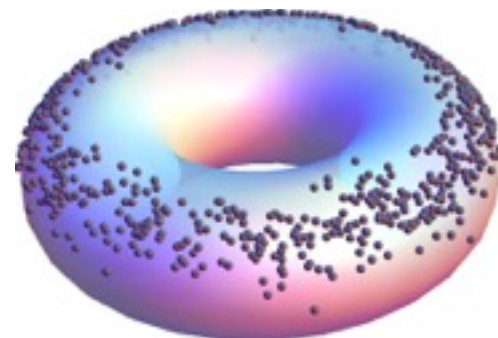
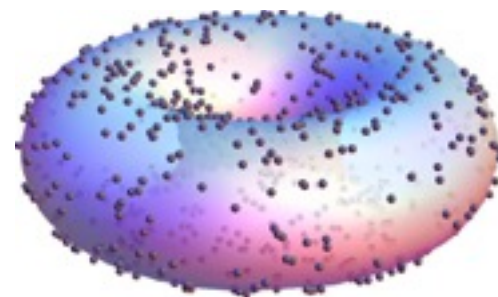
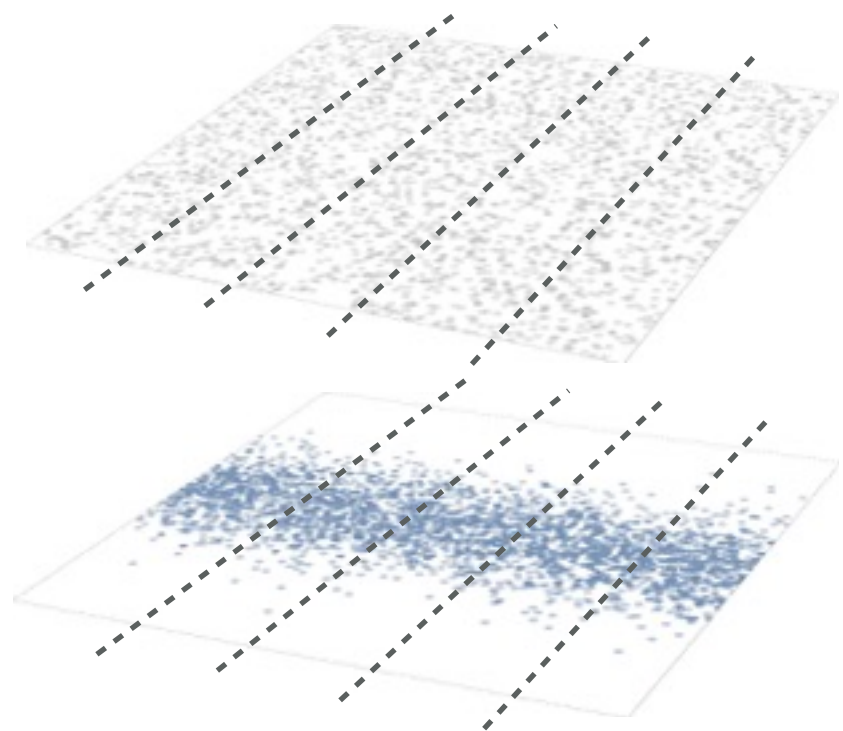
Agreement also in  
**fine angular structure**

**Non-Gaussian current**  
**fluctuations**



# ORDER PARAMETER: TOMOGRAPHIC COHERENCES

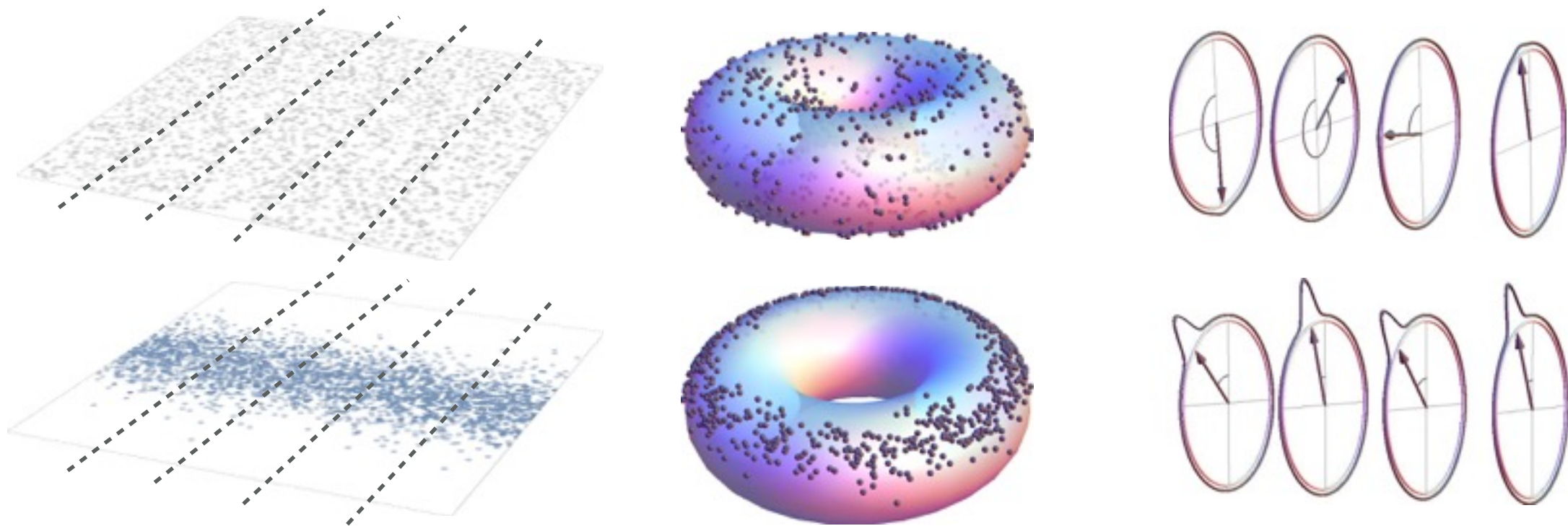
- MFT: **1d density waves** in symmetry-broken phase  $\Rightarrow$  jam particle flow
- **Tomographic analysis**: slice system along  $\alpha$ -direction  $\Rightarrow$  **j-slice is a ring in 2d** (due to pbc)  $\Rightarrow$  compute **angular position of center of mass,  $\theta_{cm}^j$**





# ORDER PARAMETER: TOMOGRAPHIC COHERENCES

- **MFT: 1d density waves** in symmetry-broken phase  $\Rightarrow$  jam particle flow
- **Tomographic analysis:** slice system along  $\alpha$ -direction  $\Rightarrow$   $j$ -slice is a **ring in 2d** (due to pbc)  $\Rightarrow$  compute **angular position of center of mass,  $\theta_{cm}^j$**



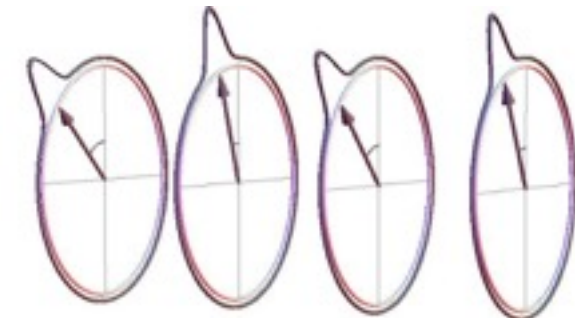
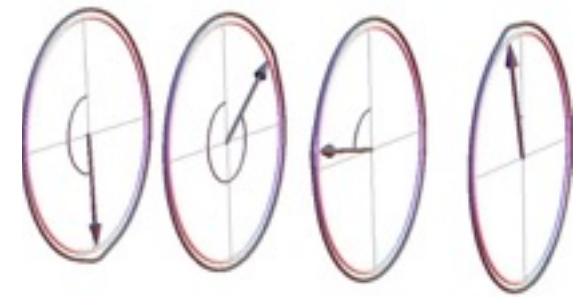
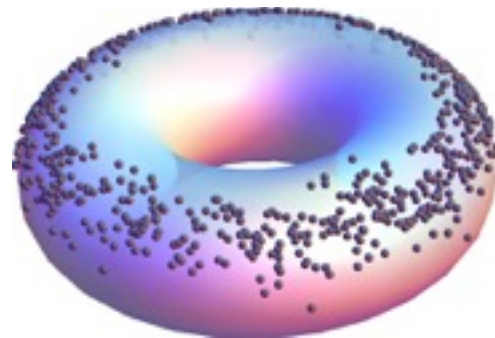
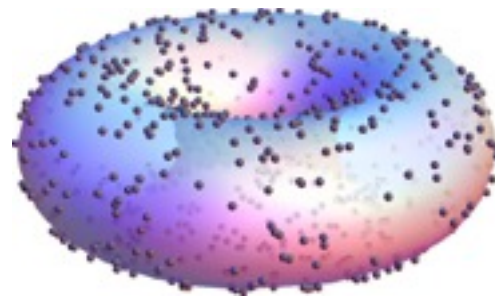
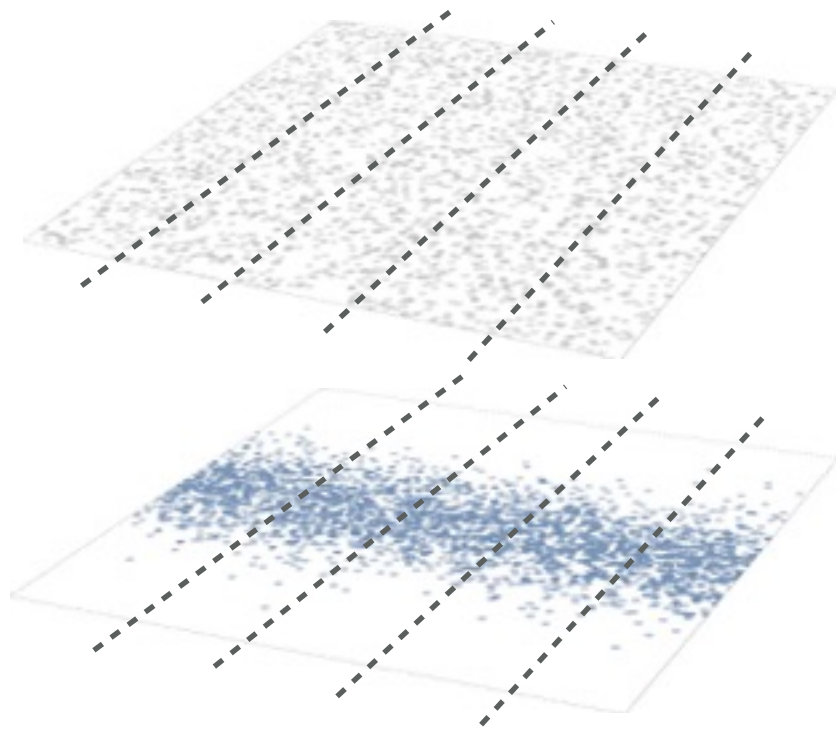
- **Small dispersion** of the angular centers of mass across slices signals the **emergence of order** Define **tomographic coherences**

$$\sigma_x^2 \equiv \langle (\theta_{cm}^{(j)})^2 \rangle_x - \langle \theta_{cm}^{(j)} \rangle_x^2$$

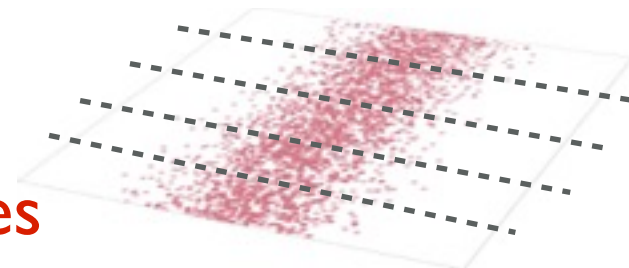
$$\Delta_x(\lambda) \equiv 1 - \langle \sigma_x^2 \rangle_\lambda$$

# ORDER PARAMETER: TOMOGRAPHIC COHERENCES

- **MFT: 1d density waves** in symmetry-broken phase  $\Rightarrow$  jam particle flow
- **Tomographic analysis:** slice system along  $\alpha$ -direction  $\Rightarrow$  **j-slice is a ring in 2d** (due to pbc)  $\Rightarrow$  compute **angular position of center of mass,  $\theta_{cm}^j$**



- **Small dispersion** of the angular centers of mass across slices signals the **emergence of order**. Define **tomographic coherences**



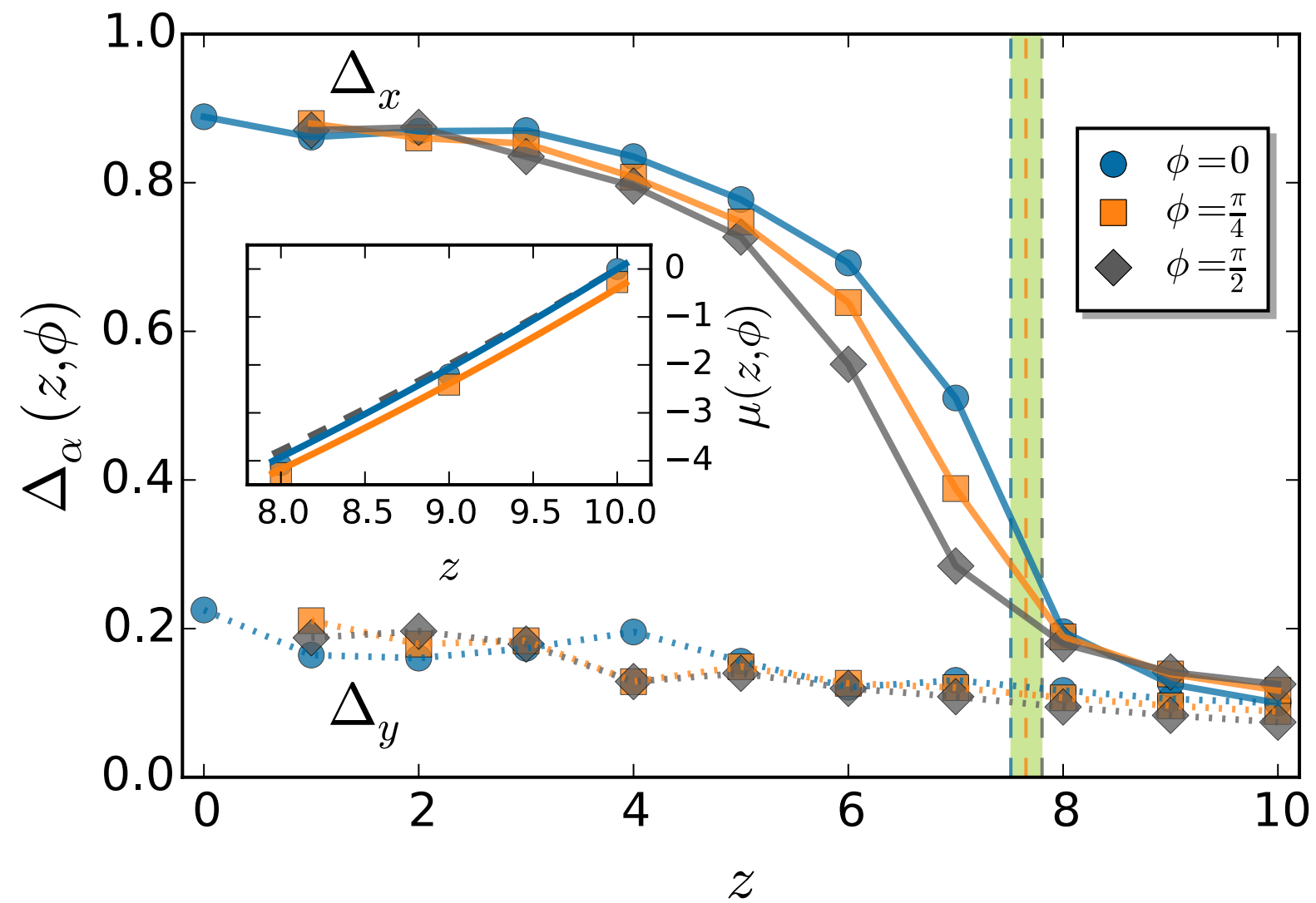
$$\sigma_x^2 \equiv \langle (\theta_{cm}^{(j)})^2 \rangle_x - \langle \theta_{cm}^{(j)} \rangle_x^2$$

$$\Delta_x(\lambda) \equiv 1 - \langle \sigma_x^2 \rangle_\lambda$$

$$\Delta_y(\lambda) \equiv 1 - \langle \sigma_y^2 \rangle_\lambda$$

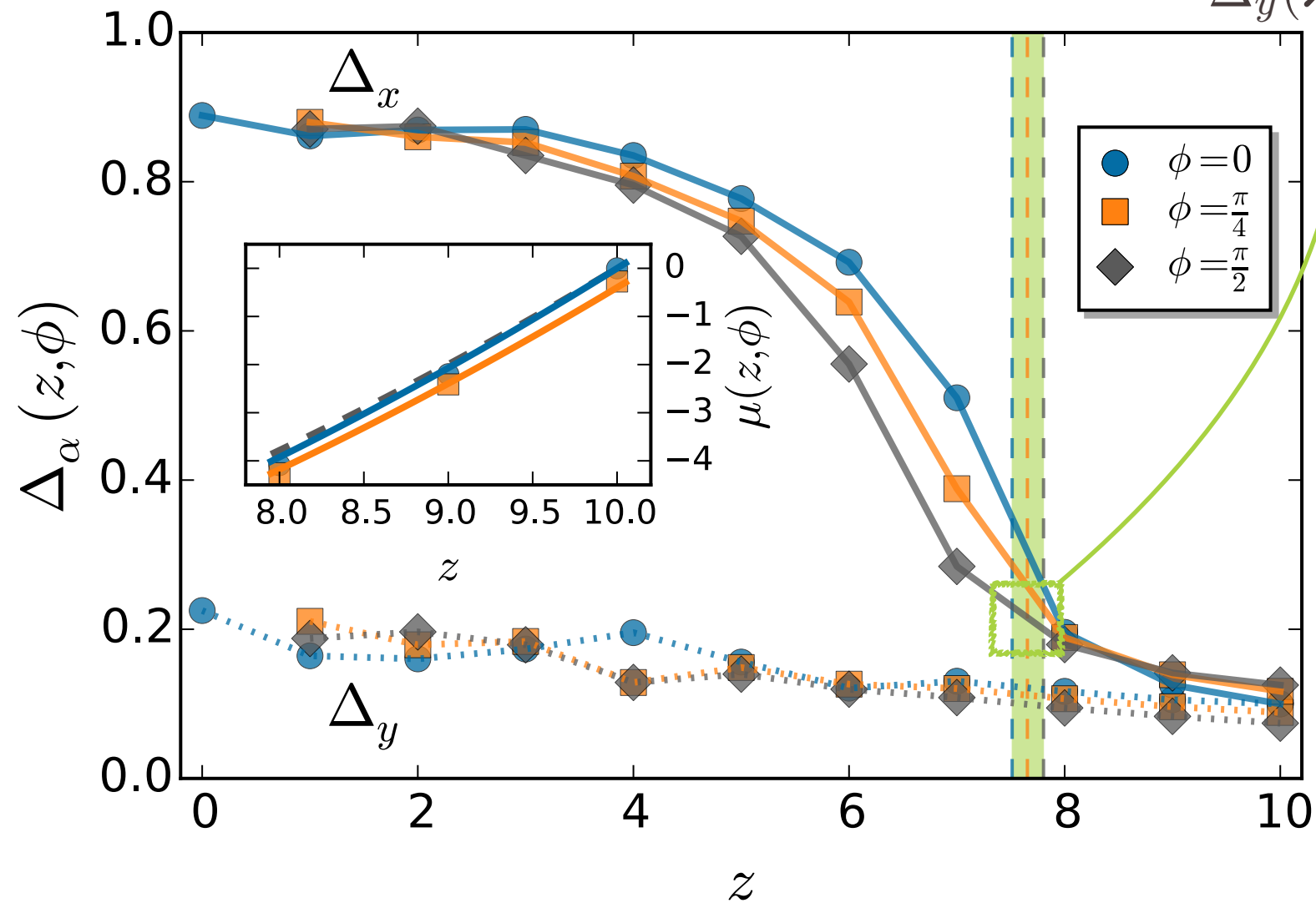


# ORDER AND DENSITY WAVE STRUCTURE

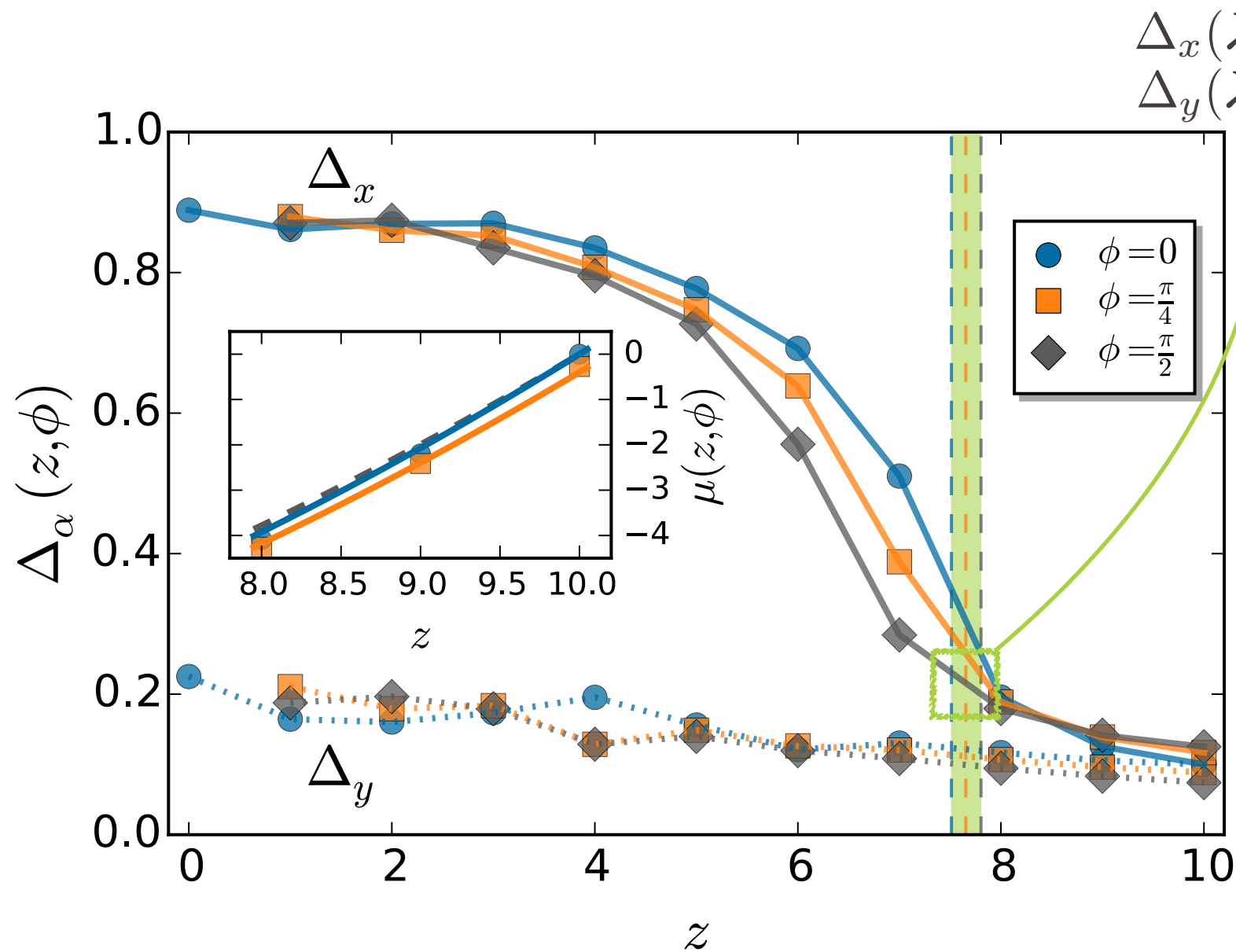


# ORDER AND DENSITY WAVE STRUCTURE

$\Delta_x(\lambda)$  increases steeply across DPT  $\forall \phi$   
 $\Delta_y(\lambda)$  remains small and unaffected

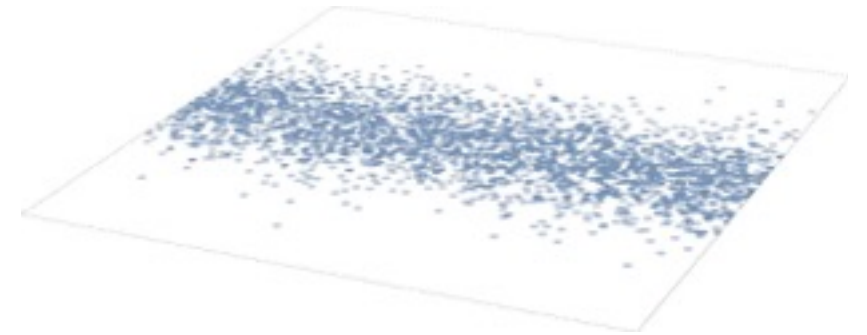


# ORDER AND DENSITY WAVE STRUCTURE



$\Delta_x(\lambda)$  increases steeply across DPT  $\forall \phi$   
 $\Delta_y(\lambda)$  remains small and unaffected

Only one symmetry-broken phase  
 Travelling wave in  $y$ , jam in  $x \forall \phi$   
 $\omega_J(y - vt)$

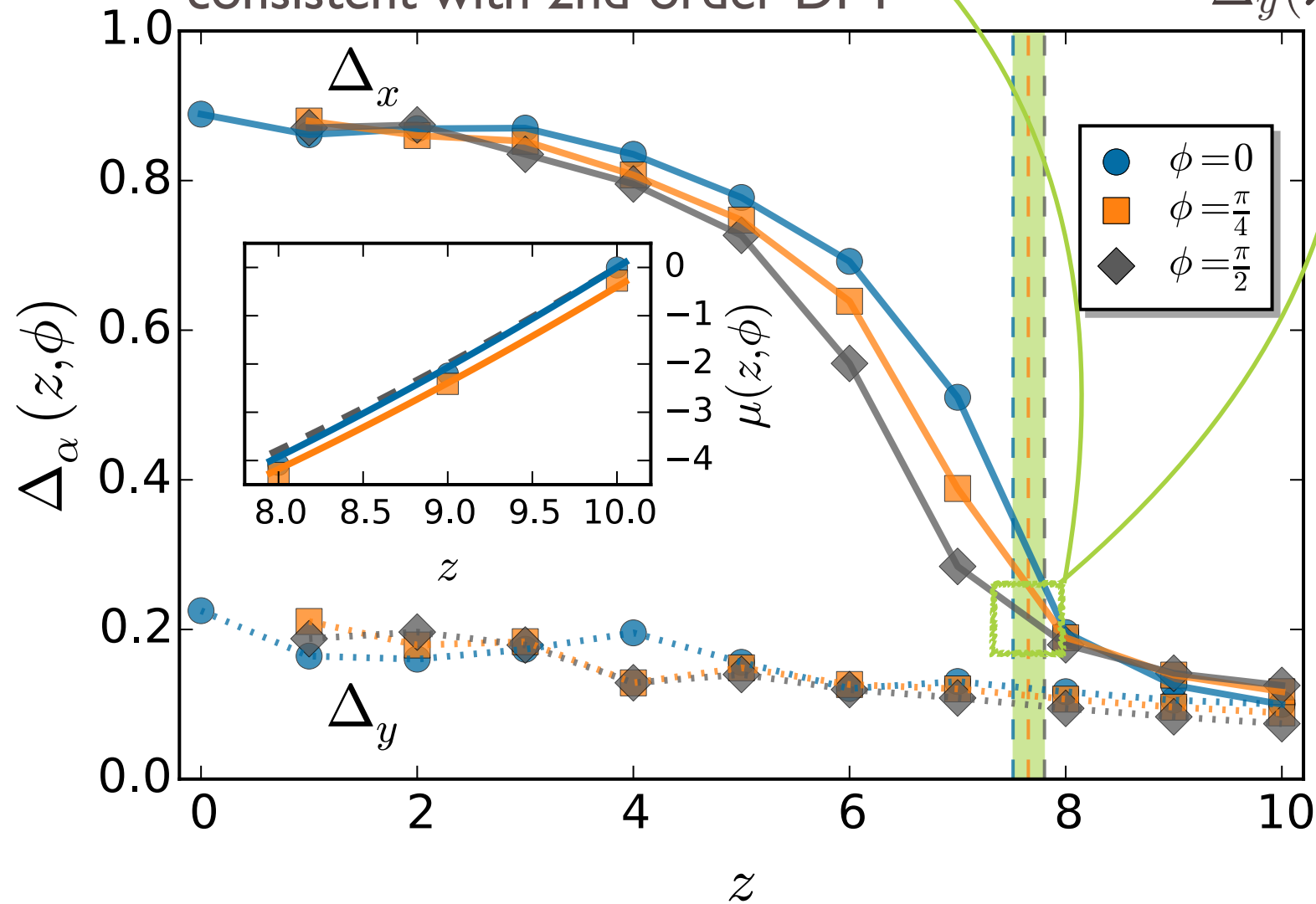


Consistent with supercritical  
 effective anisotropy  $\epsilon > \epsilon_c$

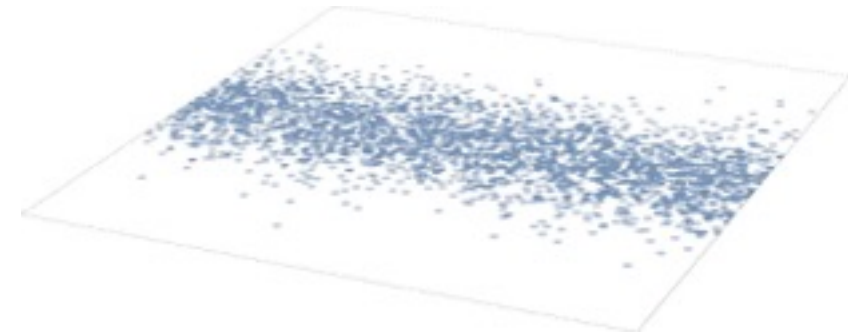
# ORDER AND DENSITY WAVE STRUCTURE

Sharp but continuous change in  $\Delta_x(\lambda)$   
consistent with 2nd-order DPT

$\Delta_x(\lambda)$  increases steeply across DPT  $\forall \phi$   
 $\Delta_y(\lambda)$  remains small and unaffected



Only one symmetry-broken phase  
Travelling wave in y, jam in x  $\forall \phi$   
 $\omega_J(y - vt)$

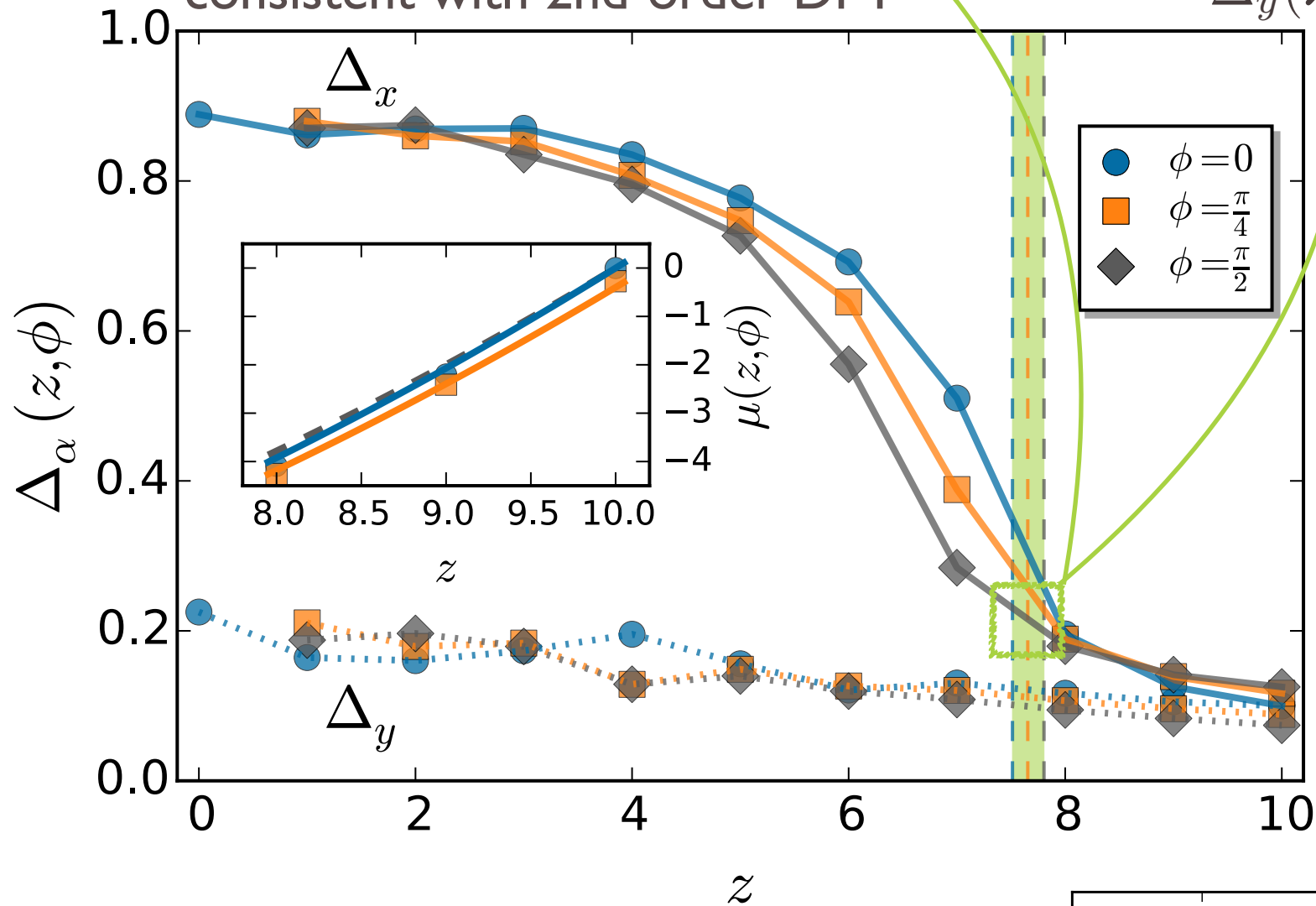


Consistent with supercritical  
effective anisotropy  $\epsilon > \epsilon_c$

# ORDER AND DENSITY WAVE STRUCTURE

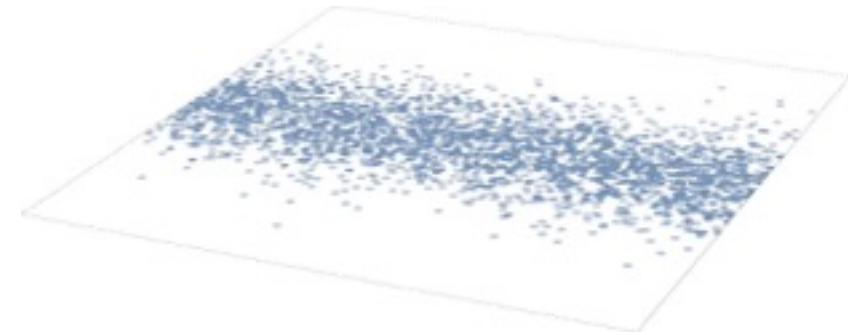
Sharp but continuous change in  $\Delta_x(\lambda)$  consistent with 2nd-order DPT

$\Delta_x(\lambda)$  increases steeply across DPT  $\forall \phi$   
 $\Delta_y(\lambda)$  remains small and unaffected



Only one symmetry-broken phase  
 Travelling wave in  $y$ , jam in  $x \forall \phi$

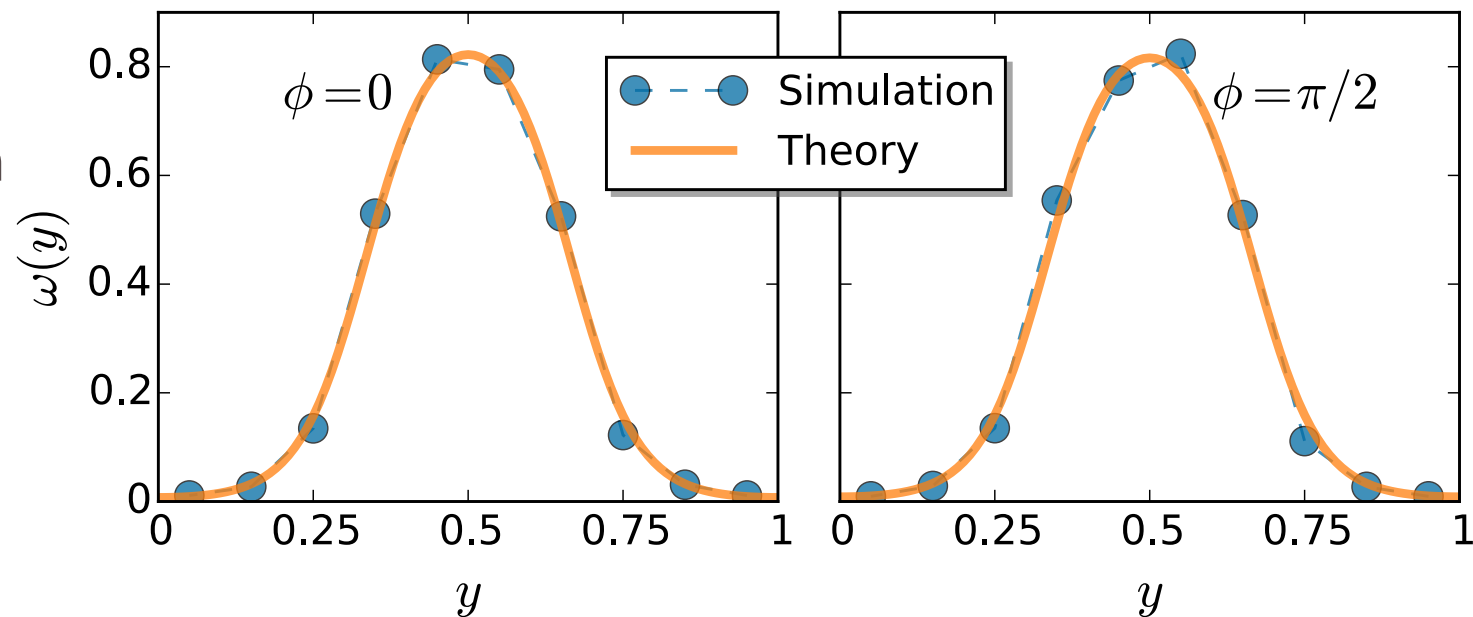
$$\omega_J(y - vt)$$



Consistent with supercritical effective anisotropy  $\epsilon > \epsilon_c$

Structure of density wave in  $y$ -direction for different  $\phi$  deep in symmetry-broken phase

Excellent theory/simulation agreement





# SUMMARY

- **Dynamic phase transitions (DPTs) at the trajectory level** are one of the most intriguing phenomena of nonequilibrium physics
- However, the **nature of DPTs** in realistic high-dimensional systems remains **puzzling**

# SUMMARY

- **Dynamic phase transitions (DPTs) at the trajectory level** are one of the most intriguing phenomena of nonequilibrium physics
- However, the **nature of DPTs** in realistic high-dimensional systems remains **puzzling**
- We report **compelling evidences of a complex DPT** in the vectorial current statistics of an archetypal 2d driven diffusive system (**WASEP**), and characterize its properties using macroscopic fluctuation theory (**MFT**)
- The **complex interplay among the external field, anisotropy and currents in 2d** leads to a **rich phase diagram**
- **Different symmetry-broken fluctuation phases** separated by lines of **1<sup>st</sup>- and 2<sup>nd</sup>-order DPTs**
- Key role of divergence-free but **structured current fields: weak additivity principle**

# SUMMARY

- **Dynamic phase transitions (DPTs) at the trajectory level** are one of the most intriguing phenomena of nonequilibrium physics
- However, the **nature of DPTs** in realistic high-dimensional systems remains **puzzling**
- We report **compelling evidences of a complex DPT** in the vectorial current statistics of an archetypal 2d driven diffusive system (**WASEP**), and characterize its properties using macroscopic fluctuation theory (**MFT**)
- The **complex interplay among the external field, anisotropy and currents in 2d** leads to a **rich phase diagram**
- **Different symmetry-broken fluctuation phases** separated by lines of **1<sup>st</sup>- and 2<sup>nd</sup>-order DPTs**
- Key role of divergence-free but **structured current fields: weak additivity principle**
- Order in the form of **coherent jammed states** emerges to hinder transport for low-current fluctuations
- **Rare events are associated with coherent, self-organized patterns** which enhance their probability, making them **far more probable than anticipated**.

Thank you

Backup slides



$$G(\mathbf{q}) = \lim_{\tau \rightarrow \infty} \frac{1}{\tau} \max_{\{\rho, \mathbf{j}\}_0^\tau} I_\tau[\rho, \mathbf{j}], \quad (\text{A8})$$

subject to constraints (A5), (A6) and (A7). The density and current fields solution of this variational problem, denoted here as  $\rho_{\mathbf{q}}(\mathbf{r}, t)$  and  $\mathbf{j}_{\mathbf{q}}(\mathbf{r}, t)$ , correspond to the optimal path the system follows in mesoscopic phase space to sustain a long-time current fluctuation  $\mathbf{q}$ . This path may be in general time-dependent, and the associated general variational problem is remarkably hard.

This problem becomes simpler however in different limiting cases. For instance, in the steady state the system exhibits translation symmetry with an homogeneous stationary density profile  $\rho_{\text{st}}(\mathbf{r}) = \rho_0$  and a constant average current  $\mathbf{j}_{\text{st}}(\mathbf{r}) = \langle \mathbf{q} \rangle = \sigma_0 \hat{\mathcal{A}} \mathbf{E}$ , where we have defined  $\sigma_0 \equiv \sigma(\rho_0)$ . Now, small fluctuations of the empirical current  $\mathbf{q}$  away from the average behavior  $\langle \mathbf{q} \rangle$  will typically result from weakly-correlated local events in different parts of the system which add up incoherently to yield the desired  $\mathbf{q}$ . Thus, the optimal density field associated to these small fluctuations still corresponds to the homogeneous, stationary one, i.e.  $\rho_{\mathbf{q}}(\mathbf{r}, t) = \rho_0$  for  $|\mathbf{q} - \langle \mathbf{q} \rangle| \ll 1$ , while the optimal current field is constant,  $\mathbf{j}_{\mathbf{q}}(\mathbf{r}, t) = \mathbf{q}$ , leading to a quadratic current LDF corresponding to Gaussian current statistics,

$$G_G(\mathbf{q}) = -\frac{1}{2\sigma_0} \left( \mathbf{q} - \sigma_0 \hat{\mathcal{A}} \mathbf{E} \right) \cdot \hat{\mathcal{A}}^{-1} \left( \mathbf{q} - \sigma_0 \hat{\mathcal{A}} \mathbf{E} \right), \quad (\text{A9})$$

as indeed corroborated in our simulations for a broad range of  $\mathbf{q}$ 's. As an interesting by-product, note that current fluctuations in this Gaussian regime obey an anisotropic version of the Isometric Fluctuation Theorem [4, 5], which links in simple terms the probability of two different but  $\hat{\mathcal{A}}$ -isometric current vector fluctuations. In particular,

$$\lim_{\tau \rightarrow \infty} \frac{1}{\tau L^d} \ln \left[ \frac{P_\tau(\mathbf{q})}{P_\tau(\mathbf{q}')} \right] = \mathbf{E} \cdot (\mathbf{q} - \mathbf{q}'), \quad (\text{A10})$$

$\forall \mathbf{q}, \mathbf{q}'$  in the Gaussian regime such that  $\mathbf{q} \cdot \hat{\mathcal{A}} \mathbf{q} = \mathbf{q}' \cdot \hat{\mathcal{A}} \mathbf{q}'$ .



Interestingly, the above *flat* profiles remain a solution of the full variational problem  $\forall \mathbf{q}$ , but the question remains as to whether other solutions with more complex spatiotemporal structure may yield a better maximizer of the MFT action (A8) for currents. To address this question, we now perturb the above flat solution with small but otherwise arbitrary functions of space and time, and study the local stability of the homogeneous solution against such perturbations. In particular, we ask whether the perturbed fields yield in some case a larger  $G(\mathbf{q})$ . With this aim in mind, we write

$$\bar{\rho}(\mathbf{r}, t) = \rho_0 + \delta\rho(\mathbf{r}, t), \quad \bar{\mathbf{j}}(\mathbf{r}, t) = \mathbf{q} + \delta\mathbf{j}(\mathbf{r}, t), \quad (\text{A11})$$

where both  $\bar{\rho}(\mathbf{r}, t)$  and  $\bar{\mathbf{j}}(\mathbf{r}, t)$  remain constrained by Eqs. (A5), (A6) and (A7). Inserting these expressions in Eq. (A8) and expanding to second order in the perturbations, we obtain the leading correction to the quadratic form  $G_G(\mathbf{q})$  of Eq. (A9) (termed here  $O2$ )

$$O2 = -\frac{1}{2\tau} \int_0^\tau dt \int_\Lambda d\mathbf{r} \left\{ A(\rho_0, \mathbf{q}) \delta\rho^2 + \nabla\delta\rho \cdot \hat{B}(\rho_0) \nabla\delta\rho + \delta\mathbf{j} \cdot \hat{C}(\rho_0) \delta\mathbf{j} + \delta\mathbf{j} \cdot \mathbf{F}(\rho_0, \mathbf{q}) \delta\rho \right\}, \quad (\text{A12})$$

where we have defined

$$A(\rho_0, \mathbf{q}) = \left( \frac{\sigma_0'^2}{\sigma_0^3} - \frac{\sigma_0''}{2\sigma_0^2} \right) \mathbf{q} \cdot \hat{\mathcal{A}}^{-1} \mathbf{q} + \sigma_0'' \mathbf{E} \cdot \hat{\mathcal{A}} \mathbf{E}, \quad \hat{B}(\rho_0) = \frac{D_0^2}{\sigma_0} \hat{\mathcal{A}}, \quad \hat{C}(\rho_0) = \frac{\hat{\mathcal{A}}^{-1}}{\sigma_0}, \quad \mathbf{F}(\rho_0, \mathbf{q}) = -\frac{\sigma_0'}{\sigma_0^2} \hat{\mathcal{A}}^{-1} \mathbf{q}, \quad (\text{A13})$$

with ' denoting derivative with respect to the argument, and  $D_0 \equiv D(\rho_0)$ . We next expand the perturbations  $\delta\rho(\mathbf{r}, t)$  and  $\delta\mathbf{j}(\mathbf{r}, t)$  in Fourier series, taking advantage of the spatial periodic boundary conditions, and imposing explicitly along the way the constraints (A5), (A6) and (A7). For simplicity we particularize hereafter our results for dimension two,  $d = 2$ , though the generalization to arbitrary  $d$  is straightforward. The  $O2$  correction above is of course a quadratic form of the perturbations with constant coefficients, so that the different Fourier modes decouple simplifying the problem. In this way the stability analysis melts down as usual to an eigenvalue problem, which in this case splits into different problems for only temporal modes, spatiotemporal modes with structure along just one dimension,  $x$  or  $y$ , and fully  $2d$  spatiotemporal modes, which can be analyzed separately [6]. This straightforward but lengthy calculation leads to the following conclusion: the flat solution corresponding to Gaussian current statistics remains stable (i.e. the  $O2$  correction is negative) whenever the following conditions hold,

$$\begin{aligned} a_{\min} k_n^2 \frac{D_0^2}{\sigma_0} + H(\mathbf{E}, \mathbf{q}) &> 0 \\ a_{\max} k_m^2 \frac{D_0^2}{\sigma_0} + H(\mathbf{E}, \mathbf{q}) &> 0 \\ (a_{\min} k_n^2 + a_{\max} k_m^2) \frac{D_0^2}{\sigma_0} + H(\mathbf{E}, \mathbf{q}) &> 0, \end{aligned} \quad (\text{A14})$$

with  $k_n = 2\pi n$  and  $k_m = 2\pi m$  the different spatial modes associated to each perturbation along either direction,  $a_{\min} = \min\{a_\alpha, \alpha \in [1, d]\}$  and  $a_{\max} = \max\{a_\alpha, \alpha \in [1, d]\}$ , and

$$H(\mathbf{E}, \mathbf{q}) = \frac{\sigma_0''}{2} \left( \mathbf{E} \cdot \hat{\mathcal{A}} \mathbf{E} - \sigma_0^{-2} \mathbf{q} \cdot \hat{\mathcal{A}}^{-1} \mathbf{q} \right) \quad (\text{A15})$$



A number of important conclusions can be directly derived from this set of conditions, namely:

- (i) The first mode to become unstable (if any) is always the fundamental mode  $k_1 = 2\pi$ .
- (ii) For any value of the anisotropy, the first perturbations to become unstable are those with structure along one spatial dimension,  $x$  or  $y$ .
- (iii) For anisotropic systems,  $a_{\min} < a_{\max}$ , the leading unstable perturbation has structure in the direction of minimum anisotropy.
- (iv) For isotropic systems,  $a_{\min} = a_{\max} \equiv a$ , both one-dimensional perturbations trigger the instability of the flat solution at the same point. In this case, the orientation of the current vector  $\mathbf{q}$  determines the most probable profile immediately after the instability kicks in, with structure only along the  $x$ - or  $y$ -direction, as dictated by the term proportional to  $\mathbf{F}(\rho_0, \mathbf{q})$  in the  $O2$  correction, see Eq. (A12).

Therefore there exists a line of critical values for the current  $\mathbf{q}_c$  at which the instability appears, given by

$$\mathbf{q}_c \cdot \hat{\mathcal{A}}^{-1} \mathbf{q}_c = \sigma_0^2 \left( \mathbf{E} \cdot \hat{\mathcal{A}} \mathbf{E} + 8\pi^2 a_{\min} \frac{D_0^2}{\sigma_0 \sigma_0''} \right) \equiv \sigma_0^2 \Xi_c. \quad (\text{A16})$$

For systems with  $\sigma_0'' > 0$  (as e.g. the Kipnis-Marchioro-Presutti model of heat transport [3, 4, 7]), the instability appears always, regardless of the value of the external field (even for  $\mathbf{E} = 0$ ), separating a regime of Gaussian current statistics for  $\mathbf{q} \cdot \hat{\mathcal{A}}^{-1} \mathbf{q} \leq \sigma_0^2 \Xi_c$  and a non-Gaussian region for  $\mathbf{q} \cdot \hat{\mathcal{A}}^{-1} \mathbf{q} > \sigma_0^2 \Xi_c$ . On the other hand, for systems with  $\sigma_0'' < 0$  (as the weakly asymmetric simple exclusion process –WASEP– studied in this paper [8–10]) a line of critical values of the external field exists, defined by

$$\mathbf{E}_c \cdot \hat{\mathcal{A}} \mathbf{E}_c = 8\pi^2 a_{\min} \frac{D_0^2}{\sigma_0 |\sigma_0''|} \equiv |\Sigma_c|. \quad (\text{A17})$$

beyond which the instability appears,  $\mathbf{E} \cdot \hat{\mathcal{A}} \mathbf{E} \geq |\Sigma_c|$ . In this strong field case, Gaussian statistics are expected for all currents except for a region around  $\mathbf{q} = 0$ , defined by  $\mathbf{q} \cdot \hat{\mathcal{A}}^{-1} \mathbf{q} \leq \sigma_0^2 \Xi_c$ , where current fluctuations are non-Gaussian. For weak external fields,  $\mathbf{E} \cdot \hat{\mathcal{A}} \mathbf{E} < |\Sigma_c|$ , only Gaussian statistics are observed.

Whenever the instability emerges, the first two frequencies to become unstable are  $\nu_c = \pm 2\pi q_{\parallel} \sigma_0' / \sigma_0$ , with  $q_{\parallel}$  the component of the current vector along the direction of structure formation (that we denote here as  $x_{\parallel}$ ). It can be then easily proved [6] that, immediately after the instability kicks in, the perturbation of the density profile takes the form of a one-dimensional traveling wave

$$\delta\rho(x_{\parallel}, t) = A \sin \left[ 2\pi \left( x_{\parallel} - x_{\parallel}^0 - \frac{q_{\parallel} \sigma_0'}{\sigma_0} t \right) \right], \quad (\text{A18})$$



with  $A$  and  $x_{\parallel}^0$  two arbitrary constants. With this result in mind, we consider now that the relevant density fields well below the instability conserve a traveling-wave structure, i.e.  $\rho(\mathbf{r}, t) = \omega(\mathbf{r} - \mathbf{v}t)$  which, taking into account constraints (A5), (A6) and (A7), implies current fields of the form

$$\mathbf{j}(\mathbf{r}, t) = \mathbf{q} - \mathbf{v} [\rho_0 - \omega(\mathbf{r} - \mathbf{v}t)] + \phi(\mathbf{r} - \mathbf{v}t) \quad (\text{A19})$$

where  $\phi(\mathbf{r} - \mathbf{v}t)$  is a possibly structured but divergence-free vector field with zero integral. Hence, under these assumptions, the current LDF of Eq. (A8) can now be written, after a change of variables  $(\mathbf{r} - \mathbf{v}t) \rightarrow \mathbf{r}$ , as

$$G(\mathbf{q}) = - \min_{\omega, \phi, \mathbf{v}} \int_{\Lambda} d\mathbf{r} \frac{1}{2\sigma(\omega)} \mathcal{J}_{\mathbf{q}}(\omega, \phi, \mathbf{v}) \cdot \hat{\mathcal{A}}^{-1} \mathcal{J}_{\mathbf{q}}(\omega, \phi, \mathbf{v}), \quad (\text{A20})$$

with the definition

$$\mathcal{J}_{\mathbf{q}}(\omega, \phi, \mathbf{v}) \equiv \mathbf{q} - \mathbf{v} [\rho_0 - \omega(\mathbf{r})] + \phi(\mathbf{r}) + D(\omega) \hat{\mathcal{A}} \nabla \omega - \sigma(\omega) \hat{\mathcal{A}} \mathbf{E}, \quad (\text{A21})$$

and with the additional constraints

$$\rho_0 = \int_{\Lambda} \omega(\mathbf{r}) d\mathbf{r} \quad (\text{A22})$$

$$\int_{\Lambda} \phi(\mathbf{r}) d\mathbf{r} = 0 \quad (\text{A23})$$

$$\nabla \cdot \phi(\mathbf{r}) = 0 \quad (\text{A24})$$

9

The optimal fields and velocity solution of this complex variational problem, denoted as  $\omega_{\mathbf{q}}(\mathbf{r})$ ,  $\phi_{\mathbf{q}}(\mathbf{r})$ , and  $\mathbf{v}_{\mathbf{q}}$ , obey the following system of coupled equations,

$$\left[ \frac{\mathbf{v}_{\mathbf{q}}}{\sigma(\omega_{\mathbf{q}})} - \frac{\sigma'(\omega_{\mathbf{q}})}{2\sigma(\omega_{\mathbf{q}})^2} \mathbf{j}_{\mathbf{q}} \right] \cdot \hat{\mathcal{A}}^{-1} \mathbf{j}_{\mathbf{q}} - \left[ \left( \frac{D(\omega_{\mathbf{q}})^2}{2\sigma(\omega_{\mathbf{q}})} \right)' \nabla \omega_{\mathbf{q}} + \frac{D(\omega_{\mathbf{q}})^2}{\sigma(\omega_{\mathbf{q}})} \nabla \right] \cdot \hat{\mathcal{A}} \nabla \omega_{\mathbf{q}} + \frac{1}{2} \sigma'(\omega_{\mathbf{q}}) \mathbf{E} \cdot \hat{\mathcal{A}} \mathbf{E} - \zeta = 0$$

$$D(\omega_{\mathbf{q}}) \nabla \omega_{\mathbf{q}} + \hat{\mathcal{A}}^{-1} \mathbf{j}_{\mathbf{q}} + \sigma(\omega_{\mathbf{q}}) [\boldsymbol{\kappa} - \nabla \Psi] = 0, \quad (\text{A25})$$

$$\int_{\Lambda} d\mathbf{r} \left( \frac{\omega_{\mathbf{q}} - \rho_0}{\sigma(\omega_{\mathbf{q}})} \right) \hat{\mathcal{A}}^{-1} \mathbf{j}_{\mathbf{q}} = 0, \quad (\text{A26})$$

where we have defined  $\mathbf{j}_{\mathbf{q}}(\mathbf{r}) \equiv \mathbf{q} - \mathbf{v}_{\mathbf{q}} [\rho_0 - \omega_{\mathbf{q}}(\mathbf{r})] + \phi_{\mathbf{q}}(\mathbf{r})$  for simplicity in notation, and  $\zeta$ ,  $\boldsymbol{\kappa}$  and  $\Psi(\mathbf{r})$  are Lagrange multipliers associated to the constraints (A22), (A23) and (A24), respectively.



As discussed above, our local stability analysis shows that whenever the transition is unleashed, the leading instability is a density wave with structure in one dimension only, determined either by the minimum-anisotropy direction, see condition (iii) above, or by the orientation of the current vector for isotropic systems, see (iv). Such a 1d traveling wave will dominate the optimal solution of our variational problem *at least* in a finite region below the transition line, so we now assume 1d optimal traveling-wave fields of the form  $\omega_{\mathbf{q}}(x_{\parallel})$  and  $\phi_{\mathbf{q}}(x_{\parallel})$  (recall that we denote as  $x_{\parallel}$  the direction of structure formation, and  $x_{\perp}$  the orthogonal, structureless direction). Next we decompose the optimal vector field  $\phi_{\mathbf{q}}$  along the  $\parallel$ - and  $\perp$ -directions,  $\phi_{\mathbf{q}}(x_{\parallel}) = [\phi_{\mathbf{q}}^{\parallel}(x_{\parallel}), \phi_{\mathbf{q}}^{\perp}(x_{\parallel})]$ . The divergence-free and zero-integral constraints on  $\phi_{\mathbf{q}}$ , see Eqs. (A23) and (A24) above, thus immediately imply that  $\phi_{\mathbf{q}}^{\parallel}(x_{\parallel}) = 0$ , while Eq. (A25) leads to  $\phi_{\mathbf{q}}^{\perp}(x_{\parallel}) = -a_{\max} \tilde{\kappa} \sigma[\omega_{\mathbf{q}}(x_{\parallel})]$ , where  $\tilde{\kappa}$  is a constant which comprises in this simplified 1d problem both Lagrange multipliers  $\kappa$  and  $\Psi(\mathbf{r})$ . In this situation, the system of coupled integro-differential equations for the optimal fields is

$$X(\omega_{\mathbf{q}}) \left( \frac{d\omega_{\mathbf{q}}}{dx_{\parallel}} \right)^2 - Y(\omega_{\mathbf{q}}) + \tilde{K} \omega_{\mathbf{q}}(x_{\parallel}) - K = 0, \quad (\text{A27})$$

$$\int_0^1 dx_{\parallel} \frac{[\omega_{\mathbf{q}}(x_{\parallel}) - \rho_0]}{a_{\min} \sigma(\omega_{\mathbf{q}})} [q_{\parallel} - v_{\parallel}(\rho_0 - \omega_{\mathbf{q}}(x_{\parallel}))] = 0, \quad (\text{A28})$$

$$\rho_0 = \int_0^1 \omega_{\mathbf{q}}(x_{\parallel}) dx_{\parallel}, \quad (\text{A29})$$

with  $K$  and  $\tilde{K}$  two constants to be specified below, and where we have defined

$$X(\omega) \equiv \frac{D(\omega)^2}{2\sigma(\omega)} a_{\min}, \quad (\text{A30})$$

$$Y(\omega) = \frac{\sigma(\omega)}{2} \left( \mathbf{E} \cdot \hat{\mathcal{A}} \mathbf{E} + \frac{[q_{\parallel} - v_{\parallel}(\rho_0 - \omega)]^2}{a_{\min} \sigma(\omega)^2} - \frac{q_{\perp}^2}{a_{\max} (\int_0^1 \sigma(\omega) dx_{\parallel})^2} \right). \quad (\text{A31})$$

In order to solve this system of equations, we now introduce a reparametrization which simplifies the numerical evaluation of the optimal 1d density wave profile and thus of the current LDF  $G(\mathbf{q})$ . First note that, in our geometry, Eq. (A27) leads to a periodic optimal profile *symmetric* around  $x_{\parallel} = 1/2$  (recall that  $x_{\parallel} \in [0, 1]$ ), i.e. with reflection symmetry  $x_{\parallel} \rightarrow 1 - x_{\parallel}$ . Next we consider the possible maxima and minima of the optimal density wave. For models with a quadratic mobility transport coefficient  $\sigma(\omega)$ , as the WASEP and KMP models typically studied in literature, the number of possible maxima  $\omega_+$  and minima  $\omega_-$  of the curve  $\omega_{\mathbf{q}}(x_{\parallel})$  is rather restricted, see Eq. (A27) once particularized for  $\omega'_{\mathbf{q}}(x_{\parallel}) = 0$ . In the simplest case [3, 6, 10], a single maximum  $\omega_+ = \omega_{\mathbf{q}}(x_{\parallel}^+)$  and minimum  $\omega_- = \omega_{\mathbf{q}}(x_{\parallel}^-)$  will appear, such that the position of two consecutive extrema  $x_{\parallel}^+$  and  $x_{\parallel}^-$  is such that  $|x_{\parallel}^+(k) - x_{\parallel}^-(k)| = 1/2n$ , with  $n$  the number of cycles in the unit interval. One can then study numerically the dependence of the current LDF on the number  $n$  of cycles, finding that  $n = 1$  is the optimal case. We hence restrict



hereafter to 1d density waves with a single maximum and minimum with  $n = 1$ . As a result, we can express now the constants  $\tilde{K}$  and  $K$  of Eq. (A27) in terms of these extrema

$$Y(\omega_{\pm}) = \tilde{K}\omega_{\pm} - K. \quad (\text{A32})$$

The values of these extrema  $\omega_{\pm}$  can be obtained from the constraints on the distance between them and the total density of the system. In particular, the first constraint leads to the following equation,

$$1 = \int_0^1 dx_{\parallel} = 2 \int_{\omega_-}^{\omega_+} \frac{d\omega_{\mathbf{q}}}{\omega'_{\mathbf{q}}} = 2 \int_{\omega_-}^{\omega_+} f(\omega_{\mathbf{q}}) d\omega_{\mathbf{q}} \quad (\text{A33})$$

with

$$f(\omega_{\mathbf{q}}) \equiv \sqrt{\frac{X(\omega_{\mathbf{q}})}{Y(\omega_{\mathbf{q}}) - \tilde{K}\omega_{\mathbf{q}} + K}} \quad (\text{A34})$$

as derived from Eq. (A27), while the constraint on the total density leads to

$$\rho_0 = \int_0^1 \omega_{\mathbf{q}}(x_{\parallel}) dx_{\parallel} = 2 \int_{\omega_-}^{\omega_+} \frac{\omega_{\mathbf{q}}}{\omega'_{\mathbf{q}}} d\omega_{\mathbf{q}} = 2 \int_{\omega_-}^{\omega_+} \omega_{\mathbf{q}} f(\omega_{\mathbf{q}}) d\omega_{\mathbf{q}}. \quad (\text{A35})$$

Note that the unknown variables  $\omega_{\pm}$  appear as integration limits in Eqs. (A33) and (A35), difficulting the numerical solution of this problem. However, a suitable change of variables allows to drop this dependence. In particular, we write now  $\omega_{\mathbf{q}}(\Omega) \equiv \omega_- + \Omega(\omega_+ - \omega_-)$ , with  $\Omega \in [0, 1]$ , and define  $h(\Omega) \equiv (\omega_+ - \omega_-) f[\omega_- + \Omega(\omega_+ - \omega_-)]$ . With this choice, constraints (A33) and (A35), together with Eq. (A28) for the velocity, now read

$$\frac{1}{2} = \int_0^1 h(\Omega) d\Omega, \quad (\text{A36})$$

$$\frac{\rho_0}{2} = \int_0^1 \omega_{\mathbf{q}}(\Omega) h(\Omega) d\Omega, \quad (\text{A37})$$

$$\int_0^1 h(\Omega) \frac{[\omega_{\mathbf{q}}(\Omega) - \rho_0]}{a_{\min} \sigma[\omega_{\mathbf{q}}(\Omega)]} [q_{\parallel} - v_{\parallel}(\rho_0 - \omega_{\mathbf{q}}(\Omega))] d\Omega = 0. \quad (\text{A38})$$

The solution of this three integral equations for a particular model and a given current vector  $\mathbf{q}$  leads to particular values of the parameters  $\omega_-$ ,  $\omega_+$  and  $v_{\parallel}$ , which can be used in turn to solve numerically the differential equation for the optimal density wave profile [3, 6, 10] and thus obtain the current LDF  $G(\mathbf{q})$ .